

**STUDIES ON THE DYNAMICS AND RHEOLOGY OF
DILUTE SUSPENSIONS OF BROWNIAN PARTICLES
IN SIMPLE SHEAR FLOW UNDER THE ACTION OF
AN EXTERNAL FORCE**

Thesis submitted to
THE COCHIN UNIVERSITY OF SCIENCE AND TECHNOLOGY
in partial fulfilment of the requirements
for the degree of
DOCTOR OF PHILOSOPHY
in
TECHNOLOGY



G 8631

by
ASOKAN K.

under the supervision of
Dr. T. R. RAMAMOCHAN

REGIONAL RESEARCH LABORATORY (CSIR)
Thiruvananthapuram
September, 2003

DECLARATION

I, Asokan K., do hereby declare that the matter embodied in this thesis entitled “ **Studies on the dynamics and rheology of dilute suspensions of Brownian particles in simple shear flow under the action of an external force** ” is the result of the investigations carried out by me in the Computational Material Science Unit of the Regional Research Laboratory(CSIR), Thiruvananthapuram, under the guidance of **Dr. T. R. Ramamohan** and that the same has not been submitted elsewhere for any other degree.

In keeping with the general practice of reporting scientific observations, due acknowledgment has been made wherever the work described is based on the findings of other investigators.



Asokan K.



वैज्ञानिक एवं औद्योगिक अनुसंधान परिषद्
Council of Scientific & Industrial Research
क्षेत्रीय अनुसंधान प्रयोगशाला
REGIONAL RESEARCH LABORATORY

इन्डस्ट्रीयल इस्टेट - डाक घर, तिरुवनन्तपुरम - 695 019, भारत
Industrial Estate - P.O., Thiruvananthapuram - 695 019, INDIA

Dr. T. R. Ramamohan
Scientist

CERTIFICATE

This is to certify that the thesis entitled "**Studies on the Dynamics and Rheology of Dilute Suspensions of Brownian Particles in Simple Shear Flow Under the Action of an External Force**" is an authentic record of the research work carried out by Mr. Asokan K. under my supervision in partial fulfillment of the requirements for the degree of **Doctor of Philosophy** of the **Cochin University of Science and Technology** and further that no part thereof has been submitted elsewhere.

T. R. Ramamohan
Dr. T. R. Ramamohan
(Supervisor)

Acknowledgments

I wish to express my deep sense of gratitude to Dr. T. R. Ramamohan, my supervisor, for meticulously overseeing my Ph.D work, right from suggesting the problem till the completion of the work. His sharp observations, insightful comments and innovative suggestions guided the work in the right direction and made the numerous discussions I had with him inspiring and enlightening. I have found in him the rare combination of a devout scientist and a noble human soul. It was a pleasure to work with him, and I cherish my association with him for the past few years as one of the most delightful experiences in my life.

My sincere thanks to Dr. B. C. Pai, Director, RRL for his support and encouragement and for the help rendered in many official matters. I am also grateful to Dr. U. Syamaprasad, Convener, Research Committee and Dr. M. Sabir, Department of Physics, CUSAT for their timely help in connection with my registration at CUSAT.

I acknowledge with thanks the help and support received from the scientists at RRL, Dr. Roschen Sasikumar, Dr. C. C. S. Bhat, Dr. Elizabeth Jacob, Dr. S. Savithri and Dr. M. Ravi.

My seniors Dr. K. Satheesh Kumar and Dr. C. V. Anil Kumar have been a great help both in my work and personal affairs. I am indebted to both for all the help received from them and for the nice time I had with them at RRL.

I appreciate the help and company offered by my friends at RRL Mr. K. Radhakrishnan, Mr. J. Dasan, Mr. Tito Paul and Mr. A. Farook on whom I relied for many things, both personal and official.

Thanks are also due to the authorities of M. G. University and Director, STAS, for kindly allowing me to continue research part time and to the Regional Director, STAS, for permitting me to use the computing facilities at STAS, Pathanamthitta.

All my colleagues at STAS, Pathanamthitta have been very helpful. In particular, I had the company of Dr. P. R. Prince and Mr. Vinod Mathew on many evenings and

holidays while doing my research work. I am grateful to them for those joyful hours.

Financial assistance from CSIR, India, in the form of a fellowship during the initial years of this work is also thankfully acknowledged.

The critical comments and suggestions from the referees of various journals, who reviewed the work as part of the process of publication, have added to the quality of the results. I express my thanks to them.

I remember the love and affection from my parents and family, and the care and guidance of my eldest brother throughout my career.

My greatest source of strength was the love and support of my wife V. Hema who was always willing to help me in every possible way. I must thank her, and also my son Kannan, for the emotional sustenance they have provided all through these years of my work. Thanks also to her parents and family for being so supportive of me.

I am thankful to the free software community for the many applications and tools that I have freely used throughout my work.

Above all, I thank God Almighty for His blessings.

Asokan K.

Abstract

We present a novel approach to computing the orientation moments and rheological properties of a dilute suspension of spheroids in a simple shear flow at arbitrary Péclet number based on a generalised Langevin equation method. This method differs from the diffusion equation method which is commonly used to model similar systems in that the actual equations of motion for the orientations of the individual particles are used in the computations, instead of a solution of the diffusion equation of the system. It also differs from the method of ‘Brownian dynamics simulations’ in that the equations used for the simulations are deterministic differential equations even in the presence of noise, and not stochastic differential equations as in Brownian dynamics simulations. One advantage of the present approach over the Fokker-Planck equation formalism is that it employs a common strategy that can be applied across a wide range of shear and diffusion parameters. Also, since deterministic differential equations are easier to simulate than stochastic differential equations, the Langevin equation method presented in this work is more efficient and less computationally intensive than Brownian dynamics simulations.

We derive the Langevin equations governing the orientations of the particles in the suspension and evolve a procedure for obtaining the equation of motion for any orientation moment. A computational technique is described for simulating the orientation moments dynamically from a set of time-averaged Langevin equations, which can be used to obtain the moments when the governing equations are harder to solve analytically. The results obtained using this method are in good agreement with those available in the literature.

The above computational method is also used to investigate the effect of rotational Brownian motion on the rheology of the suspension under the action of an external force

field. The force field is assumed to be either constant or periodic. In the case of constant external fields earlier results in the literature are reproduced, while for the case of periodic forcing certain parametric regimes corresponding to weak Brownian diffusion are identified where the rheological parameters evolve chaotically and settle onto a low dimensional attractor. The response of the system to variations in the magnitude and orientation of the force field and strength of diffusion is also analyzed through numerical experiments. It is also demonstrated that the aperiodic behaviour exhibited by the system could not have been picked up by the diffusion equation approach as presently used in the literature.

The main contributions of this work include the preparation of the basic framework for applying the Langevin method to standard flow problems, quantification of rotary Brownian effects by using the new method, the paired-moment scheme for computing the moments and its use in solving an otherwise intractable problem especially in the limit of small Brownian motion where the problem becomes singular, and a demonstration of how systems governed by a Fokker-Planck equation can be explored for possible chaotic behaviour.

Contents

List of figures	iii
List of tables	v
1 Introduction	1
1.1 Overview	1
1.2 Introduction to suspension rheology	7
1.2.1 Dilute suspension of ellipsoids	8
1.2.2 Rotary Brownian diffusion	10
1.2.3 The material functions	13
1.2.4 External Forcing	14
1.3 Introduction to stochastic processes	16
1.3.1 The theories of Brownian motion	16
1.3.2 Stochastic processes—general theory	18
1.3.3 Stochastic differential equations	20
1.4 Introduction to Chaos theory	24
1.4.1 Dynamical systems	24
1.4.2 Chaos and its implications	27
1.4.3 Detecting and characterising chaos	31
1.4.4 Experimental study of chaos	36
1.4.5 Attractor reconstruction	37

2	The Basic equations	39
2.1	The assumptions of the model	40
2.2	The dynamics of force-free particles	41
2.3	The diffusion equation approach	44
2.4	An outline of the new approach	49
2.5	A comparison of the different methods	51
3	The Langevin approach	53
3.1	The spherical Harmonics	53
3.2	The dynamics of the spherical harmonics	55
3.2.1	From the diffusion equation	55
3.2.2	The Coffey <i>et al.</i> method	60
3.2.3	From the Langevin equation	61
4	Computation of moments	66
4.1	The dynamics of the moments	66
4.2	The computation of moments	69
4.3	Results and discussion	72
5	Rheology and external forcing	76
5.1	The effect of the external field on particle orientation	77
5.2	The stress tensor	79
5.3	The stress coefficients	80
5.4	Material functions for dilute suspension	82
6	Periodic forcing and chaos	88
6.1	The dynamics of periodically forced fibres	89
6.2	The simulation of the bulk properties	90
6.3	Analysis of the time series	92

Contents

iii

6.4 Other Orientations	102
7 Conclusions	108
7.1 Summary	108
7.2 Future work and applications	110
A Program listing	113
B Notes on notation	129

List of figures

1.1	(a) The bifurcation diagram for the logistic map; (b) The strange attractor of the Lorenz system	30
2.1	(a) A Schematic of the co-ordinate system and the orientation vector. (b) The profile of the flow.	42
4.1	The discretization of the $\theta\phi$ space.	71
4.2	Plot of the orientation moments vs. Péclet number. The symbols are the results from the finite difference method and the spherical harmonics method.	74
5.1	The stress coefficients	82
5.2	Plot of intrinsic viscosity $[\eta_1]$ for dipolar suspensions for various strengths of the external field, for spheroids of aspect ratio $r=0.4, 1.0$ and 1.6 . Results for $\mathbf{k} \parallel (0, 1, 1)$ and $\mathbf{k} \parallel (0, 1, 0)$ are shown. Compare with fig. 2 of Strand and Kim (1992)	86
5.3	Plot of intrinsic viscosity $[\eta_1]$ for dipolar suspensions for various values of Pe , for spheroids of aspect ratio $r=0.4, 1.0$ and 1.6 . Results for $\mathbf{k} \parallel (0, 1, 1)$ and $\mathbf{k} \parallel (0, 1, 0)$ are shown. Compare with fig. 3 in Strand and Kim (1992).	87
6.1	A part of the time series of $[\eta_2]$ for $\tilde{P}e = 0.01, k_1 = k_3 = 0, k_2 = 0.1$ and $\omega = 1$	93

6.2	Plot of the power vs. frequency of $[\eta_2]$. The figure is typical of both chaotic and linear stochastic signals	93
6.3	Fraction of false nearest neighbors as a function of the embedding dimension m for the $[\eta_2]$ series.	95
6.4	Three-dimensional embedding of the attractor of $[\eta_2]$ reconstructed from the time series with delay 15 and $m = 3$	96
6.5	Plot of $\ln C(m, \epsilon) / \ln \epsilon$ vs. ϵ . The convergence of the curves for large m indicates low dimensionality.	97
6.6	The functions $S(\epsilon, m, \Delta n)$ vs. Δn for various embedding dimensions. The curves are approximately linear with an overall slope of 0.04. . . .	98
6.7	Three-dimensional embedding of the attractors reconstructed from the time series of $[\eta_2]$ for $Pe = 0.01$, $k_1 = k_3 = 0$ and various values of k_2 ; (a) $k_2 = 0.3$, (b) $k_2 = 0.42$, (c) $k_2 = 0.5$ and (d) $k_2 = 1.0$	100
6.8	Three-dimensional embedding of the attractors reconstructed from the time series of $[\eta_2]$ for $k_2 = 0.1$, $k_1 = k_3 = 0$ and various values of $\tilde{P}e$; (a) $\tilde{P}e = 0.0$, (b) $\tilde{P}e = 0.1$ and (c) $\tilde{P}e = 1.0$	101
6.9	Poincaré section of the attractor of $[\eta_2] \times [\tau_1]$ for $\tilde{P}e = 0.01$, $k_2 = 0.1$, $k_1 = k_3 = 0$	103
6.10	Three-dimensional embedding of the attractors reconstructed from the time series of $[\eta_1]$ and $[\tau_1]$ for $k_1 = k_2 = 0$, $k_3 = 1.0$ and various values of $\tilde{P}e$; (a) & (d) $\tilde{P}e = 0$; (b) & (e) $\tilde{P}e = 0.1$; (c) & (f) $\tilde{P}e = 1.0$	104
6.11	Three-dimensional embedding of the attractors reconstructed from the time series of $[\eta_2]$ and $[\tau_1]$ for $k_1 = 0$, $k_2 = k_3 = 0.1$ and various values of $\tilde{P}e$; (a) & (d) $\tilde{P}e = 0$; (b) & (e) $\tilde{P}e = 0.01$; (c) & (f) $\tilde{P}e = 0.1$	106
6.12	Three-dimensional embedding of the attractors reconstructed from the time series of $[\eta_1]$ and $[\tau_1]$ for $k_3 = 0$, $k_1 = k_2 = 0.1$ and various values of $\tilde{P}e$; (a) & (d) $\tilde{P}e = 0$; (b) & (e) $\tilde{P}e = 0.01$; (c) & (f) $\tilde{P}e = 0.1$	107

List of tables

4.1	The functions for generating moments	72
4.2	The steady state values of the moments for various initial conditions at different values of Pe	73
4.3	Time taken(in seconds) to compute the moments on a 500MHz, 128 RAM, Pentium III PC for two different pairs at various Pe	74
5.1	The limiting values of the stress coefficients.	81
5.2	The various moments in the expressions for the rheological parameters and the corresponding noise terms	85
6.1	The estimated Lyapunov exponents and approximate correlation dimensions of the attractors in fig. 6.11	103
6.2	The estimated Lyapunov exponents and approximate correlation dimensions of the attractors in fig. 6.12	105

Introduction

1.1 Overview

In this work we study the orientation dynamics and rheological properties of orientable particles suspended in a simple shear flow using a novel computational technique based on an extension of the traditional Langevin equation formalism. The particles are assumed to possess a dipole moment in which case an external force field can influence their orientation behaviour. The study will be limited to dilute suspensions only, implying that particle-particle interactions are neglected. The thrust of the analysis will be in the use of the Langevin method for including the effects of rotational Brownian motion in both the dynamics and the rheology of the suspension and exploring how Brownian diffusion affects the orientational as well as viscometric properties of the suspension.

Suspensions are two phase systems consisting of discrete solid particles distributed in a continuous fluid medium. Common examples of this include industrial slurries, cements, ceramics, paints, printing inks, drilling muds and many processed foods. Of particular importance to our study are suspensions of orientable particles, in which the orientations of the particles are as important a factor affecting the bulk suspension properties as their nature and spatial distribution. There are many areas in engineering, industry and natural phenomena that benefit from the study of such systems. Physi-

cal properties of heterogeneous media like composites, metal alloys, polymer solutions, electro-rheological fluids etc. are greatly influenced by the properties of the constituent materials and their internal distribution. The analysis of these systems from seemingly disparate fields can be greatly simplified by studying them in a general framework of suspensions of (possibly) dipolar particles in a shearing motion subject to an external force field, and this study has led to a unified understanding of a wide range of phenomena. In turn, the results obtained from such analyses have been useful in developing new suspensions with desired properties, new products and devices making use of the understanding gained by such analyses, new methods to characterise suspensions etc. (eg. magnetofluidization (Buevich *et al.*, 1984), magnetostriction of ferromagnetic particle suspensions (Ignatenko *et al.*, 1984), characterisation of magnetorheological suspensions (Cebers, 1993), bio-convection set-up by swimming of certain micro-organisms (Pedley and Kessler, 1990; Almog and Frankel, 1998)).

A complete knowledge of the rheology of the suspensions is desirable in the manufacturing of suspensions of industrial importance. Determining the rheological properties through experiments is prone to many artefacts and instrumental errors which are difficult to remove, particularly when the particle size is small. Numerical simulation is the preferred procedure in this case since errors caused by the deficiency of measurement techniques or unavoidable defects in the material or flow conditions can be eliminated in simulations. Also, simulations offer enough flexibility to mimic approximately any experimental set up by adding desired effects or removing unwanted ones. Experiments using conventional rheometers cannot often unravel the source of the many types of complex behaviour observed in suspensions. Hence the emphasis in our study is on devising appropriate tools for simulating the rheological properties efficiently, in the presence of Brownian motion and additional effects due to shear and external force.

If the particles are dipolar, an external force field that interact with the dipole moments of the particles imparts an additional rotational torque besides the torque due

P40

S

to shear. Further, if the particle size is comparatively small, the effects of Brownian rotations set in that tend to disorient the particles in a random manner. The interplay between these forces can become quite complicated, particularly in parameter regimes where the magnitudes of these forces are comparable. If the external force is periodic, the dynamics and the rheology can sometimes exhibit complex behaviour. Ramamohan *et al.* have studied extensively suspensions of periodically driven dipolar spheroids in the limit of negligible or zero Brownian motion and demonstrated the existence of parametric regimes where both the rotational dynamics and the intrinsic suspension properties evolve chaotically (Ramamohan *et al.*, 1994; Kumar *et al.*, 1995; Kumar and Ramamohan, 1995; Kumar *et al.*, 1996). A new type of class-I intermittency route to chaos has also been shown to exist in the system they studied (Kumar and Ramamohan, 1997), thus providing an example of a physically realizable system showing a non-hysteretic form of class-I intermittency. Further, a new and easy to implement chaos control algorithm was developed, which leads to a very efficient scheme for separating particles (Kumar and Ramamohan, 1998), and to a technique of controlling chaotic rheological parameters, so that they can be made to oscillate in a desired periodic orbit (Kumar, 1997). The micro-particle suspension they studied is also one of the few examples of a physically realizable system showing spatio-temporal chaos and non-trivial collective behaviour (Radhakrishnan *et al.*, 1999). The system is therefore important, both from a theoretical as well as a practical point of view. In this work we shall extend the applicability of the results of Ramamohan *et al.* to a wider class of suspensions by incorporating the effects of Brownian diffusion into the study.

The role of Brownian motion is prominent in many real suspensions. Experimental studies conducted on various systems also point to the importance of Brownian motion; theoretical predictions made in the absence of Brownian diffusion are largely unsupported by experimental results. Previous studies on Brownian particles in suspensions have been mostly based on the diffusion equation approach in which the orientation distribution of the particles is described in terms of an equation (the diffusion equation) for

the spatio-temporal evolution of an appropriate density function for orientations, called the orientation distribution function (ODF). Due to the difficulty of solving the diffusion equation, various numerical techniques have been used to approximate the solution, each of which may be valid for only a small range of the parameters corresponding to shear, diffusion or external fields. Further, as observed by Kumar and Ramamohan (1995), the diffusion equation approach used by Strand (1989) and Strand and Kim (1992), based on the expansion of the ODF into series of spherical harmonics, is generally invalid in regimes where the system exhibits chaotic behaviour. Hence we use in this work an alternate strategy, a generalised Langevin equation method, based on the work of Coffey *et al.* (1996) on non-linear systems with noise. In this approach the focus is on the equations for the orientations of the individual particles in the suspension rather than on the statistical distribution of the orientations. These equations, called Langevin equations, are stochastic differential equations containing a noise term arising from the random fluctuations in the orientations due to Brownian effects.

The success of the Langevin method depends largely on determining the exact form of the noise term and this may be achieved by comparing an ensemble of the Langevin equations with the diffusion equation of the system. In our problem this is done by specializing to the case of non-dipolar particles free of external forcing, and requiring that the Langevin equations and the diffusion equation give rise to the same dynamical relations for spherical harmonics. This noise term can then be used in the general case involving dipolar particles under external forcing by applying the principle of superposition which is valid since the diffusion equation is linear in the ODF. The direct simulation of the Langevin equations, as done in Brownian dynamics simulations, is generally difficult and prone to errors due to the presence of the noise term with statistically determined properties. Instead, in our method, proper time averaging of the Langevin equations leads to deterministic equations for the evolution of orientation averages which do not contain terms of the orientation distribution function. This dispenses

-p < 6
 $\psi(\omega)$
 $= \gamma(\omega)$

with the need to solve the diffusion equation and hence the diffusion equation can be completely bypassed. The moment equations are generally hard to solve analytically, but are suitable for simulation with minor modifications. We present a brute-force computational technique for generating the moments dynamically in appropriately chosen pairs. This scheme turns out to be faster and more efficient than other known computational methods and provides a unified framework for analysing the system for all ranges of the shear and Brownian parameters and for more general systems. In the case of non-dipolar orientable particles and dipolar particles under a constant, time independent external field, we reproduce certain results already known in the literature.

In the presence of an oscillatory force field, the Langevin method is the ideal tool to extend the analyses made by Ramamohan *et al.* to a more general setting that includes the diffusive effects of Brownian motion. In this case we demonstrate the interesting result that the rheological parameters may evolve chaotically even in the presence of a Brownian force, though the effects of diffusion apparently need to be relatively weak for this to occur. The chaotic attractor in this case is, however, low-dimensional, so the system behaviour can be described using a few independent variables. As the magnitude of the diffusion term increases, the attractor gradually becomes a limit cycle through the quasi-periodic route. Similar behaviour is observed when the magnitude of the force field changes; the system reverts to regular behaviour as the strength of the force field is increased. Results for many different orientations of the external field are presented and the changes in the complexity of the system behaviour for variations in the intensity of the external field are analysed through phase space plots. These analyses pertain to the region of relatively weak Brownian motion where the problem becomes singular in the limit and is rendered intractable by other methods. The suitability of this method for analysing complex system responses is brought out by showing that the diffusion equation method of Strand and Kim (1992) would not have picked up the behaviour we have observed in these range of parameters.

P102

Organization of the thesis

The thesis consists of 7 chapters.

The first chapter contains introductions to the various topics covered in this thesis. A review of the literature in suspension rheology is included with emphasis on the areas particularly relevant to us. The Langevin equation approach presented in this work builds upon some recent developments in the theory of stochastic processes, hence an introduction to this subject is given. The fluctuations in the time series generated by the methods developed in this work are further analysed using tools of nonlinear dynamics and chaos theory. Hence an introduction to chaos theory is also included in this chapter.

The basic equation for the orientation dynamics of spheroids suspended in a simple shear flow is obtained for the zero diffusion case in Chapter 2 based on the analysis of Strand and Kim (1992). The different approaches to modeling the effects of Brownian rotation are discussed. An overview of the generalised Langevin equation method along with its merits is also described in this chapter.

The contribution from Brownian diffusion on the orientational motion of the particle is considered in Chapter 3. The Langevin equation governing the particle orientation is derived by modifying the equation obtained in Chapter 2 for the deterministic case using a novel theory for nonlinear systems with noise presented by Coffey *et al.* (1996).

A method for computing the orientation moments using the Langevin equations is described in Chapter 4. A few of the orientation moments thus computed are compared with the results from other methods which show remarkable agreement.

Chapter 5 generalises the results of the previous chapters to the case of dipolar suspensions subject to an external force field. The apparent viscosity is computed for several orientations of the force field and various strengths of the external field and compared with known results.

Chapter 6 analyses the dynamics of the rheology in oscillating external force fields. The presence of chaos is demonstrated for a set of parameters corresponding to weak

diffusion. The variations in the topological properties of the attractor of the system in response to changes in the strengths of the force field and degree of diffusion are also presented in this chapter.

Conclusions and future work are the contents of Chapter 7.

We have also included two appendices in which the source code of the program used in the computations (Appendix A) and the list of notations used in this thesis (Appendix B) are listed.

The list of publications which resulted from the work presented in the thesis is attached at the end of the thesis.

1.2 Introduction to suspension rheology

A systematic theoretical study of suspensions of particles in fluids can be considered to have started with the seminal work of Einstein on Brownian motion (Einstein, 1906, 1911). Brownian motion is the irregular and random fluctuations of tiny particles suspended in a fluid, first noticed by the botanist Robert Brown while observing a suspension of pollen grains in water. Further experiments conducted by Brown confirmed that these fluctuations were not caused by the presence of any organic molecules, and this opened up the possibility of a physical explanation for the phenomenon. Einstein based his analysis of Brownian motion on the kinetic theory of fluids and conjectured that it was caused by the bombardment of the suspending particles by the fluid molecules which are always in a state of incessant motion, according to kinetic theory. Starting from these assumptions and using concepts from probability theory he proceeded to calculate the effective viscosity of the suspension. Einstein's theory laid the foundations for stochastic modeling and analysis of random processes and also served as a maiden support for kinetic theory.

1.2.1 Dilute suspension of ellipsoids

There are a number of practical situations where suspensions of a more general nature than those studied by Einstein have to be considered. This warrants considering additional effects that can influence both the dynamics of individual particles and bulk suspension properties. For example, if the suspending medium is sheared, the resulting flow field influences both the local orientations of the particles and their relative positions in the medium. Hydrodynamic interactions among particles, caused by the disturbance that the presence of each particle produces on its neighbours, is another factor that becomes important in concentrated solutions with larger volume fraction of particles. Interactions are, however, neglected in sufficiently dilute suspensions which are characterised by the limit $nl^3 \ll 1$ where n is the number of particles per unit volume and l is the linear dimension of the particles. If the particles have electric or magnetic charges, as in ferromagnetic particles immersed in a ferrofluid, an external electric or magnetic field can affect the local microstructure. The shape of the particles is also important; for example, non-spheres have definite orientation effects unlike spheres, and long fibres usually behave differently from ellipsoids. There are quite a number of studies in the literature incorporating one or more of these factors, but most of the theoretical work is in dilute suspensions in Newtonian fluids. Newtonian fluids have fairly simple flow equations and are characterised by a linear relationship between shear stress and rate of strain.

The starting point of most of these investigations is the classic work of Jeffery (1922) that describes the creeping motion of rigid, non-Brownian spheroids in an incompressible, Newtonian fluid subjected to a simple shear with flow field given by $\mathbf{v} = \dot{\gamma}y\mathbf{i}$ where $\dot{\gamma}$ is the shear rate, y the y -coordinate and \mathbf{i} the unit vector in the x -direction. The rotation of an ellipsoidal particle can be described by a pair of equations for the evolution with time of the polar angle θ and azimuthal angle ϕ of a unit vector \mathbf{u} placed along the axis

of symmetry of the particle (Jeffery, 1922; Leal and Hinch, 1971):

$$\begin{aligned}\frac{d\theta}{dt} &= \frac{\dot{\gamma}}{4} \left(\frac{r^2 - 1}{r^2 + 1} \right) \sin 2\theta \sin 2\phi \\ \frac{d\phi}{dt} &= \frac{\dot{\gamma}}{r^2 + 1} (r^2 \cos^2 \phi + \sin^2 \phi)\end{aligned}\tag{1.1}$$

Above, r is ratio of the the polar to equatorial radii of the ellipsoid, called the *aspect ratio*. The solutions θ and ϕ of the above equations are given by

$$\begin{aligned}\tan \theta &= \frac{Cr}{\sqrt{r^2 \cos^2 \phi + \sin^2 \phi}} \\ \tan \phi &= r \tan \left(\frac{\dot{\gamma}}{r + r^{-1}} + k \right)\end{aligned}$$

The constant C is called the orbit constant which, as well as the constant k , depends on the initial orientation of the spheroid. Several conclusions can be drawn from the above equations immediately. Each spheroid rotates about the z -axis with a period $(2\pi/\dot{\gamma})(r + 1/r)$ and its end describes a symmetric ellipse in orientation space (called the Jeffery Orbit). The Jeffery orbit of a given spheroid is completely determined by its initial orientation and its future life is confined to that orbit alone. Thus in the absence of diffusion and interactions, the long term particle configuration depends solely on the initial orientations and never attains a steady state. This means that the effective viscosity and the stress in a suspension of many such particles will vary periodically in a manner dictated by the initial conditions of the particles. Jeffery's equations are not restricted to spheroids alone; in fact, as shown by Bretherton (1962), the motion of any axi-symmetric particle is governed by the same equations with the aspect ratio r replaced by an effective aspect ratio r_e for the axi-symmetric particle.

Experimental studies have also been taken up by a number of investigators in fiber suspensions of varied concentrations both to observe the orientation distributions and to measure various rheological properties (Anczurowski and Mason, 1967; Folgar and Tucker, 1984; Stover *et al.*, 1992). A typical experimental setup for the study of orientations consists of a Couette device to generate a nearly simple shear flow in which

a large number of identical opaque particles are immersed, whose projections on to the flow-vorticity plane can be studied from photographs. Anczurowski and Mason (1967) observed cylindrical fibres with an aspect ratio $r = 18.4$ for concentration levels $n l^3 = 0.016, 0.066$ and 0.266 and measured the distribution $f(C)$ of orbit constants in each case. Folgar and Tucker (1984) and Stover *et al.* (1992) report experiments on semi-dilute suspensions in which C -distributions and ϕ -distributions were measured. A summary of these experiments and the inferences thereof can be found in Zirnsak *et al.* (1994). The principal fact emerging from these observations is that while at small concentrations the particles follow Jeffery orbits, at higher concentrations they rapidly forget the initial conditions and settle down to steady distributions, unlike predicted by Jeffery. The cause of this phenomenon of fading memory exhibited by real suspensions has been attributed to many factors such as particle interactions, polydispersity, non-uniformity of the flow field and Brownian diffusion which were all neglected in Jeffery's analysis (Hur, 1987). For example, Leal and Hinch (1971) showed that the action of even very weak Brownian rotation can yield in the long time limit an equilibrium distribution for the orientation of the particles that does not depend on the initial orientation state of the suspension. This implies that rotary Brownian motion, even if weak, has significant effects, in that it causes oscillations to die out in the long run.

1.2.2 Rotary Brownian diffusion

The effect of Brownian rotation is important in suspensions of orientable particles of comparatively smaller size. If interactions and other body forces are not present, the configuration of the suspension microstructure is determined by a competition between rotational fluxes due to the imposed flow and rotary Brownian motion, the former tending to orient the particles in preferred directions and the latter tending to disorient them in a random fashion. The relative importance of these fluxes is expressed in terms of the dimensionless quantity $Pe = \dot{\gamma}/Dr$ where D_r is the rotary diffusivity of the particle.

In the presence of random orientational effects due to Brownian motion, the orientation vector can be considered a time dependent stochastic variable, with a probability density $\psi(\mathbf{u}, t)$ of orientations, called the orientation distribution function (ODF). The collective variation with time of all the particles in the suspension is usually expressed as an evolution equation for ψ . This is basically a convection-diffusion equation, variously referred to as the diffusion equation or the Fokker-Planck equation, and has the general form

$$\frac{\partial \psi}{\partial t} + \frac{\partial}{\partial \mathbf{u}} \cdot (\dot{\mathbf{u}} \psi) = 0. \quad (1.2)$$

The diffusion equation is related to the dynamics of individual particles through the equation of motion for \mathbf{u} , which is a modified form of the Jeffery equations (1.1), with a general form given by;

$$\dot{\mathbf{u}} = f(\mathbf{u}, \mathbf{E}, \mathbf{\Omega}, k_i) - D_r \nabla(\log \psi).$$

The random effects due to Brownian motion is accounted for by the last term, while the deterministic effects are lumped together in the first term on the right which depends on the rate of strain tensor \mathbf{E} , the vorticity tensor $\mathbf{\Omega}$ and on other micro-mechanical parameters k_i contributed by external forces, electric or magnetic charges on the particles etc.

The theories for the macroscopic parameters of microstructured fluids relate the state of stress at a material point in the flow to the distribution function ψ , through various orientation moments of the distribution function. The orientation moment $\langle f(\mathbf{u}) \rangle$ of a function $f(\mathbf{u})$ is evaluated thus:

$$\langle f(\mathbf{u}) \rangle = \int f(\mathbf{u}) \psi \, d\mathbf{u}$$

where the integration is over the entire orientation space. The principal difficulty with this method is that we need to compute the distribution function ψ at each material point in the suspension for which the diffusion equation (1.2) must be solved. This is a non-trivial task since solving the diffusion equation in its full generality is difficult; in

particular, there exist no analytical solutions for the diffusion equation in simple shear flow. Most of the analyses, therefore, use some numerical scheme to approximate the ODF for certain ranges of flow and microstructure and under appropriate boundary conditions (Hinch and Leal, 1972, 1976; Strand and Kim, 1992; Kumar and Ramamohan, 1995; Chen and Koch, 1996; Chen and Jiang, 1999).

There are also a few techniques that do not require solving the diffusion equation to compute the rheological parameters. One method is to obtain the evolution equations for the moments directly from the diffusion equation by suitable averaging, and then attempt to solve these equations instead of the diffusion equation. In a general flow problem, this often leads to a closure problem; for example, the evolution equation for the second moment $\langle uu \rangle$ involves the fourth moment $\langle uuuu \rangle$, and that of the fourth moment involves the sixth moment and so on. This difficulty is circumvented by using approximations to the moments, called closure approximations, at some level of the higher order moment hierarchy. The closure approximations can be avoided in a few models (Lipscomb, 1986; Lipscomb *et al.*, 1988; Szeri and Lin, 1996), but for the vast majority of practical problems these approximations remain relevant and continue to evoke interest in the literature (Advani and Tucker, 1987, 1990; Cintra and Tucker, 1995; Han and Im, 1999). Useful reviews of the closure problem can be found in Barthés-Biesel and Acrivos (1973), Tucker (1991), Szeri and Leal (1992) and Advani and Tucker (1987, 1990). A second method to compute moments is due to Szeri and Leal (1992, 1994) and uses a doubly Lagrangian representation of the distribution function which leads to significant simplifications of the Brownian diffusion terms and the subsequent moment calculation.

In this work we develop yet another method for computing the moments without having to solve the full Fokker-Planck equation. This is based on a generalised Langevin equation method presented by Coffey *et al.* (1996) for non-linear systems with noise, and expresses the evolution of moments in terms of suitable time averages of the orientation

vectors over a set of sharp starting values. This formalism allows for an easy computational procedure for generating the moments dynamically by simulating a set of tracer orientational vectors.

1.2.3 The material functions

For a fluid in shearing motion the stress is defined as the force per unit area and is considered distributed continuously throughout the continuous medium. It is represented by a second order tensor having, in general, nine components representing the nine combinations of the three force components acting on three surface components at a given point. In simple shear, the stress tensor σ depends only on the shear rate $\dot{\gamma}$ and the viscosity η_s of the fluid;

$$\begin{pmatrix} \sigma_{xx} & \sigma_{xy} & \sigma_{xz} \\ \sigma_{yx} & \sigma_{yy} & \sigma_{yz} \\ \sigma_{zx} & \sigma_{zy} & \sigma_{zz} \end{pmatrix} = \begin{pmatrix} -p & \eta_s \dot{\gamma} & 0 \\ \eta_s \dot{\gamma} & -p & 0 \\ 0 & 0 & -p \end{pmatrix}.$$

The stress tensor in this case is symmetric. The components σ_{xx} , σ_{yy} and σ_{zz} are the *normal stresses* and are usually considered in pairwise differences, $\tau_1 = \sigma_{xx} - \sigma_{zz}$, $\tau_2 = \sigma_{yy} - \sigma_{zz}$, to eliminate the dependence on the pressure p , and the quantities τ_1 and τ_2 are called *normal stress differences* and have value zero in the case of simple shear. In the presence of particles under the action of an external field the stress tensor may no longer be symmetric, except for dilute suspensions of spheres in which case the average suspension behaviour is commonly measured in terms of the intrinsic viscosity

$$[\eta] = \lim_{\Phi \rightarrow 0} \frac{\sigma_{xy} - \eta_s \dot{\gamma}}{\Phi \eta_s \dot{\gamma}}.$$

Einstein estimated that $[\eta] = 2.5$ for a dilute suspension of spheres. For suspensions of force-free orientable particles σ_{xy} and σ_{yx} are identical but τ_1 and τ_2 may be different and non-zero. More generally, in the case of dilute suspensions of dipolar particles, σ_{xy} and σ_{yx} may also be different from each other and hence four different viscometric

functions are required to characterise the bulk properties in simple shear, viz.,

$$\begin{aligned} [\eta_1] &= \lim_{\Phi \rightarrow 0} \frac{\sigma_{xy} - \eta_s \dot{\gamma}}{\Phi \eta_s \dot{\gamma}}, & [\eta_2] &= \lim_{\Phi \rightarrow 0} \frac{\sigma_{yx} - \eta_s \dot{\gamma}}{\Phi \eta_s \dot{\gamma}}, \\ [\tau_1] &= \lim_{\Phi \rightarrow 0} \frac{\sigma_{xx} - \sigma_{zz}}{\Phi \eta_s \dot{\gamma}}, & [\tau_2] &= \lim_{\Phi \rightarrow 0} \frac{\sigma_{yy} - \sigma_{zz}}{\Phi \eta_s \dot{\gamma}}. \end{aligned}$$

Normal stresses for incompressible fluids are generally very small at equilibrium and bear a quadratic dependence on shear rate. The second normal stress difference is usually found to be negative and is about one tenth of the first in magnitude. However, a departure from this behavior has been observed for suspensions of dipolar particles under periodic external forcing (Kumar and Ramamohan, 1995). Brenner (1974) gives an extensive tabulation of the viscometric functions for the dilute suspension of ellipsoids of several aspect ratios. At small shear rates the suspension is nearly Newtonian with a modified viscosity which depends mainly on the shape of the particles. For smaller shear rates in which Brownian motion is nonetheless dominant, $[\eta]$ depends linearly on Pe .

1.2.4 External Forcing

If the particles in a suspension are dipolar, i.e. have electric or magnetic charges on them, the presence of an external electric or magnetic field can influence the local fluid structure. While suspensions in the absence of external forcing have been extensively studied, only a relatively few investigations are available for the case of dipolar particles and most of the later analyses are restricted to the limit of weak shear. The earliest of these studies were of Hall and Busenberg (1969) and Brenner (1970), concerning dilute suspensions of dipolar non-Brownian spheres. Brenner and Weissman (1972) extended these studies incorporating Brownian diffusion effects, and obtained results mainly for particles that are spheres or near-spheres. Further extensions analysing the effects of various relative strengths of shear, diffusion and external force on the particle dynamics and rheology are available (Jansons, 1983; Pedley and Kessler, 1990; Salueña *et al.*, 1994;

Smith and Bruce, 1979), but most of these apply to the limit of weak shear. Strand and Kim (1992) considered dilute dipolar suspensions for a wider range of shear and diffusion parameters, and analysed the rheology for various orientations of the external force. They used an expansion of the ODF into a series of surface spherical harmonics and applied the Galerkin method to an appropriately truncated form of the series. The numerical scheme, however, fails due to poor convergence of the series in regimes where the ODF has steep gradients, and is not valid in regimes where the ODF may have subharmonic periodicity or when the underlying dynamics is chaotic (Kumar and Ramamohan, 1995). Almog and Frankel (1998) furnished analytical results for moderate values of Pe , the analysis being limited to the case of weak rotary diffusion. The generalised Langevin method which we develop in this work, unlike previous studies, is not limited to any range of diffusion or advection.

Oscillatory dynamics of rheological averages may result from oscillatory shear or external fields. Oscillations resulting from time dependent shear fields have been studied by many (Leal and Hinch, 1972; Bird *et al.*, 1971, 1987), though oscillatory force fields have been considered only by a few investigators including Strand (1989) and Ramamohan *et al.*. Strand (1989) followed the diffusion equation approach, but this is not general enough to study complex system responses like chaotic behaviour, as discussed by Kumar and Ramamohan (1995). The possibility of chaotic behaviour in the orientation dynamics and rheology was demonstrated by Ramamohan *et al.* in a series of papers (Ramamohan *et al.*, 1994; Kumar *et al.*, 1995; Kumar and Ramamohan, 1995; Kumar *et al.*, 1996). This opened up a new range of possibilities like novel routes to chaos (Kumar and Ramamohan, 1997), computer controlled intelligent rheology (Kumar, 1997), efficient particle separation in suspensions (Kumar *et al.*, 1995) and an option to use dipolar particle suspensions as a paradigm for studying spatio-temporal chaos (Radhakrishnan *et al.*, 1999). This work is a generalisation of the studies by Ramamohan *et al.* to the case of systems in which Brownian motion is important.

1.3 Introduction to stochastic processes

Roughly speaking, a dynamical system whose behavior exhibits fluctuations due to the influence of some random force in the system is called a stochastic system. The process defining the system, called a stochastic process, may be modeled by a collection of time-dependent random variables. One of the most important examples of stochastic processes is the Brownian motion of tiny particles suspended in a fluid. There are numerous natural phenomena that lend themselves to stochastic modeling, a comprehensive description of which may be found in van Kampen (1981), Chandrasekhar (1943) and Coffey *et al.* (1996).

1.3.1 The theories of Brownian motion

A systematic study of stochastic processes began with the fundamental work of Einstein on Brownian motion (Einstein, 1906, 1926), the observed erratic motion of tiny particles suspended in a fluid. Einstein's analysis of Brownian motion is based on the assumption that although the exact position of any particle at any instant may be indeterminate due to the random nature of Brownian fluctuations, the shift in particle positions might obey some frequency rule, so it can be analysed using tools of probability theory. Using a series of arguments combining physical intuition with mathematical theory, Einstein arrived at a partial differential equation for the spatio-temporal variation of the density function $f(x, t)$ for the number of particles per unit volume at position x and time t ;

$$\frac{\partial f}{\partial t} = D \frac{\partial^2 f}{\partial x^2}$$

This equation is known as the *diffusion equation* and the constant D is the diffusion coefficient. The constant D was obtained using the kinetic theory of fluids, according to which the molecules in the fluid are always in an agitated state executing random motion, and the Brownian motion, according to Einstein, is the result of these molecules colliding with the suspension particles. Thus at equilibrium the Maxwell-Boltzmann

distribution of particles must set in. This, together with Stoke's law for the viscous drag on a spherical particle of radius r , gives (Einstein, 1926)

$$D = \frac{kT}{6\pi\eta r\nu} \quad (1.3)$$

The validity of this expression was verified experimentally by Perrin (Nelson, 1967). Many topics related to stochastic processes, such as the Chapman–Kolmogorov equation, the Fokker–Planck equation, the Kramers–Moyal expansion etc. all have their root in the pioneering work of Einstein.

Some time after Einstein presented his work (1908), Langevin presented an alternate approach, quite different from Einstein's and, according to him, "infinitely simpler". According to him the force acting on a Brownian particle of mass m can be resolved into two parts: (i) a regular part, which is the viscous drag on the particle, given by $-6\pi\eta r\nu$ where r is the radius of the spherical particle and ν its speed and (ii) a fluctuating part $\Gamma(t)$ resulting from the random collisions of the particles by the fluid molecules (Lemons and Gythiel, 1997). This gives an unusual differential equation for the position x of the particle containing a random function,

$$m \frac{d^2x}{dt^2} = -6\pi\eta r\nu \frac{dx}{dt} + \Gamma(t). \quad (1.4)$$

The properties of the fluctuating part $\Gamma(t)$ were specified in terms of an ensemble of such particles:

- (a) $\Gamma(t)$ is independent of the position x of the particle, so the ensemble average of the quantity $\Gamma(t)x$ over a large number of particles is zero; $\langle \Gamma(t)x \rangle = 0$.
- (b) $\Gamma(t)$ varies extremely rapidly compared to the variation in x and is positive and negative with equal probability, so $\langle \Gamma(t) \rangle = 0$.

Using these properties and results from statistical mechanics, Langevin derived the the same expression, eq. (1.3), for the diffusion coefficient which Einstein obtained through other means.

Eq. (1.4) is an example of a stochastic differential equation, a differential equation containing a noise term, with properties determined only in terms of moments of ensembles.

1.3.2 Stochastic processes—general theory

A *Stochastic process* is a random variable ξ whose density function is parametrised in time. Thus for two instances t_1 and t_2 , $\xi(t_1)$ and $\xi(t_2)$ are in general two different random variables. Hence the stochastic process ξ may be thought of as a family $\{\xi(t) : t \in T\}$ of random variables with time t belonging to an index set T . The random variable $\xi(t)$ can also be a multivariate process, $\xi(t) = \{\xi_1(t), \xi_2(t), \dots, \xi_n(t)\}$, where the components $\xi_j(t)$ are themselves random variables.

A stochastic process $\xi(t)$ is, in fact, a function of two arguments, $\{\xi(t, \omega); t \in T, \omega \in \Omega\}$, where Ω is the sample space. For a fixed t , $\xi(\omega)$ is a family of random variables, called an *ensemble*, and for a fixed ω , $x(t)$ is a function of time and is called a *sample*.

For a given division $t_1 < t_2 < \dots < t_n$ of T , the stochastic process $\xi(t)$ is completely determined by an infinite sequence $P = P_1, P_2, \dots$ of conditional probability density functions. The first of these is $P = P_1(x, t|x_1, t_1)$, which is such that the probability of finding $\xi(t)$ between x and $x + dx$ given that $\xi(t_1) = x_1$ for any $t_1 \leq t$, is $P_1(x, t|x_1, t_1) dx$. Similarly $P_n = P_n(x, t|x_n, t_n; x_{n-1}, t_{n-1}; \dots; x_1, t_1)$ is such that

$$\begin{aligned} P_n(x, t|x_n, t_n; x_{n-1}, t_{n-1}; \dots; x_1, t_1) dx \\ = \text{Prob}\{\xi(t) \in [x, x + dx) \text{ given that } \xi(t_j) = x_j, \quad j = 1 \text{ to } n\}. \end{aligned}$$

Any joint probability pertaining to the random process $\xi(t)$ can be evaluated in terms of one or more of the above conditional probabilities. Thus, for example, if $\xi(t_0) = x_0$, the joint probability that $\xi(t_1)$ will be within dx_1 of x_1 and then, at a later time t_2 , $\xi(t_2)$ will be within dx_2 of x_2 is given, according to the multiplication rule for probabilities, by

$$P_1(x_1, t_1|x_0, t_0) dx_1 \times P_2(x_2, t_2|x_1, t_1; x_0, t_0) dx_2$$

The requirement that an infinite number of conditional probabilities be specified to determine a stochastic process at a given set of instances can be simplified significantly for a class of processes known as *Markovian*.

A stochastic process is said to be Markovian if each function P_n coincides with P_1 according to

$$P_n(x, t|x_n, t_n; \dots; x_1, t_1) = P_1(x, t|x_n, t_n) \quad (t_n \leq t \text{ for } n = 1, 2, \dots)$$

This means that the conditional probability P_n depends only on the most recent observation x_n at t_n and is independent of the past history of the process prior to t_n . This is often referred to as the “memorylessness” of the Markov process. Thus a Markov process is completely determined by the transition probabilities $P(x, t|x_1, t_1) = P_1(x, t|x_1, t_1)$. The transition probabilities themselves satisfy the *Chapman–Kolmogorov* equation,

$$P(x_3, t_3|x_1, t_1) = \int P(x_3, t_3|x_2, t_2)P(x_2, t_2|x_1, t_1) dx_2$$

for $t_3 > t_2 > t_1$ (van Kampen, 1981; Gardiner, 1985; Gillespie, 1996a,b). The Chapman–Kolmogorov relation, in principle, computes the transition probabilities $P(x, t|x_1, t_1)$ for any $t > t_1$ but, this being an integral equation, is in practice difficult to solve. However, for a Markov process that is continuous in time, i.e. for which the density function $P(x, t)$ is a continuous function of the parameter t , a partial differential equation can be derived for the transition probabilities under some simplifying assumptions. This equation, called the *Fokker–Planck equation*, is the time evolution equation for the transition probability $p(x, t|x_0, t_0)$, given $\xi(t_0) = x_0$ and has the general form (van Kampen, 1981; Gardiner, 1985; Gillespie, 1996b)

$$\frac{\partial}{\partial t} P(x, t|x_0, t_0) = -\frac{\partial}{\partial x} [A(x, t)P(x, t|x_0, t_0)] + \frac{1}{2} \frac{\partial^2}{\partial x^2} [D(x, t)P(x, t|x_0, t_0)] \quad (1.5)$$

where the coefficients $A(x, t)$ and $D(x, t)$ can be computed from the change in x and its mean square over small time Δt thus:

$$\begin{aligned} A(x, t) &= \lim_{\Delta t \rightarrow 0} \frac{1}{\Delta t} \langle x(t + \Delta t) - x(t) | \xi(t) = x \rangle, \\ D(x, t) &= \lim_{\Delta t \rightarrow 0} \frac{1}{\Delta t} \langle (x(t + \Delta t) - x(t))^2 | \xi(t) = x \rangle. \end{aligned} \quad (1.6)$$

If the process has evolved a long time after the initial transience we may replace $P(x, t|x_0, t_0)$ in the above by $P(x, t)$.

The Fokker–Planck equation serves as an approximate description for any Markov process ξ whose individual jumps are small. It is easier to set up since it requires only the knowledge of the functions $A(x, t)$ and $D(x, t)$ which in any stochastic process can be determined with a minimum detailed knowledge about the underlying mechanisms thanks to the expressions (1.6). For this reason most of the stochastic systems in physical applications are studied through an appropriate Fokker–Planck equation. The literature on the Fokker–Planck equation is vast and its applications diverse (see Risken, 1984)

If $P(x, t)$ is a solution of the Fokker–Planck equation the moments of any function h with respect to the random process $\xi(t)$ can be obtained as $\langle h(x) \rangle = \int h(x)P(x, t)dx$.

Even though the Fokker–Planck equation is easier to set up and more convenient than the Chapman–Kolmogorov function, it is still difficult to solve in its full generality for the vast majority of physical systems for which it has been set up. For some simple cases, it can nevertheless be rigorously solved as, for example, when $A = 0$ and $D = 1$ in (1.5). The solution of the corresponding Fokker–Planck equation

$$\frac{\partial}{\partial t}P(x, t|x_0, t_0) = \frac{1}{2} \frac{\partial^2}{\partial x^2}P(x, t|x_0, t_0)$$

is called the Wiener Process. It can be shown that the Wiener process is a Gaussian process with statistically independent increments having a sharp initial distribution that spreads in time and non-differentiable sample paths (Gardiner, 1985). The Wiener process is fundamental to the study of diffusion processes.

1.3.3 Stochastic differential equations

A stochastic differential equation is a differential equation whose coefficients are random numbers or random functions of the independent variable, such that the ensemble of solutions to the equation constitute a stochastic process. The most important examples

of stochastic differential equations are the Langevin equations given by

$$\frac{d\xi}{dt} = A(\xi, t) + B(\xi, t)\Gamma(t) \quad (1.7)$$

where A and B are quantities depending on the physics of the process and $\Gamma(t)$ is a normal random process (Gaussian) with mean zero and autocorrelation proportional to a delta function;

$$\langle \Gamma(t) \rangle = 0$$

$$\langle \Gamma(t)\Gamma(t') \rangle = D \delta(t - t')$$

The Langevin equation generally represents a stochastic process that is continuous in time and is Markovian. The average properties of Γ signify the nature of the noise as an external force; it is irregular taking positive and negative values with equal probability and its effects are practically instantaneous and temporally uncorrelated. The Gaussian nature of Γ serves to determine the hierarchy of moments of $\Gamma(t)$ —all odd moments are zero and all even moments are expressed in terms of the second moment. A $\Gamma(t)$ defined in this way is called *Gaussian white noise* (van Kampen, 1981).

If the term B multiplying $\Gamma(t)$ is a constant, the Langevin equation (1.7) is said to possess additive noise and if B depends on ξ the noise is said to be multiplicative. If the noise is additive and A is linear, the stochastic system which the Langevin equation represents is linear and is non-linear otherwise.

For linear systems, the Langevin equations furnish an alternate description of the system completely equivalent to the Fokker–Planck equation representation. More precisely, the Langevin equation

$$\dot{\xi} = k\xi + \Gamma(t)$$

with Gaussian white noise $\Gamma(t)$ represents the same Markov process as the Fokker–Planck equation (van Kampen, 1981)

$$\frac{\partial P}{\partial t} = -k \frac{\partial}{\partial x}(xP) + \frac{D}{2} \frac{\partial^2 P}{\partial x^2}$$

Non-linear systems with multiplicative noise, however, need to be treated with much more care. Such equations suffer from an interpretation problem, arising from the presence of multiplicative noise. To see this, we first note that the existence of a stochastic differential equation such as (1.7) with Gaussian white noise, is itself questionable on strict mathematical grounds. Thus, for example, if a solution ξ of equation (1.7) is to exist, the right side must be integrable which requires that $\int B(\xi, t)\Gamma(t)dt$ exist and, in particular, for $B = 1$ the integral $u(t) = \int \Gamma(t)$ exist. If $u(t)$ is to be continuous as ordinary integrals are, it turns out that $u(t)$ is a Wiener process (Gardiner, 1985) and is as such not differentiable. This then means that the Langevin equation (1.7) does not exist. However, as demonstrated by Doob (1953, 1954), a more consistent interpretation can be given using the integral equation corresponding to (1.7), viz.,

$$\xi(t) - \xi(0) = \int_0^t A[\xi(s), s]ds + \int_0^t B[\xi(s), s]\Gamma(s)ds \quad (1.8)$$

provided we designate the integral of $\Gamma(t)$ as a Wiener process $W(t)$ and replace $\Gamma(t)dt$ in the above by the differential of $W(t)$ (Gardiner, 1985),

$$dW(t) = W(t + dt) - W(t) = \Gamma(t)dt.$$

The second integral in eq. (1.8) then becomes

$$\int_0^t B[\xi(s), s]\Gamma(s)ds = \int_0^t B[\xi(s), s]dW(s).$$

In the above dW is the differential of a random process and this causes some interpretation problems for the last integral. This stochastic integral is defined as the (mean square) limit of partial sums thus

$$\int_0^t B[\xi(s), s]dW(s) = \text{ms} \lim_{n \rightarrow \infty} \left[\sum_{i=1}^n B(\tau_i) [W(t_i) - W(t_{i-1})] \right] \quad (1.9)$$

where $t_0 \leq t_1 \leq \dots \leq t_{n-1} \leq t$ is a partition of the interval $[0, t]$ and τ_i is an arbitrary point with $t_{i-1} \leq \tau_i \leq t_i$. This limit, however, depends on the choice of the intermediate point τ_i (Gardiner, 1985) and consequently, for each such choice, we get a different value

for the integral in (1.9). In particular, the integral in eq. (1.9) with $\tau_i = t_{i-1}$ is called the *Ito stochastic integral* and with $\tau_i = (t_{i-1} + t_i)/2$ it is called the *Stratonovich stochastic integral*. The Stratonovich integrals behave like ordinary Riemann-Stieltjes integrals while Ito integrals follow different integration rules, the so called Ito calculus.

The different interpretations to the Langevin equation (1.7) in the non-linear case lead to different Fokker-Planck equations also, unlike in the linear case. For example, the non-linear Langevin equation

$$\frac{d\xi}{dt} = A(\xi) + B(\xi)\Gamma(t), \quad (1.10)$$

interpreted as a Stratonovich integral, is equivalent to the Fokker-Planck equation (van Kampen, 1981)

$$\frac{\partial P}{\partial t} = -\frac{\partial}{\partial x}[A(x) + \frac{D}{2}B(x)B'(x)]P + \frac{D}{2}\frac{\partial^2}{\partial x^2}[B(x)]^2P$$

Interpreted as an Ito integral, (1.10) is equivalent to (van Kampen, 1981)

$$\frac{\partial P}{\partial t} = -\frac{\partial}{\partial x}A(x)P + \frac{D}{2}\frac{\partial^2}{\partial x^2}[B(x)]^2P$$

The Ito calculus is commonly chosen on certain mathematical grounds since rather general results of probability theory can be applied. On the other hand, since white noise is an idealisation of physical noise with short autocorrelation time, the Stratonovich calculus is usually preferred in physical applications since the corresponding results are generally identical to those obtained from systems with finite autocorrelation time, in the limit of zero correlation time (Risken, 1984)

Coffey *et al.* (1996) have recently presented an extension of the traditional Langevin equation method to non-linear systems with noise. This method is based on the interpretation of the Langevin equation (1.7) as an integral equation in the sense of Stratonovich, which leads to a useful result that the time-averaged Langevin equation can be expressed as an equation of motion for the sharp starting values. This leads to deterministic differential equations governing the evolution of the various moments of the stochastic

variable describing the system. This is the approach we adapt in this work to study a standard problem in suspension rheology. A brief description of the Coffey *et al.* method is given in section 3.2.2

1.4 Introduction to Chaos theory

Chaos theory has emerged as one of the most important breakthroughs of this century. Roughly, chaos is the complex behaviour exhibited by some deterministic non-linear systems commonly perceived as simple and well-behaved. An exposure of what is today called chaos was initially made by the meteorologist Lorenz (1963) who found that the solution of a set of three coupled ordinary differential equations exhibited irregular and aperiodic fluctuations that never settled down to equilibrium or to a periodic state. Moreover, if he started his simulations from two slightly different initial conditions, the resulting behaviours would soon become different. Yet when the solutions were plotted in three dimensions the resulting set had a definite structure. By a careful analysis of this set through computer simulations, Lorenz was able to demonstrate that it was, in fact, an infinite complex of surfaces, an example of what is called a fractal today. Other milestones in the development of chaos theory include the analysis of turbulence in fluids by Ruelle and Takens (1971), the studies by Hénon (1976) and Rössler (1976) of the “stretching and folding” mechanism behind chaotic dynamics, the work of May (1976) on the complicated dynamics in some simple population models and the discovery by Feigenbaum (1978) of the universal scaling properties in one-dimensional maps.

1.4.1 Dynamical systems

A system that changes with time is called a dynamical system. A dynamical system is mathematically described by a state vector \mathbf{x} , which determines the state of the system at any instant, and a function $f(\mathbf{x})$ that provides the rule to determine the state of the system at the next instant given the current state. Systems which change continuously

with time are usually described by a differential equation of the form

$$\dot{\mathbf{x}} = \frac{d\mathbf{x}}{dt} = f(\mathbf{x}) \quad (\mathbf{x} \in \mathbb{R}^n) \quad (1.11)$$

and systems that change its state at discrete instances of time are expressed in terms of an iterated map

$$\mathbf{x}_{n+1} = f(\mathbf{x}_n), \quad (n = 1, 2, \dots), \quad (1.12)$$

where $\mathbf{x}_n \in \mathbb{R}^n$ denotes the state of the system at the n -th instant. Here \mathbb{R}^n is called the *state space* or *phase space* of the system. These equations then describe the future states of the system completely once an initial condition is prescribed. Since we will be mainly concerned with systems governed by differential equations our discussion will be mostly around continuous systems.

The traditional method of analysing such systems was by solving equations (1.11) or (1.12) for a given initial condition to express the state $\mathbf{x}(t)$ or \mathbf{x}_n in terms of certain known functions. However, this is almost always impossible given the complicated form the function f takes in most physical problems. The famous three-body problem, for example, was proved to defy any analytical solution in the sense of obtaining explicit formulas for the motion of the three bodies. It was Poincaré who changed this point of view in the late 1800s and demonstrated that although analytical solutions may not be obtained, useful insights into the long term behaviour of such systems can be derived using powerful geometrical approach. This approach of treating dynamical systems gained recognition since then and was further reinforced by Van der Pol, Andronov, Littlewood, Levinson, Smale, Lorenz etc. A good account of these developments as well as an introduction to the subject can be found in Guckenheimer and Holmes (1983), Ott (1993), Strogatz (1994), Alligood *et al.* (1997) and Lakshmanan and Rajasekhar (2003)

Depending on whether or not the right hand side of the equations (1.11) or (1.12) contains the time variable t explicitly, the system is called non-autonomous or autonomous respectively. An n -dimensional non-autonomous system can be written as

an $(n + 1)$ -dimensional autonomous system by introducing a new variable $x_{n+1} = t$, so that $\dot{x}_{n+1} = 1$, and rewriting the system equation in terms of $\mathbf{y} = (\mathbf{x}, x_{n+1})$ (Alligood *et al.*, 1997). A broad division of the subject of dynamical systems would be into *linear* and *nonlinear* systems. The essential difference between them is that a linear system can be analysed by decomposing it into smaller parts, studying each component separately and then recombining (the principle of superposition), while a nonlinear system cannot be analysed in this manner. Most physical systems are by nature nonlinear and the geometric approach initiated by Poincaré is the ideal way to study such systems.

Attractor

The simplest of all possible solutions of the system (1.11) or (1.12) are *fixed points* and *periodic solutions*. A fixed point of the system is a solution satisfying $\dot{\mathbf{x}} = 0$ and corresponds to an equilibrium state of the system. A solution $\mathbf{x}(t)$ of eq. (1.11) such that $\mathbf{x}(t + T) = \mathbf{x}(t)$ for some period T of time is called a periodic solution and corresponds to a closed curve in the phase space. A discrete system, eq. (1.12), is periodic if \mathbf{x}_n repeatedly takes on a finite set of values in a specific order for all values of n . An isolated periodic solution is also called a *limit cycle*. In the geometric approach we consider many solutions of (1.11) at once, not just a single solution, and try to discover patterns in the solutions. A solution of eq. (1.11) can be thought of as tracing out a curve in the phase space passing through that point as $t \rightarrow \infty$, called a *trajectory* or an *orbit*. The collection of all trajectories starting from an open connected set of initial conditions is usually called a *flow*.

Physical systems may be classified as either *conservative* or *non-conservative*. In non-conservative systems the volume of any subset of the phase space spanned by the flow contracts as the system evolves forward in time. Such systems with phase space contraction are commonly characterised by the presence of *attractors*. An attractor (repeller) is a specific subset A of the phase space which is reached asymptotically as $t \rightarrow \infty$ ($t \rightarrow -\infty$) by the flow of the system over an open set B of initial conditions; the

set B is then called the *basin of attraction*. See Guckenheimer and Holmes (1983) for the subtleties involved in defining an attractor.

The possible attractors for a linear system are fixed points or closed curves in the space space (Nayfeh and Balachandran, 1995; Glendinning, 1994). Similarly, the famous *Poincaré–Bendixson theorem* asserts that bounded two-dimensional flows, even when non-linear, can have only fixed points and limit cycles as attractors (Strogatz, 1994; Alligood *et al.*, 1997)

In higher dimensions, however, the attractors of non-linear systems can take on many intricate structures and may exhibit quite unusual dynamics. The simplest of them all, besides fixed points and limit cycles, are k -periodic quasi-periodic solutions which result from k incommensurate frequencies active in the systems, i.e., k frequencies f_1, f_2, \dots, f_k such that

$$\sum n_i f_i = 0 \implies n_i = 0 \quad (n_i \text{ integers}).$$

The k -period quasi-periodic solutions lead to an attractor which is a k -torus. A 2-torus in a 3-dimensional space resembles a doughnut. All these attractors correspond to regular motion, while aperiodic or chaotic dynamics may lead to much more complex attractors, the so called strange attractors.

1.4.2 Chaos and its implications

A striking feature of some dynamical systems is that the trajectories on the attractor may exhibit *sensitive dependence on initial conditions*. This means that trajectories starting from neighbouring initial conditions may separate from each other at an exponential rate, evolving independently of each other and in an apparently uncorrelated manner after a sufficiently long period of time, and yet remain confined to a bounded subset of the phase space. While exponential divergence of orbits in a flow is possible even in linear systems (eg. $\dot{x} = x$), the possible convergence of such a flow to a bounded region of the phase space is a feature unique to nonlinear systems.

Chaos is the bounded aperiodic behaviour in a deterministic system that shows sensitive dependence on initial conditions.

There are many subtleties in the definition of chaos and there is as yet no universally accepted definition except perhaps for one-dimensional maps (Devaney, 1989; Banks *et al.*, 1992; Touhey, 1997). Given above is a working definition that identifies chaos from its features. “Deterministic” means that the apparent complexity in the system is not due to any stochastic effects such as noise. By “aperiodic long term behaviour” it is meant that there are trajectories which do not settle down to a fixed point or a periodic or quasi-periodic state. The term chaos is reminiscent of the intricate dynamics experienced by the trajectories on the attractor; the exponential divergence stretches the flow as it evolves in time, which is then folded back to remain confined to a finite region of the phase space. The attractor is the result of these sequences of stretching and folding repeated indefinitely. Thus while the dynamics on the attractor may be quite complex, the attractor as a whole maintains some definite structure.

The attractors for a linear system are fixed points and limit cycles (Alligood *et al.*, 1997; Strogatz, 1994; Glendinning, 1994) and hence there is no possibility of chaos. The Poincaré–Bendixson theorem rules out chaos in two-dimensional (autonomous) flows. Thus a necessary condition for continuous nonlinear autonomous systems to be chaotic is that they must be at least 3-dimensional and for non-autonomous systems they must be at least 2-dimensional. As for discrete systems, chaos is known to exist even in one-dimensional non-invertible maps (eg. the logistic map (Alligood *et al.*, 1997; Strogatz, 1994)) and two-dimensional invertible maps (eg. the Hénon map (Hénon, 1976)). This means that even simple non-linear systems with very few degrees of freedom can be chaotic. A good example is the logistic map given by

$$x_{n+1} = rx_n(1 - x_n), \quad 0 \leq x_n \leq 1 \quad (n = 1, 2, \dots). \quad (1.13)$$

which is known to be chaotic for certain ranges of values of r . Fig. 1.1 (a) shows the attractor of the logistic map for various values of r . For smaller values of r the attractor is

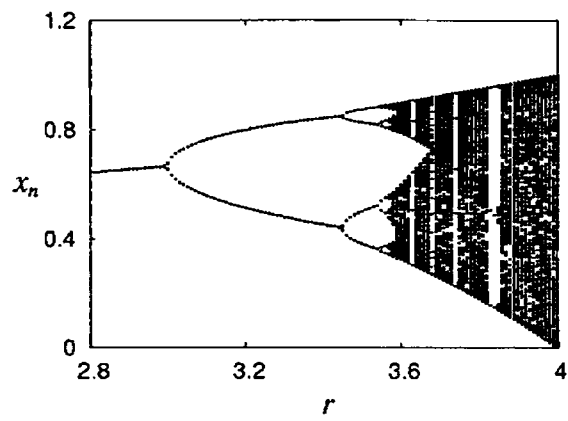
a fixed point and as r is increased the attractors also change to periodic orbits of different periods and finally at $r > 3.57$, the system becomes chaotic and the set of points visited by the attractor becomes a dense subset of the set $[0, 1]$. Similarly the Lorenz system defined by

$$\begin{aligned} \dot{x} &= \sigma(y - x) \\ \dot{y} &= rx - y - xz \\ \dot{z} &= xy - bz \end{aligned} \tag{1.14}$$

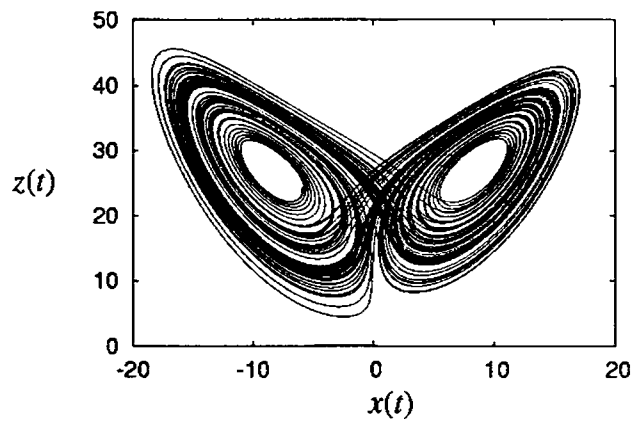
where $\sigma, r, b > 0$ are the parameters, is another example of a simple system which is chaotic for $\sigma = 10, b = 8/3$ and $r = 28$ (Lorenz, 1963). Fig. 1.1 (b) shows the attractor of the system for these values of the parameters.

The development of chaos theory has important theoretical as well as philosophical implications. With the recognition of the possibility of chaos, the difference between stochastic systems and complex deterministic systems has blurred. Earlier, an observed complexity in the response of a system used to be dubbed as either due to the presence of some external noise or due to the system having many degrees of freedom. With the advent of chaos theory it has become clear that even simple systems with very few degrees of freedom can be chaotic and hence exhibit behaviour reminiscent of stochastic processes.

Chaotic systems, even though deterministic, are unpredictable beyond a reasonable period of time due to the sensitivity of the system to initial conditions. This is due to the fact that no instrument can in practice measure the initial data with infinite precision, and any error in the initial condition, however small, will be amplified by the system by many orders of magnitude due to the exponential divergence of trajectories. Hence the state of the system as predicted based on the erroneous initial condition will be far from, and may have absolutely no correlation with, the actual state of the system after sufficiently long time. For example, one reason the various mathematical models of weather are unable to make accurate predictions beyond a period of a few days is currently attributed to a possible chaos in the system.



(a)



(b)

Figure 1.1: (a) The bifurcation diagram for the logistic map; (b) The strange attractor of the Lorenz system

1.4.3 Detecting and characterising chaos

In general it is hard to establish the existence of chaos analytically, particularly for continuous systems defined by differential equations. Instead, one tries to identify in the system various characteristics of chaotic dynamics using tools such as Poincaré section, power spectrum, Lyapunov exponents etc. with the help of computer simulations. These tools cater to the geometric approach mentioned earlier, and can be applied to non-linear systems in general, not just to chaotic systems.

Poincaré map

The Poincaré map is a classical device for analysing dynamical systems. The basic idea behind this technique, introduced by Poincaré, is to replace the flow of an n -dimensional continuous time system by an $n - 1$ dimensional discrete time system. Let Σ be an $(n - 1)$ dimensional surface in the phase space transverse to the flow of the system (1.11). If Σ is properly chosen a given trajectory in the flow will cross the surface repeatedly as $t \rightarrow \infty$. Let \mathbf{y}_k and \mathbf{y}_{k+1} be the points on Σ where the trajectory crosses it the k -th and $(k + 1)$ -th time. Since the point \mathbf{y}_{k+1} can in principle be obtained by solving the system (1.11) with \mathbf{y}_k as initial condition, \mathbf{y}_{k+1} is uniquely determined by \mathbf{y}_k and this defines a map

$$\mathbf{y}_{k+1} = P(\mathbf{y}_k), \quad (k = 1, 2, \dots)$$

which is the Poincaré map. In a non-autonomous system the function f is usually periodic in time with some period T and a Poincaré map is obtained by recording the snapshots of the trajectory at regular time intervals of length T . A periodic orbit may cross the surface a finite number of times before closing on itself and hence the Poincaré map will contain utmost a finite number of points in this case. For a quasi-periodic solution, the discrete points in the Poincaré map usually fall on a closed curve in Σ . A Poincaré section with a continuum of points may be an indication of chaos.

A construction analogous to the Poincaré section was used by Lorenz (1963) to reduce a three dimensional continuous system to a one dimensional discrete system. If $m_n(t)$ denote the n -th maximum of the function $z(t)$ in the solution of the Lorenz system eq. (1.14), the plot of m_{n+1} versus m_n falls nearly on a curve. A good deal of information about the Lorenz attractor can be extracted from the dynamics of the map defined by this curve (Lorenz, 1963; Strogatz, 1994). A similar technique has been used in analysing the Rössler system (Rössler, 1976).

Power spectrum

The time evolution of a dynamical system is represented by the time variation $x(t)$ of its dynamical variables. If $x(t)$ is periodic, under certain conditions (Arfken and Weber, 1995), it can be represented as a superposition of oscillations whose frequencies are integer multiples of a basic frequency (Fourier theorem). When f is not periodic it can be represented in terms of oscillations with a continuum frequencies and this is called the Fourier transform of $x(t)$, given by

$$a(\omega) = \frac{1}{2\pi} \int_{-\infty}^{\infty} f(t)e^{i\omega t} dt.$$

The real-valued function $P(\omega) = |a(\omega)|^2$ is called the power of the signal $x(t)$. The entire range of $P(\omega)$ for various values of ω is called the *power spectrum* and is commonly exhibited as a plot of $P(\omega)$ versus ω . The spectrum of a periodic function will contain only discrete spikes corresponding to the basic frequency and its integral multiples, and that of a quasi-periodic function will also contain numerous spikes, but not necessarily spaced at integral multiples of any particular frequency (Schuster, 1988; Nayfeh and Balachandran, 1995).

The power spectrum of any dynamical variable of a chaotic system will be broadband and continuous. The spectrum of random motions such as noise may also have a continuous broadband character, but chaotic motion can be distinguished from noise using tools such as dimension estimates and Lyapunov exponents.

Lyapunov exponents

Lyapunov exponents are dynamical invariants of an attractor which measure the average rate of divergence or convergence of neighbouring trajectories on the attractor in various directions. Let \mathbf{x}_0 be any point on the basin of attraction and consider an infinitesimal sphere of perturbed initial conditions. This sphere distorts into an ellipsoid as the system evolves in time (Alligood *et al.*, 1997). Let $\epsilon_k(t)$, $k = 1, 2, \dots, n$ denote the length of the k -th principal axis of the ellipsoid. In general we can write $\epsilon_k(t) = \epsilon_k(0)e^{\lambda_k t}$ where the λ_k s may be positive zero or negative, and are called the *Lyapunov exponents*. The existence of at least one positive Lyapunov exponent is the most striking signature of chaos in the system. In such a system the growth of the separation $\delta(t)$ between two neighbour trajectories will be eventually dominated by the maximum Lyapunov exponent λ , so that $\|\delta(t)\| = \|\delta(0)\|e^{\lambda t}$ and hence

$$\lambda = \lim_{t \rightarrow \infty} \frac{1}{t} \ln \frac{\|\delta(t)\|}{\|\delta(0)\|}$$

In practice one computes λ by plotting $\ln \delta(t)$ versus t , which should fall nearly on a straight line, the slope of which then gives an estimate of λ . The Lyapunov exponent of a discrete system can be described along similar lines with slight modifications (Alligood *et al.*, 1997). Analytic computation of Lyapunov exponents is generally difficult and many algorithms have been proposed for computing them numerically for known dynamical systems which, when combined with the technique of attractor reconstruction, can be used to extract Lyapunov exponents from time series (Wolf *et al.*, 1985; Eckmann *et al.*, 1986; Bryant *et al.*, 1990; Parlitz, 1992; Kantz, 1994).

Attractor dimension

The flow of a dissipative system should eventually fall on a manifold and occupy zero volume in the n -dimensional phase space, and if the system is chaotic, exponential divergence causes repeated stretching and folding within the attractor (Hénon, 1976; Rössler,

1976). This usually gives the attractor a self-similar structure, so repeatedly zooming in on any part of the attractor reveals the same structure but at a finer scale. Self-similar objects are commonly characterised by a fractional dimension, but this requires a generalisation of the Euclidean definition of dimension. Sets with fractional dimension are called *fractals* and if the fractal is also the attractor of a dissipative system it is called a *strange attractor*. Fractals need not always arise as attractors of chaotic systems, they may be generated using purely mathematical constructions also, eg. the Cantor set and von Koch curve (Strogatz, 1994).

The *box-counting(capacity) dimension* is the simplest extension of the Euclidean concept of dimension that applies to fractals and strange attractors as well. Let S be a subset of \mathbb{R}^n and $N(\epsilon)$ be the minimum number of n -dimensional cubes of side ϵ needed to cover S . The dimension d of the set is found to scale like a power law, $N(\epsilon) \propto \epsilon^{-d}$, even for fractals for which, however, d may not be an integer. The limiting value of d as $\epsilon \rightarrow 0$ is the box counting or capacity dimension:

$$d = \lim_{\epsilon \rightarrow 0} \frac{\ln N(\epsilon)}{\ln(1/\epsilon)}, \quad \text{if the limit exists.}$$

According to this definition a line and plane have capacity dimensions 1 and 2 respectively. The capacity dimension of the Cantor set is $\ln 2 / \ln 3$ (Strogatz, 1994).

The capacity dimension does not take care of a possible inhomogeneity of the attractor, it treats the dense and rare parts of the attractor equally. Grassberger and Procaccia (1983) introduced a more efficient approach which has now become the standard. This begins by defining the *correlation sum* $C(\epsilon)$ as the probability that a pair of points chosen randomly on the attractor is separated by a distance less than ϵ . The correlation dimension, denoted by D_2 , is empirically found to scale as $C(\epsilon) \propto \epsilon^{D_2}$ and hence is defined as

$$D_2 = \lim_{\epsilon \rightarrow 0} \frac{\ln C(\epsilon)}{\ln \epsilon}.$$

Any given trajectory in a chaotic attractor comes arbitrarily close to any point on the attractor arbitrarily often if it is observed for sufficiently long time. Hence in practice one records a single trajectory of finite length L on the attractor at N equally spaced discrete times x_i and approximates $C(\epsilon)$ by

$$C(N, \epsilon) = \frac{2}{N(N-1)} \sum_i \sum_j \Theta(\epsilon - \|x_i - x_j\|)$$

where $\Theta(x) = 1$ for $x > 0$ and $\Theta(x) = 0$ for $x \leq 0$ (Kantz and Schreiber, 1997). In the limit $L, N \rightarrow \infty$, $C(N, \epsilon) \rightarrow C(\epsilon)$. The correlation dimension estimated by Grassberger and Procaccia (1983) for the Lorenz attractor is 2.05 ± 0.01 . A marked advantage of the correlation dimension is the comparative ease with which it can be computed, particularly for time series data.

Routes to chaos

The onset of chaos in a system can be viewed as a transition from a periodic or equilibrium state through a series of qualitative changes in the dynamics as one or other control parameter is varied. A qualitative change in the dynamics as a system parameter is changed is called a *bifurcation*. For example, fig. 1.1 (a) shows that the attractor of the logistic map undergoes a series of *period doubling bifurcations* before entering the chaotic state. This is an example of a *period doubling route* to chaos. The Rössler system and the Lorenz system are other examples of systems showing period doubling route to chaos for certain ranges of parameters (Sparrow, 1982; Olsen and Degn, 1985). The B–Z reaction (*cf.* sec. 1.4.4) also takes this route to chaos (Simoyi *et al.*, 1982; Roux *et al.*, 1983).

The bifurcation points a_1, a_2, \dots in the logistic map exhibit a striking limiting behaviour. If $\rho = (a_n - a_{n-1})/(a_{n+1} - a_n)$, then $\lim_{n \rightarrow \infty} \rho_n = \delta$ where $\delta = 4.66920$. This was discovered by Feigenbaum (1978, 1979) who found that this number is *universal* in that all unimodal maps undergoing period-doubling route to chaos have this limiting

property giving the same value for δ . A fuller discussion of this quantitative universality can be found in Feigenbaum (1980) and Schuster (1988).

A second route to chaos, the *quasi-periodic route*, is usually associated with Hopf bifurcations which involve the generation of a limit cycle from a fixed point with a change in parameter. Landau (1944) suggested that the chaotic state associated with turbulence in liquids is approached through an infinite sequence of Hopf bifurcations. A modification of this model suggested by Newhouse *et al.* (1978) shows that after three Hopf bifurcations regular motion becomes highly unstable in favour of motion on a strange attractor. The later theory is also supported by some experimental results (Nayfeh and Balachandran, 1995).

The third widely known route to chaos is *intermittency* which is the occurrence of fluctuations that alternate randomly between long periods of nearly regular behaviour and short irregular bursts. The frequency and density of chaotic bursts increase with the control parameter, presenting a continuous route from regular to chaotic behaviour. A detailed study of the theory of intermittency can be found in Pomeau and Manneville (1980).

1.4.4 Experimental study of chaos

Chaotic behaviour occurs in a great number of engineering, experimental and natural systems. Hao (1990) presents a detailed list of the experimental study of chaos in various areas of applied and natural sciences.

Following the works of Belousov and Zhabotinsky, it has been known for a long time that certain chemical reactions, now known as *B-Z reactions*, exhibit oscillations before reaching equilibrium (Field and Burger, 1985). Roux *et al.* (1983) demonstrated that a properly “driven” B-Z reaction, in which reactants are constantly pumped in to compensate for the loss due to reaction, may exhibit chaos for certain ranges of the control parameter which in this case was the rate of input of reactants.

The Rayleigh–Bénard convection is also widely known for the presence of chaos in the movement of convection rolls in a fluid confined between thermally conducting plates and heated up in a controlled manner, when the temperature difference in the system crosses a threshold value (Libchaber *et al.*, 1982).

The Chua circuit (Chua *et al.*, 1986; Madan, 1993) is a nonlinear electronic system exhibiting a rich variety of bifurcations and chaos. This is also the first physical system where theoretical results agree well with computer simulations and experiments.

Lasers provide a typical class of potentially chaotic nonlinear oscillator systems (Weiss and Kische, 1984; Weiss and Brock, 1986). Chaos in optical systems has been reviewed by Harrison and Biswas (1986).

Examples of non-autonomous systems showing chaotic fluctuations can be found among forced non-linear oscillators. For example, the driven double-well oscillator is a well studied system showing a rich variety of dynamics (Moon and Holmes, 1979).

Some of the reviews of observed chaos in other areas include Lauterborn and Parlitz (1988)(acoustic chaos), Beasley and Huberman (1982) and Pederson (1988) (Chaos in Josephson junctions), Schaffer (1985) (chaos in ecology), Olsen and Degn (1985) (chaos in biological systems)

1.4.5 Attractor reconstruction

There are many occasions when we are limited to making a sequence of measurements of one or more observables, while the exact dynamics of the system which cause the observables to vary may not be known or too difficult to determine. For example, the population of different species in a given ecosystem, the air temperature and pressure at specified geographical locations, or the density of traffic at several positions on a motorway are dynamic observables which can be measured without being certain about the underlying dynamics. In such cases one can reconstruct the unknown system from a sequence of measurements of just a single observable, using a technique known as *delay*

reconstruction of the attractor, first suggested by Packard *et al.* (1980) and successfully used by many others. The embedding theorems of Takens (1981), and its extensions (Sauer *et al.*, 1991; Sauer and Yorke, 1993) elucidate the mathematical theory behind delay reconstruction. Roughly, the embedding theorems assert that for deterministic systems, the dynamics of the n -dimensional state vector $\mathbf{x}(t)$ can be recaptured from the dynamics of the delay vectors of a single scalar function of \mathbf{x} , $y(t) = h(\mathbf{x}(t))$, under rather general conditions. The mapping

$$\Phi(\mathbf{x}(t)) = (y(t), y(t + \tau), \dots, y(t + (m - 1)\tau)),$$

which maps \mathbf{x} to an m -dimensional delay vector with delay τ , is an embedding when $m \geq 2n + 1$. This means that most of the significant characteristics of the original system, both dynamical and geometrical, are carried over to the reconstructed phase space in a one-to-one manner (Kantz and Schreiber, 1997; Ott *et al.*, 1994). In particular, properties such as the fractal dimension, Lyapunov exponents and entropies are preserved under the reconstruction map Φ and can be computed from the mirror dynamical flow in the reconstructed space. There exist further generalizations which serve to reduce the bound on the embedding dimension, and in many cases the smallest integer greater than the correlation dimension is enough to fully embed the attractor (Sauer *et al.*, 1991; Sauer and Yorke, 1993).

The success of delay reconstruction depends on choosing the embedding dimension m and the delay τ suitably. There are many subtleties involved in this which will be discussed in greater detail in Chapter 6.

The Basic equations

In this chapter we introduce the problem studied in this work and present the basic assumptions made of the system to build an appropriate mathematical model. The basic equations governing the dynamics of the system are derived for a simple special case which will be extended to more general systems in subsequent chapters. These extensions arouse several theoretical as well as practical questions as to the suitability of the various methods used to model such systems. These points are discussed and an overview of the novel approach which we adopt to analyse the system is also given in this chapter.

We propose to extend the theoretical studies of Ramamohan *et al.* on the dynamics and rheology of dilute suspensions of dipolar particles in a simple shear flow by incorporating the additional effects of rotary Brownian motion which were neglected in their work. They had identified certain parametric regimes where both the orientation dynamics and the bulk orientation averages exhibited chaotic fluctuations (Ramamohan *et al.*, 1994; Kumar and Ramamohan, 1995; Kumar *et al.*, 1995). It was noted (Kumar and Ramamohan, 1995) that the diffusion equation approaches commonly used to solve similar problems were inadequate to capture a possible chaos in the system. Hence in generalising their analysis to suspensions of smaller particles in which Brownian motion is significant, we require that the resulting model should be general enough to pick up

possible chaos in the modified system also and suitable for investigating the effects of Brownian diffusion on chaos in the system. The generalised Langevin equation method which we use in this work is suitable in this respect and has several merits over the traditional diffusion equation method as discussed in sec. 2.5

The traditional method for studying Brownian effects is through the modifications to the orientation distribution function obtained as a solution of a modified diffusion equation. We shall, in subsequent sections, outline this approach and discuss the difficulties associated with it. The Langevin approach we follow in this work, allows for a direct simulation of the various orientation moments without having to solve the diffusion equation.

2.1 The assumptions of the model

We shall model a suspension of Brownian spheroids in a fluid medium subjected to a simple shear flow, using a generalised Langevin equation method advocated by Coffey *et al.* (1996). No restriction is made about the strength of either the flow field or of the diffusion and the results we present are, in principle, true for an arbitrary range of Péclet number (Pe). We develop a technique for computing the various orientation moments of the suspension and then extend it to the case of driven systems in which an external force influences the particle dynamics and the rheology. The external force considered can be constant or periodic in time and it is assumed that the suspending fluid is unaffected by the action of this field on the particles. The following are some of the further assumptions made, in order to make the problem tractable to mathematical analysis.

The suspending medium is an infinite incompressible isothermal Newtonian fluid. The particles are identical, rigid, neutrally buoyant spheroids which are sufficiently small, so the boundaries of the physical apparatus holding the fluid do not significantly affect the rheology of the bulk of the suspension.

While considering external forces, like electric or magnetic fields, it is assumed that the particles are dipolar, i.e., have electric or magnetic charges on them. In such cases the particle dipole moment is considered collinear with its physical symmetry axis.

The volume fraction Φ of the particles is so small that hydrodynamic interaction among particles or between a particle and the flow boundary may be neglected. Hydrodynamic interaction is a long range phenomenon in which the flow field experienced by a particle is affected by the velocity disturbance of other particles. Our assumption here is that the solution is *dilute*, which mathematically corresponds to the limit $nl^3 \ll 1$ where n is the number of particles per unit volume and l is the linear dimension of the particles.

The flow is considered sufficiently slow that the effects of inertial and external body forces are negligible compared to the viscous force. This means that, in the mathematical formulation of the problem, the Reynolds number, defined as the ratio of inertial forces to viscous forces, is very small and nearly zero.

2.2 The dynamics of force-free particles

In this section we derive the basic equation of motion for the orientation of a representative particle in the suspension, neglecting for now the effects of Brownian motion and external force fields. This equation can be later modified to include the contribution of Brownian and external forces by superimposing on it suitable terms corresponding to these factors.

Consider a single particle from a dilute suspension of identical, rigid, neutrally buoyant spheroids in an infinite incompressible Newtonian fluid. A spheroid has aspect ratio $r = a/b$ where a and b are respectively the polar and equatorial radii. Since for a dilute suspension the bulk properties are generally determined by the orientations of the particles alone we neglect any translatory motion of the particle by choosing a co-ordinate system that moves along with it. The origin of the co-ordinate system is placed at the

spin?

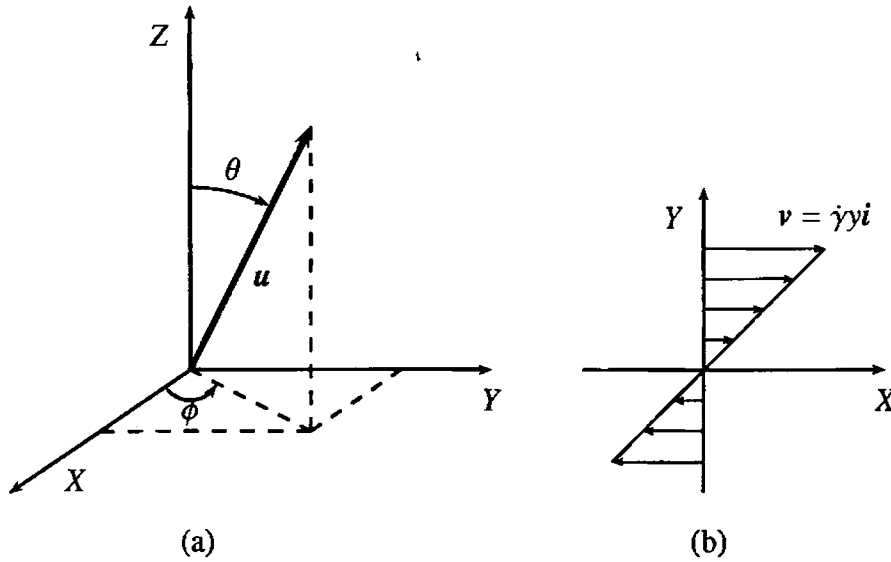


Figure 2.1: (a) A Schematic of the co-ordinate system and the orientation vector. (b) The profile of the flow.

centre of mass of the spheroid. The orientation of the spheroid is then represented by a unit vector \mathbf{u} placed along the major axis of the spheroid. Fig. 2.1(a) shows a schematic of this set up where the direction of \mathbf{u} is specified by the polar co-ordinates (θ, ϕ) , $\theta(0 \leq \theta \leq \pi)$ and $\phi(0 \leq \phi \leq 2\pi)$ being the polar and azimuthal angles determined by the vector \mathbf{u} . The Cartesian co-ordinates of \mathbf{u} are then given by the relations,

$$\begin{aligned} u_1 &= \sin \theta \cos \phi \\ u_2 &= \sin \theta \sin \phi \\ u_3 &= \cos \theta. \end{aligned} \tag{2.1}$$

The u_i being components of a unit vector they also satisfy

$$u_1^2 + u_2^2 + u_3^2 = 1$$

The suspending fluid medium is subjected to a simple shear flow with a flow field given by,

$$\mathbf{v} = \dot{\gamma} y \mathbf{i} = (\dot{\gamma} y, 0, 0) \tag{2.2}$$

where $\dot{\gamma}$ is the shear rate, y is the y -co-ordinate and i is the unit vector in the X -direction (Fig. 2.1(b)). The time rate of change of particle orientation can be expressed as

$$\dot{\mathbf{u}} = \boldsymbol{\omega} \times \mathbf{u}, \quad (2.3)$$

where $\boldsymbol{\omega}$ is the angular velocity of the particle, an expression ^{for} which may be obtained (through an angular momentum balance ~~equation~~ ^{equation}) (Strand and Kim, 1992) as follows. Without Brownian motion, the rotational torque on the particle is mainly due to hydrodynamic forces, and the conservation of angular momentum requires that

$$T^{\text{hyd}} = 0, \quad (2.4)$$

where T^{hyd} is the hydrodynamic torque which may be expressed as (Hinch and Leal, 1972),

$$T^{\text{hyd}} = \boldsymbol{\zeta} \cdot (\boldsymbol{\Omega} - \boldsymbol{\omega}) - C\boldsymbol{\zeta} \cdot [\mathbf{u} \times (\mathbf{E} \cdot \mathbf{u})]. \quad (2.5)$$

Above $\boldsymbol{\zeta}$ is the hydrodynamic resistance tensor and C is a shape factor for axi-symmetric particles defined by,

$$C = \frac{r^2 - 1}{r^2 + 1}$$

which takes value -1 for disks, 0 for spheres and +1 for long fibres (slender rods). The first term in (2.5) signifies the part of the torque caused by the interplay between the particle rotation and the local fluid motion, while the second term corresponds to the torque due to the shearing motion of the imposed flow. The strength of the flow field interferes T^{hyd} , eq. (2.5), through the rate of deformation tensor \mathbf{E} and the vorticity vector $\boldsymbol{\Omega}$ defined thus:

$$\mathbf{E} = \frac{1}{2}(\nabla \mathbf{v} + \nabla \mathbf{v}^T),$$

$$\boldsymbol{\Omega} = \frac{1}{2}(\nabla \times \mathbf{v}).$$

In simple shear, (2.2), \mathbf{E} and $\mathbf{\Omega}$ can be represented in terms of the shear rate thus,

$$\begin{aligned}\mathbf{E} &= \frac{\dot{\gamma}}{2}(\mathbf{i}\mathbf{j} + \mathbf{j}\mathbf{i}) \\ \mathbf{\Omega} &= (0, 0, -\frac{\dot{\gamma}}{2})\end{aligned}\quad (2.6)$$

The hydrodynamic resistance tensor ζ can be decomposed into components parallel and perpendicular to the particle symmetry axis (Kim and Lawrence, 1987),

$$\zeta = \zeta_{\parallel}\mathbf{u}\mathbf{u} + \zeta_{\perp}(\delta - \mathbf{u}\mathbf{u}),$$

where δ is the unit tensor. This when substituted into (2.5) eliminates terms involving ζ_{\parallel} and reduces it to,

$$\mathcal{T}^{\text{hyd}} = \zeta_{\perp}[(\mathbf{\Omega} - \boldsymbol{\omega}) - C[\mathbf{u} \times (\mathbf{E} \cdot \mathbf{u})]].$$

Hence (2.4) gives,

$$\boldsymbol{\omega} = \mathbf{\Omega} + C[\mathbf{u} \times (\mathbf{E} \cdot \mathbf{u})], \quad (2.7)$$

which, when substituted into (2.3) gives the final expression for the rate of rotation of the spheroid,

$$\dot{\mathbf{u}} = \mathbf{\Omega} \times \mathbf{u} + C[\mathbf{u} \times (\mathbf{E} \cdot \mathbf{u})] \times \mathbf{u}. \quad (2.8)$$

The Cartesian form of the above equation may be obtained by using (2.6);

$$\begin{aligned}\dot{u}_1 &= \dot{\gamma}Cu_2(1 - u_1^2) + \frac{\dot{\gamma}}{2}(1 - C)u_2, \\ \dot{u}_2 &= -\dot{\gamma}Cu_1u_2^2 - \frac{\dot{\gamma}}{2}(1 - C)u_1, \\ \dot{u}_3 &= -\dot{\gamma}Cu_1u_2u_3.\end{aligned}\quad (2.9)$$

2.3 The diffusion equation approach

Eq. (2.8) describes the orientation dynamics of a single particle in simple shear flow in the complete absence of Brownian motion, namely, the random fluctuations experienced

by the orientation of the particle due to collision by the numerous fluid molecules surrounding it. We now discuss how the effects of Brownian motion can be accounted for in the system. Brownian motion has significant effects if the particle size is comparatively smaller, typically of the order of $10 - 50 \mu\text{m}$. It affects the local dynamics of the particles by imparting additional rotational torques and influences the bulk properties by modifying the orientation distribution function. Experimental studies conducted on various flows also point to the necessity of taking Brownian effects into account (Anczurowski and Mason, 1967; Folgar and Tucker, 1984; Stover *et al.*, 1992). For example, the rotation of force-free particles in shear flows predicted by Jefferey should in principle lead to oscillations in the bulk properties(*cf.* sec. 1.2.1), while actual experiments showed that they tended to attain steady values in the long time limit. Leal and Hinch (1971) showed that one reason for this could be Brownian diffusion, since even very weak Brownian motion can kill oscillations in the dynamics and hence in the rheology. In the absence of any forcing on the particles, either due to the flow field or from an external force field, the Brownian forces tend to drive the particles to a uniform distribution. The additional torques due to the flow field or external force, which tend to align particles in preferred directions, compete with this disorienting effects of Brownian motion and make the particle dynamics depend on the various forces in a complicated manner.

shock
↓
expts
q

Brownian motion imparts rapid and random fluctuations to the particle orientation, the extent of which probably varies with time also. The particle orientation may therefore be considered a stochastic process, the sample space of which is the unit sphere that represents the set of all possible directions for the vectors \mathbf{u} . There are generally two different, but equivalent, methods for studying a stochastic system like this (*cf.* sec. 1.3). The first is the Diffusion equation (Fokker-Planck equation) formalism, in which the system is studied through a partial differential equation governing the time-space variation of an appropriate density function for the stochastic variable. In the second method, the Langevin equation formalism, the system is modelled through a set of stochastic

differential equations, called Langevin equations, governing the time dynamics of the stochastic variables.

Due to its random nature, a complete description of Brownian motion can only be made in terms of orientations of an ensemble of particles. The Fokker-Planck equation (diffusion equation) approach does this by describing the orientation state at a point in the space by a probability density function $\psi(\mathbf{u}, t)$, called the orientation distribution function (ODF), which is defined as the probability of finding a particle within the solid angle $d\mathbf{u}$ about \mathbf{u} at time t . The function ψ must satisfy some physical conditions. First, if the spheroid is not dipolar, the orientations \mathbf{u} and $-\mathbf{u}$ are indistinguishable so that

$$\psi(\mathbf{u}) = \psi(-\mathbf{u}).$$

Since every spheroid has some orientation, ψ must be normalised:

$$\int_S \psi(\mathbf{u}) d\mathbf{u} = \int_{\theta=0}^{\pi} \int_{\phi=0}^{2\pi} \psi(\theta, \phi) \sin \theta d\theta d\phi = 1,$$

the integration being over the surface S of the unit sphere. The third condition is a continuity equation, describing the change in ψ with time when the particles change orientations;

$$\frac{\partial \psi}{\partial t} + \frac{\partial}{\partial \mathbf{u}} \cdot (\dot{\mathbf{u}} \psi) = D_r \frac{\partial^2 \psi}{\partial u^2}, \quad (2.10)$$

which is referred to as the Fokker-Planck equation or Diffusion equation (Strand and Kim, 1992). This is basically a convection–diffusion equation, in which Brownian rotation is the diffusion process that tends to smooth out the distribution towards isotropy. D_r is the diffusion coefficient, called rotary diffusivity, defined by

$$D_r = k_B T / \zeta_{\perp}$$

where ζ_{\perp} represents the rotational resistance in the direction perpendicular to the particle symmetry axis, k_B is the Boltzmann constant and T is the absolute temperature.

In a dilute system, with the correlation among the orientations of neighbouring particles negligible, the ODF is assumed to be a complete description of the orientation state.

The above equation, eq. (2.10), usually appears in scaled form, either with the shear rate or the diffusion coefficient D_r , to express it in terms of the dimensionless quantity Pe , called *Péclet number*, defined by

$$Pe = \frac{\dot{\gamma}}{D_r}.$$

The flow parameter $\dot{\gamma}$ and the Brownian coefficient D_r influence the particle distribution in opposing directions, the former tending to drive the suspension towards an anisotropic state and the latter trying to maintain an isotropic equilibrium. Hence the magnitude of Pe determines the degree of anisotropy of the suspension. At steady state Pe is the only dimensionless parameter that dictates the suspension behaviour for the above system.

The average orientation properties of the suspension are estimated through appropriate moments of the orientation distribution function and the bulk suspension properties are then expressed in terms of these moments. For a given orientation function $B(\mathbf{u})$, the moment $\langle B(\mathbf{u}) \rangle$ is $B(\mathbf{u})$ averaged over an ensemble of orientations \mathbf{u} , weighted by ψ ,

$$\langle B(\mathbf{u}) \rangle = \int_S B(\mathbf{u}) \psi d\mathbf{u}. \quad (2.11)$$

Above, ψ can be obtained by solving the diffusion equation eq. (2.10) at steady state where $\dot{\mathbf{u}}$ is given by eq. (2.8). A major impediment to the success of this approach is the fact that the diffusion equation is usually very difficult to solve in its fully generality, except for some comparatively simpler cases like steady uniaxial and planar extensional flows, for which there exist rigorous solutions of the diffusion equation (Brenner, 1974; Brenner and Condiff, 1974). What is done in practice is to attempt various numerical schemes, guided by physical intuition, to approximate the solution for various ranges of shear and diffusion parameters. Thus, for example, if diffusion is weak compared to shear, the particles tend to spend most of the time along the flow direction and diffusion

can be neglected except in a small region of the orientation space near the flow direction (Hinch and Leal, 1972). Hinch and Leal (1972) used a regular perturbation method around $1/Pe$ to approximate the ODF in this regime ($Pe^{\frac{1}{2}} \gg r$). On the other hand, if the Brownian diffusion is stronger ($Pe \ll 1$), the weak flow disturbs the uniform orientation distribution caused by the randomizing effect of diffusion only slightly; hence a regular perturbation about Pe may be used to approximate the ODF (Hinch and Leal, 1976). When the flow strength is in between these extremes, the perturbation methods fail. Chen and Koch (1996) developed a spherical harmonic method to determine the orientation distribution function of fibers of large aspect ratio in this intermediate regime where diffusion and advection are comparable. This involves expanding the steady state orientation distribution function into a double series of spherical harmonics and substituting a suitably truncated form of this series into the diffusion equation for the system, leaving a set of linear equations in the expansion coefficients. The number of terms in the truncated series and hence the number of linear equations to be solved generally increases with increasing Pe to achieve a given accuracy. Hence the procedure becomes computationally formidable for larger values of Pe , but the technique can be successfully applied for Pe upto 1000 (Chen and Jiang, 1999). Chen and Jiang (1999) present another approach, in which the diffusion equation of the system is numerically solved for the steady state ODF using a finite difference scheme with a pair of boundary conditions. This method is applicable when the flow is moderate (Pe upto 1000), but even for small Pe , the numerical scheme requires a large number of mesh points to achieve a given accuracy and so the computation time is longer even in the weak flow regime. For very large Pe they suggest another method in which the diffusion equation is numerically solved for the time evolution of the ODF with a given initial state until steady state is reached. This is particularly useful for $Pe > 1000$ where spherical harmonics methods become computationally difficult.

2.4 An outline of the new approach

It is clear from the above discussion that the numerical schemes currently used for solving the diffusion equation vary as the flow and Brownian parameters are changed. In this work, we present an alternate approach to computing the orientation moments without having to solve the diffusion equation. This method is based on a generalized Langevin equation approach presented recently by Coffey *et al.* (1996) for non-linear systems with noise, and provides a unified strategy for modeling such systems placing little restriction on the Péclet number of the flow. Each Langevin equation is an equation of motion for the orientation of a single particle depicting the irregular part of the motion due to Brownian effects in terms of a suitable random noise term whose properties are determined only on the average. An ensemble of these equations must be identical to the governing diffusion equation of the entire system. For the system we study, the Langevin equation would be obtained by superposing on eq. (2.8) for the regular part of the motion in the complete absence of Brownian diffusion, suitable terms for the random fluctuations arising from Brownian effect and hence will have the general form,

$$\dot{\mathbf{u}} = \boldsymbol{\Omega} \times \mathbf{u} + C[\mathbf{u} \times (\mathbf{E} \cdot \mathbf{u})] \times \mathbf{u} + g(\mathbf{u}, \boldsymbol{\Gamma}, t).$$

$\boldsymbol{\Gamma}$ is a white noise vector which takes care of the random fluctuations due to the additional Brownian effect. The components Γ_i of $\boldsymbol{\Gamma}$ are Gaussian random variables, the conditions on which are known only on the average, usually determined by demanding that an ensemble of these Langevin equations be mathematically equivalent to the corresponding Fokker-Planck equation of the system. Generally, it turns out that Γ_i are delta-correlated random variables with zero mean. The exact form of the function g in the above Langevin equation is presently unknown and will be determined in Chapter 3 by comparing the moments of spherical harmonics as obtained from the diffusion equation and an ensemble of the Langevin equations. We note that the spherical harmonics form a complete set of eigen functions for the expansion of any orientation average into

an infinite series. Accordingly, we first derive a differential recurrence formula for the moments of surface spherical harmonics starting from the diffusion equation (sec. 3.2.1) and then reproduce it from the Langevin equation method with a presumed noise term for the Langevin equations as suggested by some heuristic arguments (sec. 3.2.3). The exact agreement between the two formulae then justifies the form of noise we started with. We then obtain the *exact equation of motion for any desired orientation average* using a modification of a novel idea of Coffey *et al.* (1996)(Chapter 4). These moment equations being ordinary differential equations are easier to handle than the original Langevin equations which are stochastic differential equations. These equations are easily solved in the zero shear limit giving the familiar result that the orientations tend to a uniform distribution at equilibrium due to the randomization effect caused by the Brownian diffusion. In other cases, we transform each pair of moment equations into a pair of coupled ODEs and a set of such equations is simulated over a finite number of initial conditions until the properties of the solutions are invariant in time. The desired moments can be easily obtained from these solutions and the results are in good agreement with previously known ones, when obtained for some special cases.

The basic idea behind the Coffey *et al.* (1996) treatment of non-linear systems with noise is that by interpreting a Langevin equation for a stochastic variable as an integral equation in the Stratonovich sense with a sharp initial condition, it is possible to express suitable time averages of the stochastic variable in terms of a *deterministic* equation of motion for the sharp values. From an ensemble of these time averaged Langevin equations it is possible to determine the dynamics of the various moments in terms of deterministic ordinary differential equations, without having to solve the diffusion equation. For the system we consider, the bulk suspension properties are related to orientation averages over the particles aligned along a set of common directions. The most realistic model for such a suspension may be a set of Langevin equations starting off from sharp initial conditions in a time-averaged sense over an appropriate white

noise term. Thus this system is an ideal one for applying the Coffey *et al.* approach. The technique presented here can be easily generalized and applied to other similar systems with noise.

2.5 A comparison of the different methods

As we have seen, most of the methods for solving the diffusion equation involve expanding the ODF into a series of orthogonal basis functions and then numerically solving for the coefficients. The method is suited for systems in which the variations in the density function over the orientation space are ^{small!} smooth. If the density has steep gradients many more terms in the expansion will have to be retained and solving for the coefficients then becomes computationally intensive. Furthermore this technique of eigen function expansion is difficult to apply to systems for which the governing equations are complicated.

As an alternative to the Fokker-Planck equation approach, the Langevin model with Brownian dynamics simulations has been proposed by some authors (Hua and Schieber, 1995). This method deals directly with stochastic differential equations, the Langevin equations of motion for the suspension elements. However, this requires a large number of equations to be tracked in order to obtain statistically accurate results, and therefore takes large computational time and effort.

In contrast to the aforementioned treatment of stochastic systems, the method presented in this work has several advantages. First, it directly describes the time evolution of the random variables rather than the probability function underlying the process. Second, the need to construct the Fokker-Planck equation from the Langevin equation is dispensed with, nonetheless the averages generated are identical to those obtained from the Fokker-Planck equation. Further, in actual experiments one measures only time averages over small time intervals and not instantaneous values and so the description of the evolution of time averages by a deterministic equation in the new method appears to

be more suitable for comparison with experiments. It is also advantageous over the usual Langevin treatment in that the time averages of the stochastic variable can be expressed in terms of ordinary differential equations for a set of sharp starting values, the trajectories of which can be more accurately simulated numerically than those of stochastic differential equations as in Brownian dynamics simulations.

From the point of view of the problem we study, the new method provides a unified strategy that can be applied over a wider range of Pe than is possible by other methods. It can be easily generalized to more complex systems like suspensions of charged particles or suspensions of dipolar particles with external forcing. Also it offers a considerable saving of computational time, as we shall see in subsequent chapters when we compare our methods with existing ones. The Langevin method, together with a paired moment scheme for computing the orientation moments developed in subsequent chapters, will be found suitable in certain regions such as the limit of weak Brownian motion where the regular methods fail due to singularity problems.

Kumar and Ramamohan (1995) demonstrated that the presence of chaos or subharmonic frequencies in the orientation dynamics or the rheology of the suspension might not be identifiable in the diffusion equation method used by Strand (1989) or similar methods. The Langevin equation method is the ideal tool in such situations as we shall elucidate in later chapters.

The Langevin approach

In the last chapter we observed that the Langevin equations governing the orientation dynamics of the spheroids in the suspension system we study has the general form,

$$\dot{\mathbf{u}} = \boldsymbol{\Omega} \times \mathbf{u} + C[\mathbf{u} \times (\mathbf{E} \cdot \mathbf{u})] \times \mathbf{u} + g(\mathbf{u}, \Gamma, t). \quad (3.1)$$

with an undetermined form for the noise term g . In this chapter we determine the form of this noise term, by requiring that the ensemble of equations (3.1) becomes identical to the diffusion equation eq. (2.10), Chapter 2 for the system. This is done by expanding the distribution function ψ into an infinite series of surface spherical harmonics. This set of Langevin equations will then be used to generate the equations for the dynamics of the desired orientation averages. The following section is a review of the definition and properties of the spherical harmonics which will be put to use in the subsequent sections. The rest of the chapter is devoted to fixing the form of the stochastic term in the Langevin equation, by exploiting the equivalence between the diffusion equation and the system of Langevin equations.

3.1 The spherical Harmonics

The spherical harmonics are an infinite class of functions defined over the surface of the unit sphere, with θ the polar angle and ϕ the azimuthal angle, defined thus (Arfken and

Weber, 1995):

$$Y_{n,m} = N_{n,m} P_n^m(\cos \theta) e^{im\phi}, \quad -n \leq m \leq n.$$

Above, the normalization constants $N_{n,m}$ are given by

$$N_{n,m} = (-1)^m \sqrt{\frac{(2n+1)(n-m)!}{4\pi(n+m)!}}.$$

The P_n^m are associated Legendre functions defined for non-negative m by

$$P_n^m(x) = (1-x^2)^{m/2} \frac{d^m}{dx^m} (P_n(x)), \quad -1 \leq x \leq 1$$

where $P_n(x)$ is the Legendre polynomial, and for negative m by

$$P_n^{-m}(x) = (-1)^m \frac{(n-m)!}{(n+m)!} P_n^m(x)$$

The $Y_{n,m}$ therefore satisfy the relation $Y_{n,m} = (-1)^m Y_{n,-m}^*$ where $*$ denotes the complex conjugate. An important property of the spherical harmonics is that they form a complete set in the space of all square integrable functions defined over the surface of the unit sphere. This means that

- (i) the spherical harmonics form an orthonormal set, pairwise satisfying the orthogonality relation (Arfken and Weber, 1995),

$$\int_{\theta=0}^{\pi} \int_{\phi=0}^{2\pi} Y_{q,p} Y_{n,m}^* \sin \theta d\theta d\phi = \delta_{qn} \delta_{pm}, \quad (3.2)$$

- (ii) any function $f(\theta, \phi)$ in the above space can be expanded in a uniformly convergent double series of spherical harmonics (Arfken and Weber, 1995)

$$f(\theta, \phi) = \sum_{n=0}^{\infty} \sum_{m=-n}^n a_{n,m} Y_{n,m}. \quad (3.3)$$

The last equation allows for expressing the orientation moment $\langle f(\theta, \phi) \rangle$ in terms of the moments of the spherical harmonics thus,

$$\langle f(\theta, \phi) \rangle = \sum_{n=0}^{\infty} \sum_{m=-n}^n a_{n,m} \langle Y_{n,m} \rangle. \quad (3.4)$$

Theoretically, this means that the dynamical variations of the moment $\langle f(\theta, \phi) \rangle$, as the distribution function ψ changes due to change in particle orientations, can be completely determined from the dynamics of the moments of the spherical harmonics.

We now proceed to determine the undetermined function g in eq. (3.1) by requiring that the diffusion equation and an ensemble of the Langevin equations (3.1), generate the same set of orientation averages. Equivalently, since any orientation average can be expanded in terms of spherical harmonics (cf. eq. (3.4)), we may require that both the methods give rise to the same evolution equations for moments of spherical harmonics and use this as a matching condition for obtaining the noise term. Towards this end, we derive a set of differential recurrence relations for the evolution of the moments of surface spherical harmonics for the system governed by the Fokker-Planck equation (2.10) and compare them in section 3.2.3 with a similar set of equations to be obtained from the set of Langevin equations (3.1) for the same system with a presumed value for the unknown function g .

3.2 The dynamics of the spherical harmonics

3.2.1 From the diffusion equation

We note that eq. (2.9) gives the regular part of the evolution equation for the orientation of a single particle in the complete absence of Brownian diffusion, while the effect of diffusion is taken care of by the diffusive term on the right side of eq. (2.10). The transformations eqs. (2.1) can be used to express eq. (2.9) in their spherical co-ordinates counter parts,

$$\begin{aligned}\dot{\theta} &= \dot{\gamma} C \sin \theta \cos \theta \sin \phi \cos \phi, \\ \dot{\phi} &= -\dot{\gamma} C \sin^2 \phi - \dot{\gamma} \left(\frac{1-C}{2} \right).\end{aligned}\tag{3.5}$$

We can use the above expressions in (2.10) to write it in spherical co-ordinates thus:

$$\frac{\partial \psi}{\partial t} + \dot{\gamma} C \bar{\Omega}(\psi) - \frac{\dot{\gamma}}{2} (1-C) \frac{\partial \psi}{\partial \phi} = D_r \bar{\Lambda}(\psi).\tag{3.6}$$

The $\bar{\Omega}$ and $\bar{\Lambda}$ appearing in the above equation are linear operators defined by

$$\begin{aligned}\bar{\Omega}(\psi) &= \frac{\sin \phi \cos \phi}{\sin \theta} \frac{\partial}{\partial \theta} (\psi \sin^2 \theta \cos \theta) - \frac{\partial}{\partial \phi} (\psi \sin^2 \phi), \\ \bar{\Lambda}(\psi) &= \frac{1}{\sin \theta} \frac{\partial}{\partial \theta} \left(\sin \theta \frac{\partial \psi}{\partial \theta} \right) + \frac{1}{\sin^2 \theta} \frac{\partial^2 \psi}{\partial \phi^2}\end{aligned}\quad (3.7)$$

We may now expand ψ into a double series of spherical harmonics (*cf.* eq. (3.3)), assuming that $\psi(\theta, \phi, t)$ satisfies the boundary conditions $\psi|_{\theta=\pi, \phi=2\pi} = \psi|_{\theta=0, \phi=0}$

$$\psi = \sum_{n=0}^{\infty} \sum_{m=-n}^n a_{n,m}(t) Y_{n,m}. \quad (3.8)$$

Since ψ is to be real the expansion coefficients $a_{n,m}$ satisfy $a_{n,-m} = (-1)^m a_{n,m}^*$. Again, since ψ is a probability density function it must satisfy the normalization condition,

$$\int_{\theta=0}^{\pi} \int_{\phi=0}^{2\pi} \psi(\theta, \phi, t) \sin \theta d\theta d\phi = 1.$$

This constrains the first term in the expansion for ψ to satisfy $a_{0,0} Y_{0,0} = 1/(4\pi)$ due to orthogonality of the spherical harmonics, eq. (3.2). In polar co-ordinates, the expression (2.11) for the moment $\langle B(\theta, \phi) \rangle$ becomes

$$\langle B(\theta, \phi) \rangle = \int_{\theta=0}^{\pi} \int_{\phi=0}^{2\pi} B(\theta, \phi) \psi \sin \theta d\theta d\phi$$

Fixing $m \geq 0$ and multiplying (3.6) through by $Y_{n,m}^*$ and integrating over the unit sphere we get

$$\begin{aligned}\int_{\theta=0}^{\pi} \int_{\phi=0}^{2\pi} \frac{\partial \psi}{\partial t} Y_{n,m}^* \sin \theta d\theta d\phi + \gamma C \int_{\theta=0}^{\pi} \int_{\phi=0}^{2\pi} \bar{\Omega}(\psi) Y_{n,m}^* \sin \theta d\theta d\phi \\ - \gamma \left(\frac{1-C}{2} \right) \int_{\theta=0}^{\pi} \int_{\phi=0}^{2\pi} \frac{\partial \psi}{\partial \phi} \sin \theta Y_{n,m}^* d\theta d\phi \\ = D_r \int_{\theta=0}^{\pi} \int_{\phi=0}^{2\pi} \bar{\Lambda}(\psi) Y_{n,m}^* \sin \theta d\theta d\phi\end{aligned}\quad (3.9)$$

The first term on the left side of (3.9) is evidently $\frac{d}{dt} \langle Y_{n,m}^* \rangle$. To evaluate the second term on the left we first note that

$$\begin{aligned}
& \int_{\theta=0}^{\pi} \int_{\phi=0}^{2\pi} \bar{\Omega}(\psi) Y_{n,m}^* \sin \theta \, d\theta \, d\phi \\
&= \int_{\theta=0}^{\pi} \int_{\phi=0}^{2\pi} \frac{\sin \phi \cos \phi}{\sin \theta} \frac{\partial}{\partial \theta} (\psi \sin^2 \theta \cos \theta) Y_{n,m}^* \sin \theta \, d\theta \, d\phi \\
&\quad - \int_{\theta=0}^{\pi} \int_{\phi=0}^{2\pi} \frac{\partial}{\partial \phi} (\psi \sin^2 \phi) \sin \theta Y_{n,m}^* \, d\theta \, d\phi \\
&= - \int_{\theta=0}^{\pi} \int_{\phi=0}^{2\pi} \sin \phi \cos \phi \frac{\partial}{\partial \theta} (Y_{n,m}^*) \psi \sin^2 \theta \cos \theta \, d\theta \, d\phi \\
&\quad + \int_{\theta=0}^{\pi} \int_{\phi=0}^{2\pi} \sin \theta \frac{\partial}{\partial \phi} (Y_{n,m}^*) \psi \sin^2 \phi \, d\theta \, d\phi
\end{aligned} \tag{3.10}$$

In the foregoing expressions the last step follows by integrating the first term of the previous step by parts with respect to θ and the second term with respect to ϕ . Now using the relations

$$\begin{aligned}
\frac{\partial}{\partial \theta} (Y_{n,m}^*) \sin^2 \theta \cos \theta &= \frac{\partial}{\partial \theta} (Y_{n,m}^* \sin^2 \theta \cos \theta) - \frac{\partial}{\partial \theta} (\sin^2 \theta \cos \theta) Y_{n,m}^* \\
\frac{\partial}{\partial \phi} (Y_{n,m}^*) \sin^2 \phi &= \frac{\partial}{\partial \phi} (Y_{n,m}^* \sin^2 \phi) - Y_{n,m}^* \sin(2\phi)
\end{aligned} \tag{3.11}$$

in (3.10) and simplifying we get

$$\begin{aligned}
\int_{\theta=0}^{\pi} \int_{\phi=0}^{2\pi} \bar{\Omega}(\psi) Y_{n,m}^* \sin \theta \, d\theta \, d\phi &= - \int_{\theta=0}^{\pi} \int_{\phi=0}^{2\pi} \bar{\Omega}(Y_{n,m}^*) \psi \sin \theta \, d\theta \, d\phi \\
&\quad - \frac{3}{2} \int_{\theta=0}^{\pi} \int_{\phi=0}^{2\pi} Y_{n,m}^* \sin^3 \theta \sin(2\phi) \psi \, d\theta \, d\phi.
\end{aligned} \tag{3.12}$$

The effects of $\bar{\Omega}$ on $P_n^m(\cos \theta)$ and $P_n^m(\sin \theta)$ have been evaluated previously (Bird *et al.*, 1987) (here and in what follows we have abbreviated $P_n^m(\cos \theta)$ by P_n^m *etc.*):

$$\begin{aligned}
\bar{\Omega}(P_n^m \sin(m\phi)) &= \sum_{j=m-2}^{m+2} \sum_{k=n-2}^{n+2} a_{n,k}^{m,j} P_k^j \cos(j\phi), \quad m \geq 0 \\
\bar{\Omega}(P_n^m \cos(m\phi)) &= - \sum_{j=m-2}^{m+2} \sum_{k=n-2}^{n+2} a_{n,k}^{m,j} P_k^j \sin(j\phi), \quad m > 0
\end{aligned}$$

The constants $a_{n,k}^{m,j}$ are the Bird-Warner coefficients (Bird *et al.*, 1987). Hence it follows that

$$\bar{\Omega}(Y_{n,m}^*) = \sum_{j=m-2}^{m+2} \sum_{k=n-2}^{n+2} b_{n,k}^{m,j} Y_{k,j}^* \quad (3.13)$$

where we have written $b_{n,k}^{m,j} = -i(N_{n,m}/N_{k,j})a_{n,k}^{m,j}$. This can now be used in (3.12) to complete the evaluation for the second term on the left of (3.9):

$$\begin{aligned} \dot{\gamma} C \int_{\theta=0}^{\pi} \int_{\phi=0}^{2\pi} \bar{\Omega}(\psi) Y_{n,m}^* \sin \theta \, d\theta \, d\phi \\ = -\dot{\gamma} C \sum_{j=m-2}^{m+2} \sum_{k=n-2}^{n+2} b_{n,k}^{m,j} \langle Y_{k,j}^* \rangle - \frac{3}{2} \dot{\gamma} C \langle \sin^2 \theta \sin(2\phi) Y_{n,m}^* \rangle \end{aligned} \quad (3.14)$$

The integral in the third term on the left of (3.9) can be integrated by parts with respect to ϕ and the boundary conditions for ψ applied to show that

$$-\dot{\gamma} \left(\frac{1-C}{2} \right) \int_{\theta=0}^{\pi} \int_{\phi=0}^{2\pi} \frac{\partial \psi}{\partial \phi} \sin \theta Y_{n,m}^* \, d\theta \, d\phi = -\dot{\gamma} \left(\frac{1-C}{2} \right) i m \langle Y_{n,m}^* \rangle \quad (3.15)$$

To evaluate the right side of (3.9) we use the known effects of $\bar{\Lambda}$ on real spherical harmonics (Bird *et al.*, 1987);

$$\bar{\Lambda}(P_n^m \cos(m\phi)) = -n(n+1) P_n^m \sin(m\phi)$$

$$\bar{\Lambda}(P_n^m \sin(m\phi)) = -n(n+1) P_n^m \cos(m\phi).$$

Hence using the linearity of $\bar{\Lambda}$ we have $\bar{\Lambda}(Y_{n,m}^*) = -n(n+1)Y_{n,m}^*$ and then invoking the eigen function expansion of ψ ,

$$\bar{\Lambda}(\psi) = \bar{\Lambda} \left(\sum_{q=0}^{\infty} \sum_{p=-q}^q a_{q,p} Y_{q,p} \right) = \sum_{q=0}^{\infty} \sum_{p=-q}^q (-q)(q+1) a_{q,p} Y_{q,p}.$$

This result together with the orthogonality relation for the spherical harmonics, (3.2), and term by term integration yields

$$\begin{aligned}
& \int_{\theta=0}^{\pi} \int_{\phi=0}^{2\pi} \bar{\Lambda}(\psi) \sin \theta Y_{n,m}^* d\theta d\phi \\
&= \int_{\theta=0}^{\pi} \int_{\phi=0}^{2\pi} \left(\sum_{q=0}^{\infty} \sum_{p=-q}^q (-q)(q+1) a_{q,p} Y_{q,p} \right) Y_{n,m}^* \sin \theta d\theta d\phi \\
&= \sum_{q=0}^{\infty} \sum_{p=-q}^q \left(-q(q+1) a_{q,p} \int_{\theta=0}^{\pi} \int_{\phi=0}^{2\pi} Y_{q,p} Y_{n,m}^* \sin \theta d\theta d\phi \right) \\
&= (-n)(n+1) a_{n,m}.
\end{aligned}$$

In a similar fashion, using the orthogonality relation (3.2) and the expansion for ψ , we can prove that the expansion coefficients $a_{n,m}$ are related to $Y_{n,m}^*$ by $a_{n,m} = \langle Y_{n,m}^* \rangle$. The final expression for the right side of (3.9), therefore, becomes

$$D_r \int_{\theta=0}^{\pi} \int_{\phi=0}^{2\pi} \bar{\Lambda}(\psi) \sin \theta Y_{n,m}^* d\theta d\phi = D_r n(n+1) \langle Y_{n,m}^* \rangle. \quad (3.16)$$

Putting together (3.14), (3.15) and (3.16) in (3.9) we get the following differential recurrence relation for $\langle Y_{n,m}^* \rangle$

$$\begin{aligned}
\frac{d}{dt} \langle Y_{n,m}^* \rangle &= \dot{\gamma} C \sum_{j=m-2}^{m+2} \sum_{k=n-2}^{n+2} b_{n,k}^{m,j} \langle Y_{k,j}^* \rangle + \frac{3}{2} \dot{\gamma} C \langle \sin^2 \theta \sin(2\phi) Y_{n,m}^* \rangle \\
&+ \dot{\gamma} \left(\frac{1-C}{2} \right) i m \langle Y_{n,m}^* \rangle - D_r n(n+1) \langle Y_{n,m}^* \rangle
\end{aligned} \quad (3.17)$$

The above recurrence relation has been derived on the assumption that m is non-negative.

If m is negative $-m$ is positive and the Bird-Warner coefficients $\alpha_{n,k}^{-m,j}$ are defined. We will then get a similar recurrence relation by complex conjugation using $Y_{n,m} = (-1)^m Y_{n,-m}^*$ with appropriate modifications.

Special cases

In the absence of shear (i.e., $\dot{\gamma} = 0$) eq. (3.17) reduces to

$$\frac{d}{dt} \langle Y_{n,m}^* \rangle = -D_r n(n+1) \langle Y_{n,m}^* \rangle,$$

which has solution

$$\langle Y_{n,m}^* \rangle = k e^{-D_r n(n+1)} \quad (k \text{ some constant}).$$

For $n > 0$, $\langle Y_{n,m}^* \rangle \rightarrow 0$ as $n \rightarrow \infty$, while for $n = 0$, $\langle Y_{0,0}^* \rangle = a_{0,0} = 1/\sqrt{4\pi}$ by normalisation. A similar result holds when the particles are spheres (i.e, $C = 0$). In this case the recurrence relation becomes

$$\frac{d}{dt} \langle Y_{n,m}^* \rangle = i c_1 \langle Y_{n,m}^* \rangle - c_2 \langle Y_{n,m}^* \rangle$$

where $c_1 = \dot{\gamma} m(1 - C/2)$ and $c_2 = D_r n(n+1)$. In terms of real spherical harmonics this can be written as a linear system,

$$\begin{aligned} \frac{d}{dt} \langle P_n^m \cos m\phi \rangle &= c_1 \langle P_n^m \sin m\phi \rangle - c_2 \langle P_n^m \cos m\phi \rangle \\ \frac{d}{dt} \langle P_n^m \sin m\phi \rangle &= -c_1 \langle P_n^m \cos m\phi \rangle - c_2 \langle P_n^m \sin m\phi \rangle. \end{aligned}$$

The coefficient matrix of the system has eigen values $\lambda_i = -c_2 \pm i c_1$. Since $Re(\lambda_i) < 0$ for $n > 0$, $\langle Y_{n,m}^* \rangle \rightarrow 0$ in this case, while for $n = 0$, $\langle Y_{0,0}^* \rangle = 1/\sqrt{4\pi}$ as before. Thus in the absence of shear or when the particles are spheres we get $\psi = 1/\sqrt{4\pi}$ in the long time limit, which corresponds to uniform particle distribution. This is the familiar result that in these cases the randomization effect due to Brownian motion leads to a uniform distribution of the suspension at equilibrium.

3.2.2 The Coffey *et al.* method

Before deriving the differential recurrence relations for the spherical harmonics by the Langevin equation approach, we give a brief mathematical description of the Coffey *et al.* (1996) approach which we will use in the coming sections. Let $\xi = (\xi_1, \xi_2, \dots, \xi_n)$ be an n -dimensional stochastic variable whose components satisfy a set of Langevin equations with multiplicative noise terms,

$$\dot{\xi}_i(t) = h_i(\xi(t), t) + g_{ij}(\xi(t), t) \Gamma_j(t), \quad 1 \leq i \leq n, \quad 1 \leq j \leq m, \quad (3.18)$$

where Γ_j are Gaussian random variables with zero mean and auto-correlation functions proportional to the δ function:

$$\overline{\Gamma_j(t)} = 0, \quad \overline{\Gamma_i(t)\Gamma_j(t')} = 2D\delta_{ij}\delta(t-t'), \quad (3.19)$$

where δ_{ij} is the Kronecker delta, $\delta(t)$ is the Dirac delta function and D is the spectral density. We start with interpreting (3.18) as an integral equation (in the Stratonovich sense) for the values of ξ at a later time $t + \delta t$,

$$\xi_i(t + \delta t) = x_i(t) + \int_t^{t+\delta t} \left[h_i(\xi(t'), t') + g_{ij}(\xi(t'), t')\Gamma_j(t') \right] dt' \quad (3.20)$$

where $x_i(t)$ is the sharp starting values for $\xi_i(t)$ at the instant t . Let \dot{x}_i (without the time argument) denote the time average of $\xi_i(t)$ starting from the sharp value $x_i(t)$, calculated by the Stratonovich rule. Then the time averages can be expressed as a *deterministic* equation of motion for the set of sharp starting values \mathbf{x} (Coffey *et al.*, 1996),

$$\begin{aligned} \dot{x}_i &= \lim_{\delta t \rightarrow 0} \frac{\overline{[\xi_i(t + \delta t) - x_i(t)]}}{\delta t} \\ &= h_i(\mathbf{x}) + D g_{kj}(\mathbf{x}, t) \frac{\partial}{\partial x_k} (g_{ij}(\mathbf{x}, t)), \end{aligned} \quad (3.21)$$

where $1 \leq i \leq n$, $1 \leq j, k \leq m$. In the above we have used Einstein's summation convention so that the second term on the right represents a sum over j and k . Similarly it can also be proved that for any well behaved function $f_i(\mathbf{x})$ (Coffey *et al.*, 1996),

$$f_i(\mathbf{x})\dot{x}_i = f_i(\mathbf{x})h_i(\mathbf{x}) + D g_{kj}(\mathbf{x}, t) \frac{\partial}{\partial x_k} (f_i(\mathbf{x}) g_{ij}(\mathbf{x}, t)), \quad (3.22)$$

where again the summation over j and k is understood.

3.2.3 From the Langevin equation

To obtain the exact form of the noise term g in the Langevin equation (3.1), we heuristically suppose that the rotary Brownian motion causes the angular velocity of the particle

to change and we incorporate this effect by superposing on the equation (2.7) for ω a white noise vector term:

$$\omega = \Omega + C [\mathbf{u} \times (\mathbf{E} \cdot \mathbf{u})] + \Gamma(t)$$

where the Cartesian components $\Gamma_i(t)$ of Γ satisfy (3.19) with $D = D_r$. A justification for this form of the noise will be available only later when we reproduce from the system of Langevin equations with this noise term, the same dynamics for the moments of the spherical harmonics, eq. (3.17), as induced by the Fokker-Planck equation. The expression for $\dot{\mathbf{u}}$, eq. (2.8), then changes into

$$\dot{\mathbf{u}} = \Omega \times \mathbf{u} + C [\mathbf{u} \times (\mathbf{E} \cdot \mathbf{u})] \times \mathbf{u} + \Gamma \times \mathbf{u}. \quad (3.23)$$

When converted into spherical co-ordinates the equation becomes (cf. eq. (3.5))

$$\begin{aligned} \dot{\theta} &= \gamma C \sin \theta \cos \theta \sin \phi \cos \phi - \sin \phi \Gamma_1(t) + \cos \phi \Gamma_2(t) \\ \dot{\phi} &= -\gamma C \sin^2 \phi - \gamma \left(\frac{1-C}{2} \right) - \cot \theta \cos \phi \Gamma_1(t) \\ &\quad - \sin \phi \cot \theta \Gamma_2(t) + \Gamma_3(t) \end{aligned} \quad (3.24)$$

These equations are now in the form (3.18) with h_1 and h_2 corresponding to the deterministic parts of $\dot{\theta}$ and $\dot{\phi}$ in (3.24) respectively and with

$$\begin{aligned} g_{11} &= -\sin \phi & g_{12} &= \cos \phi & g_{13} &= 0 \\ g_{21} &= -\cot \theta \cos \phi & g_{22} &= -\cot \theta \sin \phi & g_{23} &= 1 \end{aligned}$$

To obtain the differential recurrence relations for the spherical harmonics $Y_{n,m}^*$ for $m \geq 0$ note first that

$$\frac{d}{dt} (Y_{n,m}^*) = \frac{\partial}{\partial \theta} (Y_{n,m}^*) \dot{\theta} + \frac{\partial}{\partial \phi} (Y_{n,m}^*) \dot{\phi}. \quad (3.25)$$

Writing $f_1 = \partial Y_{n,m}^* / \partial \theta$, $f_2 = \partial Y_{n,m}^* / \partial \phi$, $\theta_1 = \theta$ and $\theta_2 = \phi$ and applying the results of (3.21) in (3.24) and of (3.22) in (3.25) we get the equation of motion for the sharp values $Y_{n,m}^*$ as

$$\frac{d}{dt} (Y_{n,m}^*) = f_1 h_1 + f_2 h_2 + D_r g_{kj} \frac{\partial}{\partial \theta_k} (f_1 g_{1j} + f_2 g_{2j}) \quad (3.26)$$

where the last term represents a sum over j and k . We first write out the deterministic part of (3.26) using (3.24)

$$f_1 h_1 + f_2 h_2 = \dot{\gamma} C \left[\frac{\partial}{\partial \theta} (Y_{n,m}^*) \sin \theta \cos \theta \sin \phi \cos \phi - \frac{\partial}{\partial \phi} (Y_{n,m}^*) \sin^2 \phi \right] - \dot{\gamma} \left(\frac{1-C}{2} \right) \frac{\partial}{\partial \phi} (Y_{n,m}^*). \quad (3.27)$$

Now multiply the first of the relations in (3.11) by $(\dot{\gamma} C \sin \phi \cos \phi) / \sin \theta$ and the second by $\dot{\gamma} C$ and subtract to get

$$\begin{aligned} & \dot{\gamma} C \left[\frac{\partial}{\partial \theta} (Y_{n,m}^*) \sin \theta \cos \theta \sin \phi \cos \phi - \frac{\partial}{\partial \phi} (Y_{n,m}^*) \sin^2 \phi \right] \\ &= \dot{\gamma} C \left[\frac{\sin \phi \cos \phi}{\sin \theta} \frac{\partial}{\partial \theta} (Y_{n,m}^* \sin^2 \theta \cos \theta) - \frac{\partial}{\partial \phi} (Y_{n,m}^* \sin^2 \phi) \right] \\ &+ \dot{\gamma} C \left[Y_{n,m}^* \sin(2\phi) - \frac{Y_{n,m}^* \sin \phi \cos \phi}{\sin \theta} \frac{\partial}{\partial \theta} (\sin^2 \theta \cos \theta) \right] \\ &= \dot{\gamma} C \bar{\Omega} (Y_{n,m}^*) + \frac{3}{2} \dot{\gamma} C \sin^2 \theta \sin(2\phi) Y_{n,m}^*. \end{aligned} \quad (3.28)$$

Substituting (3.28) in (3.27) and using eq. (3.13) we get the following form for the deterministic part of (3.26)

$$f_1 h_1 + f_2 h_2 = \dot{\gamma} C \sum_{j=-m-2}^{m+2} \sum_{k=n-2}^{n+2} b_{n,k}^{m,j} Y_{k,j}^* + \frac{3}{2} \dot{\gamma} C \sin^2 \theta \sin(2\phi) Y_{n,m}^* + \dot{\gamma} \left(\frac{1-C}{2} \right) i m Y_{n,m}^* \quad (3.29)$$

Now the noise part of (3.26) simplifies as follows:

$$\begin{aligned} & D_r g_{kj} \frac{\partial}{\partial \theta_k} (f_1 g_{1j} + f_2 g_{2j}) \\ &= D_r \left[g_{11} \frac{\partial}{\partial \theta} (f_1 g_{11} + f_2 g_{21}) + g_{12} \frac{\partial}{\partial \theta} (f_1 g_{12} + f_2 g_{22}) \right. \\ &\quad + g_{13} \frac{\partial}{\partial \theta} (f_1 g_{13} + f_2 g_{23}) + g_{21} \frac{\partial}{\partial \phi} (f_1 g_{11} + f_2 g_{21}) \\ &\quad \left. + g_{22} \frac{\partial}{\partial \phi} (f_1 g_{12} + f_2 g_{22}) + g_{23} \frac{\partial}{\partial \phi} (f_1 g_{13} + f_2 g_{23}) \right] \\ &= D_r \left[\frac{\partial^2}{\partial \theta^2} (Y_{n,m}^*) + \frac{1}{2 \sin^2 \theta} \left(2 \frac{\partial^2}{\partial \phi^2} (Y_{n,m}^*) + \sin(2\theta) \frac{\partial}{\partial \theta} (Y_{n,m}^*) \right) \right] \end{aligned}$$

$$\begin{aligned}
&= D_r N_{n,m} e^{-im\phi} \left[\frac{d^2}{d\theta^2} (P_n^m) + \frac{\cos\theta}{\sin\theta} \frac{dP_n^m}{d\theta} - \frac{m^2}{\sin^2\theta} P_n^m \right] \\
&= D_r N_{n,m} e^{-im\phi} \left[\frac{1}{\sin\theta} \frac{d}{d\theta} \left(\sin\theta \frac{dP_n^m}{d\theta} \right) - \frac{m^2}{\sin^2\theta} P_n^m \right] \\
&= -D_r n(n+1) N_{n,m} e^{-im\phi} P_n^m \\
&= -D_r n(n+1) Y_{n,m}^*. \tag{3.30}
\end{aligned}$$

In the above we have used the fact that P_n^m satisfies

$$\frac{1}{\sin\theta} \frac{d}{d\theta} \left(\sin\theta \frac{dP_n^m}{d\theta} \right) + \left[n(n+1) - \frac{m^2}{\sin^2\theta} \right] P_n^m = 0$$

Putting together (3.29) and (3.30) in (3.26) we get

$$\begin{aligned}
\frac{d}{dt} Y_{n,m}^* &= \dot{\gamma} C \sum_{j=m-2}^{m+2} \sum_{k=n-2}^{n+2} b_{n,k}^{m,j} Y_{k,j}^* + \frac{3}{2} \dot{\gamma} C \sin^2\theta \sin(2\phi) Y_{n,m}^* \\
&\quad + \dot{\gamma} \left(\frac{1-C}{2} \right) i m Y_{n,m}^* - D_r n(n+1) Y_{n,m}^*. \tag{3.31}
\end{aligned}$$

Taking now a second average over the probability density of the sharp values (θ, ϕ) we finally get

$$\begin{aligned}
\frac{d}{dt} \langle Y_{n,m}^* \rangle &= \dot{\gamma} C \sum_{j=m-2}^{m+2} \sum_{k=n-2}^{n+2} b_{n,k}^{m,j} \langle Y_{k,j}^* \rangle + \frac{3}{2} \dot{\gamma} C \langle \sin^2\theta \sin(2\phi) Y_{n,m}^* \rangle \\
&\quad + \dot{\gamma} \left(\frac{1-C}{2} \right) i m \langle Y_{n,m}^* \rangle - D_r n(n+1) \langle Y_{n,m}^* \rangle. \tag{3.32}
\end{aligned}$$

which is in the same form as (3.17) which was obtained through the diffusion equation. The extension to negative m is obvious as before. This demonstrates that an ensemble of equations (3.31) for the sharp $Y_{n,m}^*$ has the same dynamics as the moments $\langle Y_{n,m}^* \rangle$ as determined by the Fokker-Planck equation. Further, the equivalence between the two formulae justifies the form of the noise term we started with and demonstrates that Langevin equations (3.23), in ensemble, furnish an alternate but equivalent representation of the system governed by the Fokker-Planck equation (2.10). It also shows that in the Brownian regime we can use the time averaged Langevin equations to generate averages using the new method.

Note that the recurrence relation (3.32) for the moments are deterministic equations unlike the governing equations (3.23) for the orientations of individual spheroids, which are stochastic differential equations. This means that the current method expresses the dynamics of the moments in terms of deterministic equations. This is a major advantage from the computational point of view, since deterministic equations are far more suitable for simulations than stochastic ones as we demonstrate in the subsequent chapters.

Computation of moments

Having developed the Langevin equation for the evolution of the orientation behaviour of the spheroids in the suspension system under study, we now proceed to apply the Coffey *et al.* (1996) method of time-averaging the Langevin equations, to determine the equations for the temporal evolution of the various moments. In fact the moments are completely determined by the recurrence relations (3.32), but since the equations are difficult to solve, we now apply the same technique to generate the moment equations directly. It turns out that although these moments are governed by deterministic ordinary differential equations, which in itself is a significant advantage, they are nonetheless difficult to solve analytically. However, the methods of the previous chapters allow us to develop a computational technique to simulate the averages in pairs with comparative ease. Several advantages of this approach over existing computing methods are also discussed in this chapter.

4.1 The dynamics of the moments

In this section we describe how the equations governing the time evolution of the orientation moments can be developed based on the methods of the previous chapter. We shall study the dynamics of the three orientation moments $\langle u_3^2 \rangle = \langle \cos^2 \theta \rangle$, $\langle u_1 u_2 \rangle =$

$\langle \sin^2 \theta \sin \phi \cos \phi \rangle$, and $\langle u_1^2 u_2^2 \rangle = \langle \sin^4 \theta \sin^2 \phi \cos^2 \phi \rangle$ for a wide range of parameters using the new method and compare our results with those of Chen and Jiang (1999) and Chen and Koch (1996)

Each term in eq. (3.23) has dimension (1/time) and may be scaled with respect to D_r . The scaled form of the Langevin equation, in Cartesian co-ordinates is as follows.

$$\begin{aligned}\dot{u}_1 &= Pe C u_2 (1 - u_1^2) + Pe \left(\frac{1-C}{2} \right) u_2 + \Gamma_2(t) u_3 - \Gamma_3(t) u_2 \\ \dot{u}_2 &= -Pe C u_1 u_2^2 - Pe \left(\frac{1-C}{2} \right) u_1 + \Gamma_3(t) u_1 - \Gamma_1(t) u_3 \\ \dot{u}_3 &= -Pe C u_1 u_2 u_3 + \Gamma_1(t) u_2 - \Gamma_2(t) u_1.\end{aligned}$$

where $Pe = \dot{\gamma}/D_r$ is the Péclet number introduced earlier. Note that in the scaled form the Γ_i satisfy (3.19) with $D = 1$. When converted into spherical co-ordinates these equations become,

$$\begin{aligned}\dot{\theta} &= Pe C \sin \theta \cos \theta \sin \phi \cos \phi - \sin \phi \Gamma_1(t) + \cos \phi \Gamma_2(t) \\ \dot{\phi} &= -Pe C \sin^2 \phi - Pe \left(\frac{1-C}{2} \right) - \cot \theta \cos \phi \Gamma_1(t) \\ &\quad - \sin \phi \cot \theta \Gamma_2(t) + \Gamma_3(t)\end{aligned}\tag{4.1}$$

The above equations may now be time-averaged using eq. (3.22) to express them as an equation of motion for the sharp starting values. We retain the same notation of the random variables θ, ϕ for their sharp values at t . Following a procedure similar to that leading to eq. (3.26) we obtain for any orientation moment $\langle B(\theta, \phi) \rangle$, the following expression for the sharp values $B(\theta, \phi)$:

$$\frac{d}{dt} B(\theta, \phi) = f_1 h_1 + f_2 h_2 + g_{kj} \frac{\partial}{\partial \theta_k} (f_1 g_{1j} + f_2 g_{2j})\tag{4.2}$$

where $f_1 = \partial B / \partial \theta$, $f_2 = \partial B / \partial \phi$, $\theta_1 = \theta$ and $\theta_2 = \phi$ and h_1 and h_2 are the deterministic parts in (4.1). A set of these equations averaged over the density of the sharp values has the same evolution dynamics as $\langle B(\theta, \phi) \rangle$ and hence yields the equation of motion for the moment. We thus get the governing equations for the time evolution of the moments

$\langle u_3^2 \rangle$, $\langle u_1 u_2 \rangle$ and $\langle u_1^2 u_2^2 \rangle$:

$$\begin{aligned}
 \frac{d}{dt} \langle u_3^2 \rangle &= -\frac{d}{dt} \langle \cos^2 \theta \rangle \\
 &= \left(\frac{Pe}{4} \right) C \langle \sin^2 2\theta \sin 2\phi \rangle - 2(3 \langle \cos^2 \theta \rangle - 1), \\
 \frac{d}{dt} \langle u_1 u_2 \rangle &= \frac{d}{dt} \langle \sin^2 \theta \sin \phi \cos \phi \rangle \\
 &= 2CPe \langle \sin^2 \theta \cos^2 \theta \sin^2 \phi \cos^2 \phi \rangle - CPe \langle \sin^2 \theta \sin^2 \phi \cos 2\phi \rangle \\
 &\quad - Pe \left(\frac{1-C}{2} \right) \langle \sin^2 \theta \cos 2\phi \rangle - 3 \langle \sin^2 \theta \sin 2\phi \rangle, \\
 \frac{d}{dt} \langle u_1^2 u_2^2 \rangle &= \frac{d}{dt} \langle \sin^4 \theta \sin^2 \phi \cos^2 \phi \rangle \\
 &= 4CPe \langle \sin^4 \theta \cos^2 \theta \sin^3 \phi \cos^3 \phi \rangle \\
 &\quad - 2CPe \langle \sin^4 \theta \sin^3 \phi \cos \phi \cos 2\phi \rangle \\
 &\quad - Pe \left(\frac{1-C}{2} \right) \langle \sin^4 \theta \sin^2 \phi \cos 2\phi \rangle \\
 &\quad + 2 \langle \sin^2 \theta \rangle - 20 \langle \sin^4 \theta \sin^2 \phi \cos^2 \phi \rangle.
 \end{aligned} \tag{4.3}$$

The above system, as well as similar ones we might get for other moments, are generally hard to solve, either individually (because the equation may not be expressible in terms of the moment alone) or a set of them simultaneously (because the system may not be closed). For example, for $Pe \neq 0$ the above system of equations is not closed, but for $Pe = 0$ (i.e., in the absence of shear), they have a simple form, namely,

$$\begin{aligned}
 \frac{d}{dt} \langle u_3^2 \rangle &= -2(3 \langle u_3^2 \rangle - 1), \\
 \frac{d}{dt} \langle u_1 u_2 \rangle &= -\frac{3}{2} \langle u_1 u_2 \rangle, \\
 \frac{d}{dt} \langle u_1^2 u_2^2 \rangle &= 2 - 2 \langle u_3^2 \rangle - 20 \langle u_1^2 u_2^2 \rangle.
 \end{aligned}$$

Solving them we get the following results in the zero shear limit.

$$\begin{aligned}
 \langle u_3^2 \rangle &= \frac{1}{3} + k_1 e^{-6t}, \\
 \langle u_1 u_2 \rangle &= k_2 e^{-\frac{3}{2}t}, \\
 \langle u_1^2 u_2^2 \rangle &= \frac{1}{15} + k_3 e^{-2t} + k_4 e^{-20t},
 \end{aligned}$$

where the k_i are constants depending on the initial conditions. In the limit $t \rightarrow \infty$, the solutions approach, as expected, the values of the moments when the orientation distribution is uniform ($\psi = 1/4\pi$). An advantage of the equations (4.3) for the moments is that they are ordinary differential equations unlike the original Langevin equations for the orientations.

4.2 The computation of moments

We now discuss a computational technique for approximating the solutions of the moment equations in the general case. We note that in general the evolution of the moments is governed by two variables θ and ϕ and not by the moment itself. This necessitates considering two moment equations simultaneously for generating the averages. Our computational procedure is based on the fact that the dynamics of any moment $\langle B(\theta, \phi) \rangle$ can be captured by simulating an ensemble of equations (4.2) for the sharp values $B(\theta, \phi)$. Equivalently, we may set up the equations of motion for the tracer variables θ and ϕ and compute the averages dynamically by iterating a set of such equations.

To find the equations for the dynamics of the variables θ and ϕ , we proceed as follows. For the sharp values $B_1(\theta, \phi)$ and $B_2(\theta, \phi)$ of any two desired orientation averages, we may write from (4.2)

$$\begin{aligned} f_1 \dot{\theta} + f_2 \dot{\phi} &= f_1 h_1 + f_2 h_2 + g_{kj} \frac{\partial}{\partial \theta_k} (f_1 g_{1j} + f_2 g_{2j}), \\ f'_1 \dot{\theta} + f'_2 \dot{\phi} &= f'_1 h_1 + f'_2 h_2 + g_{kj} \frac{\partial}{\partial \theta_k} (f'_1 g_{1j} + f'_2 g_{2j}), \end{aligned} \quad (4.4)$$

where f_i are the partial derivatives of B_1 and f'_i those of B_2 . We can solve the above system for $\dot{\theta}$ and $\dot{\phi}$ assuming that the coefficient determinant $\Delta = f_1 f'_2 - f'_1 f_2$ is not zero,

$$\begin{aligned} \dot{\theta} &= h_1 + \frac{1}{\Delta} \left[f'_2 g_{kj} \frac{\partial}{\partial \theta_k} (f_1 g_{1j} + f_2 g_{2j}) - f_2 g_{kj} \frac{\partial}{\partial \theta_k} (f'_1 g_{1j} + f'_2 g_{2j}) \right] \\ \dot{\phi} &= h_2 - \frac{1}{\Delta} \left[f'_1 g_{kj} \frac{\partial}{\partial \theta_k} (f_1 g_{1j} + f_2 g_{2j}) - f_1 g_{kj} \frac{\partial}{\partial \theta_k} (f'_1 g_{1j} + f'_2 g_{2j}) \right]. \end{aligned} \quad (4.5)$$

This gives a system of two coupled ODE's and an ensemble of such systems for the sharp values θ and ϕ collectively determine the pair of averages B_1 and B_2 . Thus for each pair of moments for which Δ is non-zero, we consider an ensemble of systems of coupled ODE's of the type (4.5) for the tracer variables (θ, ϕ) over a set of sharp initial conditions and follow their trajectories to compute the temporal evolution of the moments.

To actually carry out the calculations, we first fix a set of finite but large number of sharp initial conditions for the random variables (θ, ϕ) distributed uniformly over the orientation space, with each initial condition representing a large number of random variables starting from that point. Accordingly we fix a positive integer n , say $n = 10$, and define n^2 squares in the $\theta\phi$ space $[0, \pi] \times [0, 2\pi]$ by the discrete points (θ_i, ϕ_i) , with

$$\left. \begin{aligned} \theta_i &= \cos^{-1}[(2i/n) - 1] \\ \phi_i &= 2\pi/n \end{aligned} \right\} i = 0, 1, \dots, n.$$

Each square $[\theta_i, \theta_{i+1}] \times [\phi_j, \phi_{j+1}]$ in the $\theta\phi$ space now corresponds to a region or bin of area $[\theta_i, \theta_{i+1}] \times [\phi_j, \phi_{j+1}] \sin \theta$ on the surface of the unit sphere. For a given pair of moments $B_1(\theta, \phi)$ and $B_2(\theta, \phi)$, we then start off with n^2 copies of the associated equations (4.5), each one with a different initial condition, the (i, j) th one taking the initial value (θ_{i0}, ϕ_{j0}) where,

$$\left. \begin{aligned} \theta_{i0} &= (\theta_i + \theta_{i+1})/2 \\ \phi_{j0} &= (\phi_j + \phi_{j+1})/2 \end{aligned} \right\} i, j = 0, 1, \dots, n$$

This corresponds to a set of tracer orientations directed approximately along the centres of the above bins and distributed almost uniformly in the orientation space (fig. 4.1). It may be noted that these initial conditions need not correspond to an initial orientation state of the actual particles in the suspension, but merely to a set of initial starting values for an ensemble of the sharp variables θ and ϕ evolving according to eq. (4.5) which together determine the moments $\langle B_1(\theta, \phi) \rangle$ and $\langle B_2(\theta, \phi) \rangle$.

ensemble
size
B.D
of
4.1
?

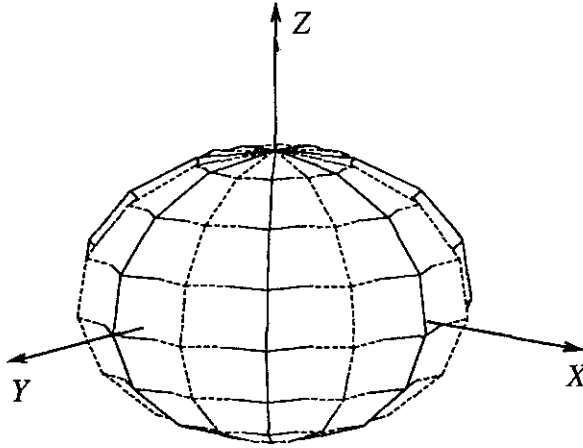


Figure 4.1: The discretization of the $\theta\phi$ space.

The sharp values (θ, ϕ) may themselves be considered a random variable with density $\psi(\theta, \phi, t)$ with sharp peaks at the sites of the vectors (θ, ϕ) at any instant. This gives the following estimate for the moment $\langle B_1(\theta, \phi) \rangle$ at that instant t ,

$$\begin{aligned} \langle B_1(\theta, \phi) \rangle &= \frac{\int \int B(\theta, \phi) \delta(\theta - \theta_{i_t}) \delta(\phi - \phi_{j_t}) d(\cos \theta) d\phi}{\int \int \delta(\theta - \theta_{i_t}) \delta(\phi - \phi_{j_t}) d(\cos \theta) d\phi} \\ &= \frac{1}{n^2} \sum_{i=1}^n \sum_{j=1}^n B(\theta_{i_t}, \phi_{j_t}) \end{aligned} \quad (4.6)$$

and a similar estimate for the moment $\langle B_2(\theta, \phi) \rangle$. The values $(\theta_{i_t}, \phi_{j_t})$ of the vectors (θ_i, ϕ_i) at the various time instances t are obtained by numerically integrating the n^2 equations (4.5) simultaneously. At the end of each iteration of the numerical integration, the numbers $B_1(\theta, \phi)$, $B_2(\theta, \phi)$ are calculated using the iterated values of each of (θ_i, ϕ_j) and summed up according to formula (4.6) to obtain an estimate for the moments for the time instance of that iteration. These computations are repeated for successive time steps using, at each step, the values (θ_i, ϕ_j) obtained from numerical integration, and continued until the values of the moments stabilize. This procedure generates a numerical approximation to the dynamics of the moments B_1 and B_2 .

Moments	Partial derivatives	Noise terms
$\langle u_3^2 \rangle$	$\begin{cases} f_1 = -\sin 2\theta \\ f_2 = 0 \end{cases}$	$-2(3 \cos^2 \theta - 1)$
$\langle u_1 u_2 \rangle$	$\begin{cases} f_1 = -\sin \theta \cos \theta \sin(2\phi) \\ f_2 = \sin^2 \theta \cos(2\phi) \end{cases}$	$\sin^2 \theta \sin(2\phi)$
$\langle u_1^2 u_2^2 \rangle$	$\begin{cases} f_1 = 4 \sin^3 \theta \cos \theta \sin^2 \phi \cos^2 \phi \\ f_2 = \sin^4 \theta \sin(2\phi) \cos(2\phi) \end{cases}$	$\begin{aligned} &2 \sin^2 \theta \\ &-20 \sin^4 \phi \cos^2 \phi \sin^2 \theta \end{aligned}$

Table 4.1: The functions for generating moments

4.3 Results and discussion

We applied the computational technique of the previous section to the moments in pairs of $\langle u_3^2 \rangle$ and $\langle u_1^2 u_2^2 \rangle$, $\langle u_1 u_2 \rangle$ and $\langle u_2^2 \rangle$ and $\langle u_3^2 \rangle$ and $\langle u_1 u_2 \rangle$ for various values of Pe , keeping the number of initial conditions at $n^2 = 100$. We used the integrator `odeint` of Press *et al.* (1986) with a tolerance of 0.001% to integrate equations (4.5). This integrator features adaptive step-size control, so the step-size of the integration is automatically adjusted to achieve an accuracy to within the tolerance specified. Note that the coefficient determinant Δ does not vanish for the pairs of moments we have chosen. The simulations may run into trouble if any of the subsequent iterations approach a singularity of (4.5), but our computations did not lead to any such problems. Table 4.1 gives the partial derivatives and the time-averaged noise terms for the the above sets of functions.

The computations were repeated changing the number of initial conditions from 64 to 2500, but the results practically stabilised for $n^2 = 100$ onwards and so n^2 was fixed at 100 in subsequent computations. Table 4.2 shows the variation of the moments with the number of initial conditions for typical values of the parameters. With $Pe = 0$, the computations reproduced the theoretical values 1/3, 0 and 1/15 for $\langle u_3^2 \rangle$, $\langle u_1 u_2 \rangle$

n^2	$Pe = 0.0$		$Pe = 1.0$		$Pe = 100.0$		$Pe = 500.0$	
	$\langle u_3^2 \rangle$	$\langle u_1 u_2 \rangle$	$\langle u_3^2 \rangle$	$\langle u_1 u_2 \rangle$	$\langle u_3^2 \rangle$	$\langle u_1 u_2 \rangle$	$\langle u_3^2 \rangle$	$\langle u_1 u_2 \rangle$
64	0.3333	0.0000	0.3293	0.0532	0.2376	0.1325	0.1763	0.0950
81	0.3333	0.0000	0.3280	0.0473	0.2082	0.1199	0.1537	0.0778
100	0.3333	0.0000	0.3288	0.0322	0.1730	0.0910	0.1285	0.0576
121	0.3333	0.0000	0.3283	0.0321	0.1721	0.0907	0.1294	0.0598
144	0.3333	0.0000	0.3285	0.0317	0.1728	0.0911	0.1277	0.0568

Table 4.2: The steady state values of the moments for various initial conditions at different values of Pe .

and $\langle u_1^2 u_2^2 \rangle$ respectively. Also we had scaled time with respect to $1/D_r$, which makes the right side of (4.5) large for larger values of Pe . Hence to minimize the round of errors we changed the scaling to $1/\dot{\gamma}$ for $Pe > 10$ while for $Pe < 10$ the earlier scaling was retained. The results obtained for Pe between 0 and 1000 are plotted in fig.4.2. These results are in good agreement with those obtained from other methods, namely the spherical harmonics method of Chen and Koch (1996) and the finite difference method of Chen and Jiang (1999) (compare fig. 3 of Chen and Jiang (1999)). An advantage of this method is the internal check it provides on the computations by way of making one average common to each pair of averages. Thus in our simulations we paired $\langle u_3^2 \rangle$ with both $\langle u_1 u_2 \rangle$ and $\langle u_2^2 u_3^2 \rangle$ and found that the results were consistent.

With a given number of initial conditions, the time taken by the simulations to settle down to steady values depends both on the Péclet number and the pair of averages chosen. Table 4.3 summarises the time data for our computations on a Pentium III, 500 MHz, 128 MB RAM PC, with 100 initial conditions for typical values of Pe . It seems that the current method offers significant improvement in terms of the computation time of various moments compared to the other methods (Chen and Jiang, 1999). For example, the finite difference method of Chen and Jiang (1999) takes 50 minutes on the SGI Onyx VTX computer, while the present method takes 32 min. in a comparatively

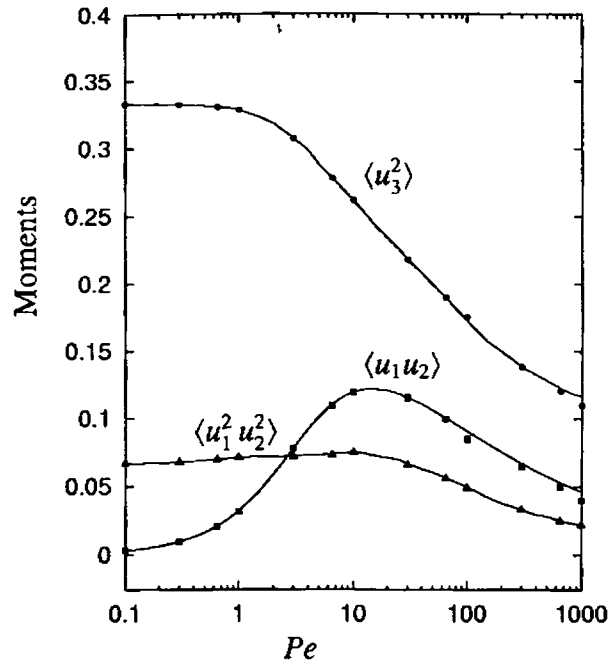


Figure 4.2: Plot of the orientation moments vs. Péclet number. The symbols are the results from the finite difference method and the spherical harmonics method.

Pe	$\langle u_3^2 \rangle$ & $\langle u_1 u_2 \rangle$	$\langle u_3^2 \rangle$ & $\langle u_1^2 u_2^2 \rangle$
0.0	1 s.	1 s.
1.0	2 s.	2 s.
10.0	4 s.	10 s.
50.0	7 s.	823 s.
100.0	10 s.	1920 s.
250.0	28 s.	2030 s.
500.0	86 s.	2800 s.

Table 4.3: Time taken (in seconds) to compute the moments on a 500MHz, 128 RAM, Pentium III PC for two different pairs at various Pe

less powerful computer. Another advantage of this approach is that it can be applied for an arbitrary range of Péclet number, with only a possible change of scaling, unlike

earlier methods which apply only to specific ranges of the parameters. This feature of the Langevin method can be used to advantage in regions where the normal methods fail due to changes in the fundamental character of the diffusion equation. An example is the region of very small Brownian motion, where the problem becomes singular in the limit and hence intractable using normal methods. The Langevin method is suitable in such cases as we will illustrate in later chapters.

Rheology and external forcing

In this chapter we shall study how the generalised Langevin equation can be used to model the rheology of a suspension under the action of an external field. External forces are usually the result of electric or magnetic fields acting on suspension particles which are dipolar having electric or magnetic charges. Ferrofluids are an example, which contain small single domain particles in a non-magnetic solvent. They have many industrial applications such as rotary seals, inertia dampers, magnetic domain detection and biomedical uses like concentration of drugs at body sites (Strand and Kim, 1992). If brought under the influence of a magnetic field, the particles in a ferrofluid no longer rotate freely with the fluid due to the action of the external field, and this introduces additional stress. Similarly charged polymers in aqueous solutions can be modelled by a long dipolar fibre. The macroscopic behaviour of such suspensions is substantially affected by the orientational torques exerted by an external electric field which tends to align the particle dipole axis along the field direction. As an example of natural phenomena analogues to the above, Pedley and Kessler (1990) refer to certain bacteria containing magnetic dipoles and various species of algae possessing an asymmetric internal mass distribution whose swimming directions are affected by gravity. All of these orientational effects can be collectively modelled by the response of a permanent dipole exposed to an external field.

The effect of fluid microstructure on macroscopic behaviour is usually measured by determining the stress tensor of the suspension. We shall determine the stress tensor in a sheared suspension of spheroids under the action of hydrodynamic forces due to the flow, Brownian rotations and an external force field on dipole moments of the particles of the suspension. Most of the analyses of external fields interacting with particle dipole moments are limited to the case of weak shear or of weak diffusion (Hall and Busenberg, 1969; Brenner, 1970; Brenner and Weissman, 1972; Jansons, 1983), except the work of Strand and Kim (1992) who present results for a wide range of shear and Brownian parameters as well as external field strength. Since the measurable stress components such as the first and second normal stress differences can be expressed in terms of orientation moments, the methods of the previous chapter can be adapted to compute these bulk properties for a wide range of parameters. We shall closely follow the work of Strand and Kim (1992), and compare our results with theirs.

5.1 The effect of the external field on particle orientation

As mentioned previously, an external orientational torque on a particle can arise from several sources;

- the interaction of an external magnetic field and the magnetic moment of a ferromagnetic particle,
- the response of an electric dipole induced on a charged particle to an electric field,
- the interaction of a gravitational field and a suspension particle possessing a gravitational dipole due to an asymmetric internal mass distribution.

In all the above cases the external field can be modelled as the cross product of the particle dipole moment \mathbf{m} and the uniform external field vector \mathbf{H} ;

$$\mathbf{T}^{\text{ext}} = \mathbf{m} \times \mathbf{H}$$

The dipole moment \mathbf{m} is assumed to be parallel to the particle symmetry axis so that we can write

$$\mathbf{m} = m\mathbf{u}$$

where m is the magnitude of the dipole moment. The conservation of angular momentum now gives (cf. eq. (2.4))

$$\mathcal{T}^{\text{hyd}} + \mathcal{T}^{\text{ext}} = 0.$$

From this we get the new expression for the angular velocity

$$\boldsymbol{\omega} = \boldsymbol{\Omega} + C[\mathbf{u} \times (\mathbf{E} \cdot \mathbf{u})] + \zeta_{\perp}^{-1} \mathbf{m} \times \mathbf{H}$$

and the equation for the orientation becomes (cf. eq. (2.8)),

$$\dot{\mathbf{u}} = \boldsymbol{\Omega} \times \mathbf{u} + C[\mathbf{u} \times (\mathbf{E} \cdot \mathbf{u})] \times \mathbf{u} + \zeta_{\perp}^{-1} \mathbf{m} \times \mathbf{H} \times \mathbf{u}.$$

The effect of Brownian motion term eq. (3.23) can now be included by superposition, giving

$$\dot{\mathbf{u}} = \boldsymbol{\Omega} \times \mathbf{u} + C[\mathbf{u} \times (\mathbf{E} \cdot \mathbf{u})] \times \mathbf{u} + \zeta_{\perp}^{-1} \mathbf{m} \times \mathbf{H} \times \mathbf{u} + \boldsymbol{\Gamma} \times \mathbf{u}. \quad (5.1)$$

where the components of $\boldsymbol{\Gamma}$ satisfy eqs. (3.19). This is the full Langevin equation for particle orientation, in the presence of constant external forcing and Brownian diffusion.

In Cartesian co-ordinates these equations become

$$\begin{aligned} \dot{u}_1 &= \dot{\gamma} C u_2 (1 - u_1^2) + \dot{\gamma} \left(\frac{1 - C}{2} \right) u_2 \\ &\quad + \frac{m}{\zeta_{\perp}} [u_3 (u_3 \bar{h}_1 - u_1 \bar{h}_3) - u_2 (u_1 \bar{h}_2 - u_2 \bar{h}_1)] + \Gamma_2(t) u_3 - \Gamma_3(t) u_2 \\ \dot{u}_2 &= -\dot{\gamma} C u_1 u_2^2 - \dot{\gamma} \left(\frac{1 - C}{2} \right) u_1 \\ &\quad + \frac{m}{\zeta_{\perp}} [u_1 (u_1 \bar{h}_2 - u_2 \bar{h}_1) - u_3 (u_2 \bar{h}_3 - u_3 \bar{h}_2)] + \Gamma_3(t) u_1 - \Gamma_1(t) u_3 \\ \dot{u}_3 &= -\dot{\gamma} C u_1 u_2 u_3 \\ &\quad + \frac{m}{\zeta_{\perp}} [u_2 (u_2 \bar{h}_3 - u_3 \bar{h}_2) - u_1 (u_3 \bar{h}_1 - u_1 \bar{h}_3)] - \Gamma_3(t) u_1 - \Gamma_1(t) u_3 \end{aligned} \quad (5.2)$$

where the \bar{h}_i denote the Cartesian components of \mathbf{H} .

5.2 The stress tensor

The averaged bulk fluid stress in a suspension is the sum of the Newtonian stress τ^s , which is the stress of the solvent in the absence of any particles and the particle stress σ^p contributed by the suspension particles alone (Batchelor, 1970; Hinch and Leal, 1972);

$$\boldsymbol{\sigma} = \boldsymbol{\tau}^s + \boldsymbol{\sigma}^p \quad (5.3)$$

The Newtonian stress can be expressed in terms of pressure p , the viscosity η_s of the solvent and the rate of strain tensor \mathbf{E} thus;

$$\boldsymbol{\tau}^s = -p\boldsymbol{\delta} + 2\eta_s\mathbf{E}$$

In the absence of force fields, the stress tensor of a Newtonian fluid is symmetric, but in a suspension of dipolar particles the particle stress will be asymmetric in general and can, in fact, be written as the sum of symmetric and antisymmetric parts;

$$\boldsymbol{\sigma}^p = \boldsymbol{\sigma}^s + \boldsymbol{\sigma}^a$$

The antisymmetric part of the stress depends on the external field strength and the volume concentration Φ of particles thus (Strand and Kim, 1992);

$$\boldsymbol{\sigma}^a = 3\eta_s\Phi D_0 \left(\frac{m}{kT} \right) \langle \mathbf{u}\mathbf{H}_\perp - \mathbf{H}_\perp\mathbf{u} \rangle$$

The term \mathbf{H}_\perp is the projection of \mathbf{H} in the direction perpendicular to \mathbf{u} , $\mathbf{H}_\perp = \mathbf{H} \cdot (\boldsymbol{\delta} - \mathbf{u}\mathbf{u})$ and D_0 denotes the rotary diffusivity of a sphere of volume equal to that of the particle.

The symmetric part of the stress can be given in terms of the second and fourth order moments (Brenner, 1974; Hinch and Leal, 1972; Jansons, 1983);

$$\begin{aligned} \boldsymbol{\sigma}^s = 2\eta_s\Phi \left\{ 2A_H\mathbf{E} : \langle \mathbf{u}\mathbf{u}\mathbf{u}\mathbf{u} \rangle + 2B_H \left(\mathbf{E} \cdot \langle \mathbf{u}\mathbf{u} \rangle + \langle \mathbf{u}\mathbf{u} \rangle \cdot \mathbf{E} - \frac{2}{3}\boldsymbol{\delta}\mathbf{E} : \langle \mathbf{u}\mathbf{u} \rangle \right) \right. \\ \left. + C_H\mathbf{E} + F_H D_r \left(\langle \mathbf{u}\mathbf{u} \rangle - \frac{1}{3}\boldsymbol{\delta} \right) - \frac{1}{6}F_H D_r \left(\frac{m}{kT} \right) \langle \mathbf{H}_\perp\mathbf{u} + \mathbf{u}\mathbf{H}_\perp \rangle \right\}. \end{aligned}$$

Combining the various expressions and substituting back in eq. (5.3) we get the following for the dimensional stress in the suspension. Here A_H , B_H , C_H and F_H are functions depending on the shape of the particles, general expressions for which are presented in the next section.

$$\begin{aligned}
 \sigma = & -p\delta + 2\eta_s \mathbf{E} + 2\eta_s \Phi \left\{ 2A_H \mathbf{E} : \langle \mathbf{u}\mathbf{u}\mathbf{u}\mathbf{u} \rangle \right. \\
 & + 2B_H \left(\mathbf{E} \cdot \langle \mathbf{u}\mathbf{u} \rangle + \langle \mathbf{u}\mathbf{u} \rangle \cdot \mathbf{E} - \frac{2}{3} \delta \mathbf{E} : \langle \mathbf{u}\mathbf{u} \rangle \right) + \\
 & C_H \mathbf{E} + F_H D_r \left(\langle \mathbf{u}\mathbf{u} \rangle - \frac{1}{3} \delta \right) \\
 & \left. + 3D_0 \frac{m}{k_B T} \left[\frac{(1-C)}{2} \langle \mathbf{u}\mathbf{H}_\perp \rangle - \frac{(1+C)}{2} \langle \mathbf{H}_\perp \mathbf{u} \rangle \right] \right\}
 \end{aligned} \tag{5.4}$$

5.3 The stress coefficients

The expressions for the various coefficients appearing in eq. (5.4) have been listed by a number of authors and are presented here for spheroids, keeping the notations and terminology as in Strand and Kim (1992) and Hinch and Leal (1972). These stress coefficients depend on certain elliptic integrals, expressions for which are also given.

$$\begin{aligned}
 A_H &= \frac{J_3}{I_3 J_1} + \frac{1}{I_3} - \frac{2}{I_1} \\
 B_H &= \frac{1}{I_1} - \frac{1}{I_3} \\
 C_H &= \frac{2}{I_3} \\
 F_H &= \frac{6(r^2 - 1)}{r^2 K_3 + K_1}
 \end{aligned} \tag{5.5}$$

The quantities I_1 , I_3 , J_1 , J_3 , K_1 and K_3 are elliptic integrals which can be evaluated for spheroids as follows.

$$\begin{aligned}
 I_1 &= \int_0^\infty \frac{ab^2(a^2 + b^2) d\lambda}{(a^2 + \lambda)^{3/2}(b^2 + \lambda)^2} = \frac{2(r^2 + 1)}{(r^2 - 1)^2} \left[1 + \frac{r^2}{2} + \frac{3rA_s}{4} \right] \\
 I_3 &= \int_0^\infty \frac{2ab^4 d\lambda}{(a^2 + \lambda)(b^2 + \lambda)^3} = \frac{r^2}{2(r^2 - 1)^2} \left[2r^2 - 5 - \frac{3A_s}{2r} \right]
 \end{aligned}$$

Coeff.	$r \rightarrow \infty$	$r = 1 + \epsilon (\epsilon \rightarrow 0)$
A_H	$\frac{r^2}{4(\ln(2r) - 3/2)}$	$\frac{395}{294}\epsilon^2$
B_H	$\frac{3 \ln(2r) - 11/2}{r^2}$	$\frac{15}{28}\epsilon - \frac{895}{1175}\epsilon^2$
C_H	2	$\frac{5}{2} - \frac{5}{7}\epsilon + \frac{235}{294}\epsilon^2$
F_H	$\frac{3r^2}{\ln(2r) - 1/2}$	9ϵ

Table 5.1: The limiting values of the stress coefficients.

$$J_1 = \int_0^\infty \frac{ab^2(a^2 + b^2)\lambda d\lambda}{(a^2 + \lambda)^{3/2}(b^2 + \lambda)^2} = \frac{2r^2}{(r^2 - 1)^2} \left[-\frac{3}{2} - \frac{(2r^2 + 1)A_s}{4r} \right]$$

$$J_3 = \int_0^\infty \frac{2ab^4 d\lambda}{(a^2 + \lambda)(b^2 + \lambda)^3} = \frac{2r^2}{(r^2 - 1)^2} \left[\frac{r^2}{4} + \frac{1}{8} + \frac{(4r^2 - 1)A_s}{16r} \right]$$

$$K_1 = \int_0^\infty \frac{ab^2 d\lambda}{(a^2 + \lambda)^{1/2}(b^2 + \lambda)^2} = \frac{r}{(r^2 - 1)} \left[r + \frac{A_s}{2} \right]$$

$$K_3 = \int_0^\infty \frac{ab^2 d\lambda}{(a^2 + \lambda)^{3/2}(b^2 + \lambda)} = \frac{r}{(r^2 - 1)} \left[-\frac{2}{r} - A_s \right]$$

The factor A_s has different forms based on whether the spheroids are prolate ($r > 1$) or oblate ($r < 1$);

$$A_s = \frac{-2 \cosh^{-1}(r)}{(r^2 - 1)^{1/2}} = \frac{1}{(r^2 - 1)^{1/2}} \ln \left[\frac{r - (r^2 - 1)^{1/2}}{r + (r^2 - 1)^{1/2}} \right], \quad (r > 1)$$

$$A_s = \frac{-2 \cos^{-1}(r)}{(1 - r^2)^{1/2}}, \quad (r < 1)$$

For general spheroids the coefficients depend on the aspect ratio in a complicated manner, but for some limiting cases such as spheres and long fibres, these expressions can be considerably simplified. The limiting values of the coefficients for long fibres ($r \rightarrow \infty$) and near spheres ($r \rightarrow 1$) are enlisted in Table 5.1 (Strand and Kim, 1992). Fig. 5.1 shows a plot of the various stress coefficients for various values of r .

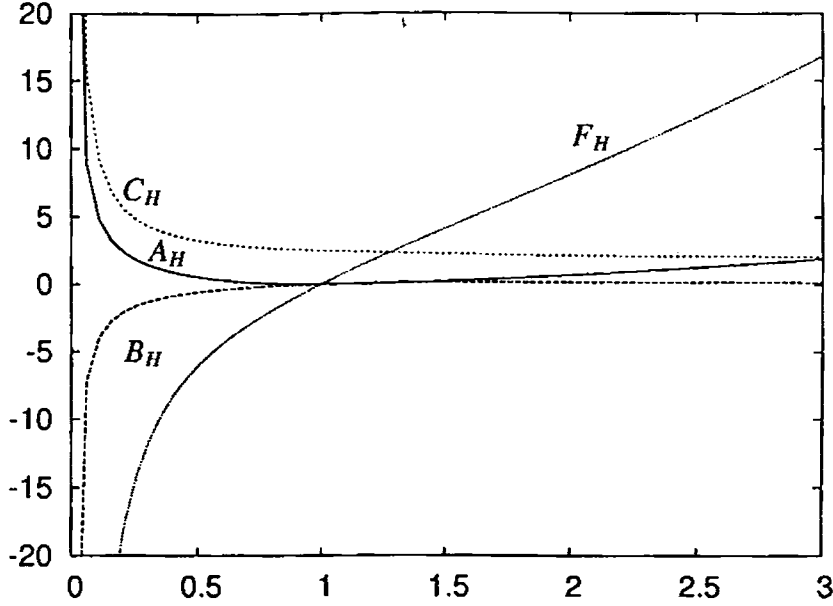


Figure 5.1: The stress coefficients

5.4 Material functions for dilute suspension

The rheological properties of a suspension are usually expressed in terms of material functions, such as the apparent viscosities and the first and second normal stress differences. For dilute suspensions these quantities involve the limit $\Phi \rightarrow 0$ and are therefore called intrinsic properties. The expressions for these rheological properties for the case of simple shear, defined below, can be obtained from eq. (5.4) by using eq. (2.6).

$$\begin{aligned}
 [\eta_1] &= \lim_{\Phi \rightarrow 0} \left(\frac{\sigma_{xy} - \eta_s \dot{\gamma}}{\Phi \eta_s \dot{\gamma}} \right) \\
 &= 4A_H \langle u_1^2 u_2^2 \rangle + 2B_H \langle u_1^2 + u_2^2 \rangle + C_H \\
 &\quad + \left(\frac{2F_H}{3CPe} \right) \left[C \langle (\Sigma k_i u_i) u_1 u_2 \rangle + \left(\frac{1-C}{2} \right) \langle u_1 \rangle k_2 - \left(\frac{1+C}{2} \right) \langle u_2 \rangle k_1 \right] \quad (5.6)
 \end{aligned}$$

$$\begin{aligned}
 [\eta_2] &= \lim_{\Phi \rightarrow 0} \left(\frac{\sigma_{yx} - \eta_s \dot{\gamma}}{\Phi \eta_s \dot{\gamma}} \right) \\
 &= 4A_H \langle u_1^2 u_2^2 \rangle + 2B_H \langle u_1^2 + u_2^2 \rangle + C_H \\
 &\quad + \left(\frac{2F_H}{3CPe} \right) \left[C \langle (\Sigma k_i u_i) u_1 u_2 \rangle + \left(\frac{1-C}{2} \right) \langle u_2 \rangle k_1 - \left(\frac{1+C}{2} \right) \langle u_1 \rangle k_2 \right] \quad (5.7)
 \end{aligned}$$

$$\begin{aligned}
[\tau_1] &= \lim_{\Phi \rightarrow 0} \left(\frac{\sigma_{xx} - \sigma_{zz}}{\Phi \eta_s \dot{\gamma}} \right) \\
&= 4A_H (\langle u_1^3 u_2 \rangle - \langle u_1 u_2 u_3^2 \rangle) + 4B_H \langle u_1 u_2 \rangle \\
&\quad + \left(\frac{2F_H}{3Pe} \right) \left[\langle (\sum k_i u_i) u_1^2 \rangle - \langle (\sum k_i u_i) u_3^2 \rangle + \langle k_3 u_3 \rangle - \langle k_1 u_1 \rangle \right]
\end{aligned} \tag{5.8}$$

$$\begin{aligned}
[\tau_2] &= \lim_{\Phi \rightarrow 0} \left(\frac{\sigma_{yy} - \sigma_{zz}}{\Phi \eta_s \dot{\gamma}} \right) \\
&= 4A_H (\langle u_1 u_2^3 \rangle - \langle u_1 u_2 u_3^2 \rangle) + 4B_H \langle u_1 u_2 \rangle \\
&\quad + \left(\frac{2F_H}{3Pe} \right) \left[\langle (\sum k_i u_i) u_2^2 \rangle - \langle (\sum k_i u_i) u_3^2 \rangle + \langle k_3 u_3 \rangle - \langle k_2 u_2 \rangle \right]
\end{aligned} \tag{5.9}$$

In obtaining the above forms for the intrinsic properties from eq. (5.4) we have followed the scaling of Strand and Kim (1992) to make comparisons easier, namely, time is scaled with respect to $6D_r$ and force with respect to kT . The external force is assumed constant (ie, without fluctuations), the scaled dimensionless form of which is denoted by k in the above equations with $k = mH/k_B T$. We have also used the fact that $D_0/D_r = F_H/(9C)$ to clear the expressions of the constant D_0 . In the scaled form the Langevin equations for the orientation behaviour of the spheroids, eq. (5.2), after being converted to spherical co-ordinates, take the following form

$$\begin{aligned}
\dot{\theta} &= h_1 - \sin \phi \Gamma_1(t) + \cos \phi \Gamma_2(t) \\
\dot{\phi} &= h_2 - \cot \theta \cos \phi \Gamma_1(t) - \sin \phi \cot \theta \Gamma_2(t) + \Gamma_3(t)
\end{aligned} \tag{5.10}$$

where h_1 and h_2 are the deterministic parts given by (cf. eq. (4.1))

$$\begin{aligned}
h_1 &= \left(\frac{Pe}{6} \right) C \sin \theta \cos \theta \sin \phi \cos \phi \\
&\quad + \frac{1}{6} (k_1 \cos \theta \cos \phi + k_2 \cos \theta \sin \phi - k_3 \sin \theta) \\
h_2 &= -\left(\frac{Pe}{6} \right) C \sin^2 \phi - \left(\frac{Pe}{6} \right) \left(\frac{1-C}{2} \right) \\
&\quad + \frac{1}{6} (-k_1 \sin \phi + k_2 \cos \phi) \left(\frac{1}{\sin \theta} \right) - \cot \theta \cos \phi \Gamma_1(t)
\end{aligned} \tag{5.11}$$

Note that the Gaussian random variables $\Gamma_i(t)$ now satisfy, after scaling, eq. (3.19) with $D = 1/6$;

$$\overline{\Gamma_j(t)} = 0, \quad \overline{\Gamma_i(t) \Gamma_j(t')} = \frac{1}{3} \delta_{ij} \delta(t - t').$$

We now evaluate the intrinsic viscosity $[\eta] = [\eta_1]$ for a number of ranges of k and Pe and compare the results with those of Strand and Kim (1992) and of Brenner and Weissman (1972). To compute the various orientation moments appearing on the right of (5.6), we revert to the techniques developed in section 4.2. In the new scaling the equation eq. (4.2) for the sharp value $B(\theta, \phi)$ corresponding to any moment $\langle B(\theta, \phi) \rangle$ modifies to

$$\frac{d}{dt}B(\theta, \phi) = f_1 h_1 + f_2 h_2 + \frac{1}{6}g_{kj} \frac{\partial}{\partial \theta_k} (f_1 g_{1j} + f_2 g_{2j}) \quad (5.12)$$

We note that the deterministic parts h_1 and h_2 in the foregoing equation are common to all pairs of moments and are given by eq. (5.11), while the other terms vary with the choice of moment. Table (5.2) lists the various moments required in the evaluation of the intrinsic viscosity and the corresponding noise terms appearing in eq. (5.12).

The computational technique, as described in section 4.2, requires considering the moments in pairs and simulating an ensemble of the following associated equations (notations as in eq. (4.5))

$$\begin{aligned} \dot{\theta} &= h_1 + \frac{1}{6\Delta} \left[f_2' g_{kj} \frac{\partial}{\partial \theta_k} (f_1 g_{1j} + f_2 g_{2j}) - f_2 g_{kj} \frac{\partial}{\partial \theta_k} (f_1' g_{1j} + f_2' g_{2j}) \right] \\ \dot{\phi} &= h_2 - \frac{1}{6\Delta} \left[f_1' g_{kj} \frac{\partial}{\partial \theta_k} (f_1 g_{1j} + f_2 g_{2j}) - f_1 g_{kj} \frac{\partial}{\partial \theta_k} (f_1' g_{1j} + f_2' g_{2j}) \right]. \end{aligned}$$

The choice of the pairs is made based on the symmetry in the noise terms (Table 5.2) and the condition that Δ be not identically zero for the chosen pairs. The pairs chosen in our simulations are also shown in Table 5.2. As in the previous chapter, the number of initial conditions were kept at $n^2 = 100$ at which the results more or less stabilized.

Figure 5.2 shows plots of the intrinsic viscosity $[\eta_1]$ verses the external field strength k for a fixed shear rate $Pe = 2$, and two different external field orientations. The azimuthal direction ϕ is held at 90° while the polar directions are 45° and 90° . The results for three different aspect ratios are shown, prolate spheroids with $r = 1.6$, oblate spheroids with $r = 0.4$ and spheres. The calculations are greatly simplified for spheres for which $A_H = B_H = F_H = 0$, $C_H = 5/2$ and $F_H/Pe = 9/2$ (see table 5.1). These results are

Moments	Noise terms
$\begin{cases} \langle u_1^2 u_2^2 \rangle \\ \langle u_3^2 \rangle \end{cases}$	$\begin{cases} 2 \sin^2 \theta - 20 \sin^4 \theta \sin^2 \phi \cos^2 \phi \\ 2(3 \cos^2 \theta - 1) \end{cases}$
$\begin{cases} \langle u_1^2 \rangle \\ \langle u_2^2 \rangle \end{cases}$	$\begin{cases} 2 - 6 \sin^2 \theta \cos^2 \phi \\ 2 - 6 \sin^2 \theta \cos^2 \phi \end{cases}$
$\begin{cases} \langle u_1^2 u_2 \rangle \\ \langle u_1 u_2^2 \rangle \end{cases}$	$\begin{cases} 2 \sin \theta \sin \phi - 12 \sin^3 \theta \sin \phi \cos^2 \phi \\ 2 \sin \theta \cos \phi - 12 \sin^3 \theta \cos \phi \sin^2 \phi \end{cases}$
$\begin{cases} \langle u_1 u_2 u_3 \rangle \\ \langle u_3^3 \rangle \end{cases}$	$\begin{cases} -6 \cos \theta \sin^2 \theta \sin 2\phi \\ -3(\cos \theta + \cos 3\theta) \end{cases}$
$\begin{cases} \langle u_1 \rangle \\ \langle u_2 \rangle \end{cases}$	$\begin{cases} -2 \sin \theta \cos \phi \\ -2 \sin \theta \sin \phi \end{cases}$
$\begin{cases} \langle u_1 u_2 \rangle \\ \langle u_3^2 \rangle \end{cases}$	$\begin{cases} -3 \sin^2 \theta \sin 2\phi \\ -2(3 \cos^2 \theta - 1) \end{cases}$
$\begin{cases} \langle u_1 u_2^3 \rangle \\ \langle u_1^3 u_2 \rangle \end{cases}$	$\begin{cases} 3 \sin^2 \theta \sin 2\phi - 10 \sin^4 \theta \sin^2 \phi \sin 2\phi \\ 3 \sin^2 \theta \sin 2\phi - 10 \sin^4 \theta \cos^2 \phi \sin 2\phi \end{cases}$
$\begin{cases} \langle u_1^2 u_3 \rangle \\ \langle u_3 u_2^2 \rangle \end{cases}$	$\begin{cases} 2 \cos \theta - 12 \sin^2 \theta \cos^2 \phi \cos \theta \\ 2 \cos \theta - 12 \sin^2 \theta \sin^2 \phi \cos \theta \end{cases}$
$\begin{cases} \langle u_1^3 \rangle \\ \langle u_2^3 \rangle \end{cases}$	$\begin{cases} 6 \sin \theta \cos \phi - 12 \sin^3 \theta \cos^3 \phi \\ 6 \sin \theta \sin \phi - 12 \sin^3 \theta \sin^3 \phi \end{cases}$

Table 5.2: The various moments in the expressions for the rheological parameters and the corresponding noise terms

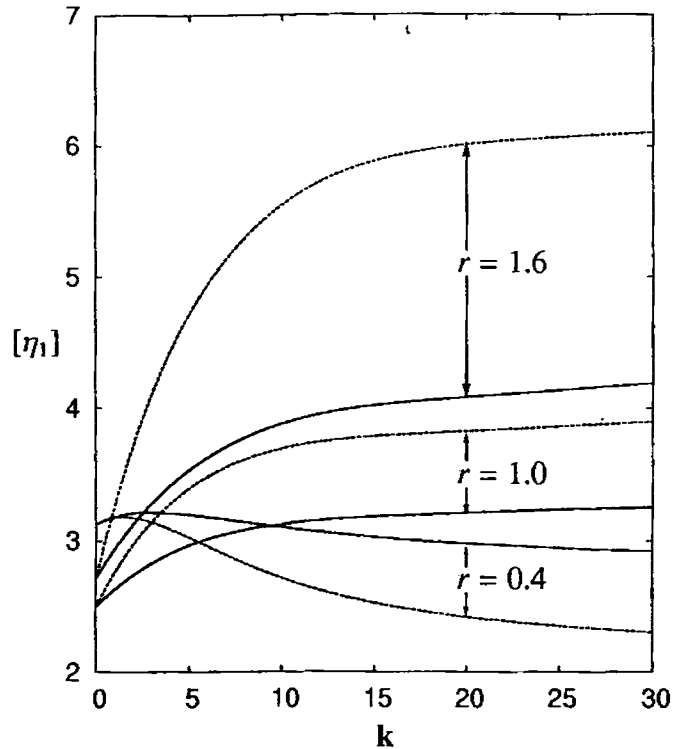


Figure 5.2: Plot of intrinsic viscosity $[\eta_1]$ for dipolar suspensions for various strengths of the external field, for spheroids of aspect ratio $r=0.4$, 1.0 and 1.6 . Results for $\mathbf{k} \parallel (0, 1, 1)$ and $\mathbf{k} \parallel (0, 1, 0)$ are shown. Compare with fig. 2 of Strand and Kim (1992)

in good agreement with those of Strand and Kim (1992) and Brenner and Weissman (1972) (see Fig. 2 in Strand and Kim (1992)). For external force fields higher (> 5) $[\eta_1]$ stabilizes rapidly to the values shown in the figure, but for smaller field strengths it takes longer for the values to stabilise.

The effect of the Brownian and shear parameters on the intrinsic viscosity $[\eta_1]$ are plotted in Fig. 5.3 for spheroids of aspect ratio $r=0.4$, 1.0 and 1.6 at two different field orientations keeping the strength of the external field constant at $k = 1$. A comparison with fig. 3 in Strand and Kim (1992) shows that the results are in good agreement with those obtained by the spherical harmonics method.

usual magnitude?

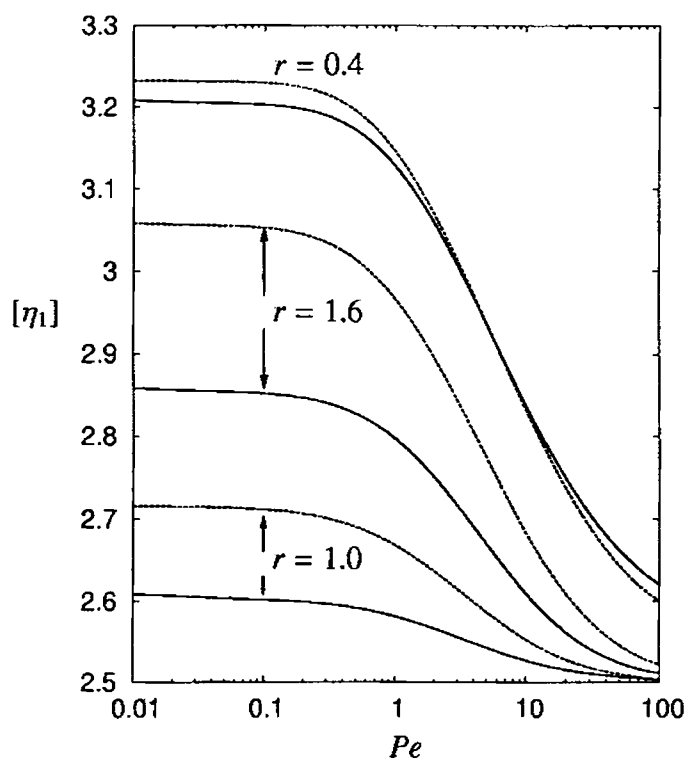


Figure 5.3: Plot of intrinsic viscosity $[\eta_1]$ for dipolar suspensions for various values of Pe , for spheroids of aspect ratio $r=0.4$, 1.0 and 1.6 . Results for $k \parallel (0, 1, 1)$ and $k \parallel (0, 1, 0)$ are shown. Compare with fig. 3 in Strand and Kim (1992).

$[\eta_2] - ?$

Periodic forcing and chaos

In this chapter we study the oscillatory dynamics of the bulk properties resulting from a sinusoidally varying external force field using and extending the methods developed in the previous chapters. Oscillatory dynamics caused by oscillatory shear flows has been studied extensively for many polymer and particulate systems, but the effect of an oscillatory force field has only rarely been considered. Leal and Hinch (1972) presented solutions for the case of general time dependent flows valid for non-dipolar near spheres. Bird *et al.* (1971) and Bird *et al.* (1987) obtained results for the rheological properties for the case of dumbbells in time-dependent flows of specialised types. Strand (1989) considered oscillatory fields in both shear and external fields and obtained results for the stress response using the Galerkin method, but as we will demonstrate, there exist parametric regimes where the approach used by Strand is fundamentally inappropriate.

We consider a sinusoidally varying force field acting on a suspension of dipolar Brownian particles in a simple shear flow, so that the temporal oscillations are limited to the force field alone. The significance of this problem was discussed earlier (*cf.* Chapter 1) where we had observed that this system exhibited a rich variety of dynamics in the absence of Brownian diffusion, which were theoretically interesting and had potential technological applications. In particular, the orientation dynamics of the system exhibit chaotic evolution for certain parametric regimes and presents a new class-I intermittency

route to chaos (Ramamohan *et al.*, 1994; Kumar *et al.*, 1995; Kumar and Ramamohan, 1997). Further, the rheological parameters such as the apparent viscosities and normal stress differences also evolve chaotically when the dynamics is chaotic (Kumar and Ramamohan, 1995; Kumar *et al.*, 1996). Chaos in the rheology can be controlled using simple chaos control algorithms and this can be used to force desired rheological behaviour using carefully controlled parameters (Kumar, 1997). The system is also useful as a paradigm for certain aspects of spatio-temporal chaos and non-trivial collective behaviour (Radhakrishnan *et al.*, 1999). All these investigations were limited to zero or negligible Brownian motion. This chapter is devoted to exploring the effect of Brownian rotation on the observed chaos in the system.

As noted earlier, the diffusion equation approach used by Strand and Kim (1992) and Strand (1989) is inadequate to study such irregular behaviour in the system (Kumar and Ramamohan, 1995) and it turns out that the Langevin equation method we developed in the earlier chapters is an ideal tool to analyse possible complexities in the dynamics of the system in the presence of noise. It is also the natural generalisation of the method of Ramamohan *et al.* to systems with noise.

As mentioned earlier, the experimental feasibility of setting up a suspension system under constant external forcing has been reported by many authors (Okagawa and Mason, 1974; McTague, 1969; Sudou *et al.*, 1983; Weser and Stierstadt, 1985) and periodic forcing should cause no additional problem.

6.1 The dynamics of periodically forced fibres

The analysis in this chapter will be restricted to the case of slender rods (fibres) which correspond to the limit $r \rightarrow \infty$. This results in considerable reduction in the computations by way of simple expressions for the stress coefficients (see Table 5.1). Typical second phase fibres in composites and polymeric solutions can be modelled as fibres to an excellent approximation since their aspect ratio is generally greater than 50. Under a

sinusoidally varying force field the Langevin equation (5.1) modifies to

$$\dot{\mathbf{u}} = \boldsymbol{\Omega} \times \mathbf{u} + C[\mathbf{u} \times (\mathbf{E} \cdot \mathbf{u})] \times \mathbf{u} + \zeta_{\perp}^{-1} \mathbf{m} \times \mathbf{H} \cos(\omega t) \times \mathbf{u} + \boldsymbol{\Gamma} \times \mathbf{u}, \quad (6.1)$$

where ω is the frequency of the external driver. We choose a scaling that is appropriate to explore the system behavior vis a vis change in the Brownian flux, so time is scaled with respect to the shear rate ($\dot{\gamma}$) and force with $\dot{\gamma}\zeta_{\perp}$ and write $\mathbf{k} = m\mathbf{H}/\dot{\gamma}\zeta_{\perp}$. In this setting, the Langevin equation (6.1) takes the following form in spherical co-ordinates;

$$\dot{\theta} = h_1 - \sin \phi \Gamma_1(t) + \cos \phi \Gamma_2(t),$$

$$\dot{\phi} = h_2 - \cot \theta \cos \phi \Gamma_1(t) - \sin \phi \cot \theta \Gamma_2(t) + \Gamma_3(t),$$

where h_1 and h_2 are, as before, the deterministic parts given by

$$\begin{aligned} h_1 &= C \sin \theta \cos \theta \sin \phi \cos \phi \\ &\quad + (k_1 \cos \theta \cos \phi + k_2 \cos \theta \sin \phi - k_3 \sin \theta) \cos(\omega t), \\ h_2 &= -C \sin^2 \phi - \left(\frac{1-C}{2}\right) \\ &\quad + (-k_1 \sin \phi + k_2 \cos \phi) \left(\frac{1}{\sin \theta}\right) \cos(\omega t). \end{aligned} \quad (6.2)$$

In the present scaling $\Gamma(t)$ satisfy (3.19) with $D = D_r/\dot{\gamma}$ which we denote by $\tilde{P}e$ so that $\tilde{P}e = 0$ when Brownian motion is negligible.

6.2 The simulation of the bulk properties

$$Pe = \frac{\dot{\gamma}}{D_r}$$

As in the case of constant external force field, the stress tensor in the suspension under periodic forcing is in general non-Newtonian and gives rise to four different non-zero viscometric functions in simple shear. The total stress tensor varies from eq. (5.4) only by the periodic term $\cos(\omega t)$;

$$\begin{aligned} \boldsymbol{\sigma} &= -p\boldsymbol{\delta} + 2\eta_s \mathbf{E} + 2\eta_s \Phi \left\{ 2A_H \mathbf{E} : \langle \mathbf{u}\mathbf{u}\mathbf{u}\mathbf{u} \rangle \right. \\ &\quad \left. + 2B_H \left(\mathbf{E} \cdot \langle \mathbf{u}\mathbf{u} \rangle + \langle \mathbf{u}\mathbf{u} \rangle \cdot \mathbf{E} - \frac{2}{3} \boldsymbol{\delta} \mathbf{E} : \langle \mathbf{u}\mathbf{u} \rangle \right) + \right. \\ &\quad \left. C_H \mathbf{E} + F_H D_r \left(\langle \mathbf{u}\mathbf{u} \rangle - \frac{1}{3} \boldsymbol{\delta} \right) \right. \\ &\quad \left. + 3D_0 \frac{m}{k_B T} \left[\frac{(1-C)}{2} \langle \mathbf{u}\mathbf{H}_{\perp} \rangle - \frac{(1+C)}{2} \langle \mathbf{H}_{\perp} \mathbf{u} \rangle \right] \cos(\omega t) \right\} \end{aligned} \quad (6.3)$$

The expressions for the stress coefficients take particularly simple form in the case of fibres and are given in Table 5.1. These expressions have the following limiting behaviour which can be used to further simplify the equations for the rheological parameters.

$$\begin{aligned} \lim_{r \rightarrow \infty} A_H B_H &= \frac{3}{4}, & \lim_{r \rightarrow \infty} C_H B_H &= 0, \\ \lim_{r \rightarrow \infty} B_H B_H &= 0, & \lim_{r \rightarrow \infty} F_H B_H &= 9. \end{aligned}$$

Hence by additionally scaling each of the rheological parameters with B_H and redefining the rheological parameters by taking a second limit as $r \rightarrow \infty$, we get

$$\begin{aligned} [\eta_1] &= \lim_{\substack{\Phi \rightarrow 0 \\ r \rightarrow \infty}} \left[\left(\frac{\sigma_{xy} - \eta_s \dot{\gamma}}{\Phi \eta_s \dot{\gamma}} \right) B_H \right] \\ &= 3 \langle u_1^2 u_2^2 \rangle + 18 \tilde{P}e \langle u_1 u_1 \rangle \\ &\quad + \left(\frac{6 \tilde{P}e}{C} \right) \left[C \langle (\Sigma k_i u_i) u_1 u_2 \rangle + \left(\frac{1-C}{2} \right) \langle u_1 \rangle k_2 - \left(\frac{1+C}{2} \right) \langle u_2 \rangle k_1 \right], \\ [\eta_2] &= \lim_{\substack{\Phi \rightarrow 0 \\ r \rightarrow \infty}} \left[\left(\frac{\sigma_{yx} - \eta_s \dot{\gamma}}{\Phi \eta_s \dot{\gamma}} \right) B_H \right] \\ &= 3 \langle u_1^2 u_2^2 \rangle + 18 \tilde{P}e \langle u_1 u_1 \rangle \\ &\quad + \left(\frac{6 \tilde{P}e}{C} \right) \left[C \langle (\Sigma k_i u_i) u_1 u_2 \rangle + \left(\frac{1-C}{2} \right) \langle u_2 \rangle k_1 - \left(\frac{1+C}{2} \right) \langle u_1 \rangle k_2 \right], \\ [\tau_1] &= \lim_{\substack{\Phi \rightarrow 0 \\ r \rightarrow \infty}} \left[\left(\frac{\sigma_{xx} - \sigma_{zz}}{\Phi \eta_s \dot{\gamma}} \right) B_H \right] \\ &= 3 \langle (u_1^3 u_2) - \langle u_1 u_2 u_3^2 \rangle \rangle + 18 \tilde{P}e \langle u_1^2 - u_3^2 \rangle \\ &\quad + 6 \tilde{P}e \left[\langle (\Sigma k_i u_i) u_1^2 \rangle - \langle (\Sigma k_i u_i) u_3^2 \rangle + k_3 \langle u_3 \rangle - k_1 \langle u_1 \rangle \right], \\ [\tau_2] &= \lim_{\substack{\Phi \rightarrow 0 \\ r \rightarrow \infty}} \left[\left(\frac{\sigma_{yy} - \sigma_{zz}}{\Phi \eta_s \dot{\gamma}} \right) B_H \right] \\ &= 3 \langle (u_1 u_2^3) - \langle u_1 u_2 u_3^2 \rangle \rangle + 18 \tilde{P}e \langle u_2^2 - u_3^2 \rangle \\ &\quad + 6 \tilde{P}e \left[\langle (\Sigma k_i u_i) u_2^2 \rangle - \langle (\Sigma k_i u_i) u_3^2 \rangle + k_3 \langle u_3 \rangle - k_2 \langle u_2 \rangle \right]. \end{aligned}$$

To simulate these averages we use the methods of the previous chapters with appropriate modifications to generate the moments in chosen pairs. In the new scaling the equation for the dynamics of any moment $\langle B(\theta, \phi) \rangle$ becomes (cf. eq. (4.2))

$$\frac{d}{dt} \langle B(\theta, \phi) \rangle = \langle f_1 h_1 \rangle + \langle f_2 h_2 \rangle + \tilde{P}e \langle g_{kj} \frac{\partial}{\partial \theta_k} (f_1 g_{1j} + f_2 g_{2j}) \rangle \quad (6.4)$$

The moment equations eq. (6.4) for any two moments $\langle B_1(\theta, \phi) \rangle$ and $\langle B_2(\theta, \phi) \rangle$ are collectively equivalent to the following simultaneous equations over a set of tracer orientations (cf. eq. (4.5))

$$\begin{aligned}\dot{\theta} &= h_1 + \frac{\tilde{P}e}{\Delta} \left[f_2' g_{kj} \frac{\partial}{\partial \theta_k} (f_1 g_{1j} + f_2 g_{2j}) - f_2 g_{kj} \frac{\partial}{\partial \theta_k} (f_1' g_{1j} + f_2' g_{2j}) \right] \\ \dot{\phi} &= h_2 - \frac{\tilde{P}e}{\Delta} \left[f_1' g_{kj} \frac{\partial}{\partial \theta_k} (f_1 g_{1j} + f_2 g_{2j}) - f_1 g_{kj} \frac{\partial}{\partial \theta_k} (f_1' g_{1j} + f_2' g_{2j}) \right].\end{aligned}$$

The same pairing of moments as in the case of constant forcing can be used here also (see Table 5.2). The time series for various rheological parameters were simulated using the computational technique presented in sec. 4.2. The topological features of the plots of the time series were found stabilised at the number of initial conditions $n^2 = 100$ onwards, hence n^2 was fixed at 100 in further computations as in the case of a constant external field.

6.3 Analysis of the time series

We generated a time series for each of the bulk suspension parameters above over a period of 100000 dimensionless time units and deleted the first 20000 data points to remove any transients. Fig. 6.1 shows a part of the time series corresponding to the set of parameters $k_1 = k_3 = 0$, $k_2 = 0.10$, $\omega = 1$ and $\tilde{P}e = 0.01$ (weak diffusion) and it is clear from the figure that the apparent viscosity exhibits persistent temporal fluctuations. A detailed study of these fluctuations using the tools of non-linear time series analysis may reveal significant features of the dynamical system. A critical review of the various topological and geometrical methods for analyzing non-linear data can be found in Kantz and Schreiber (1997). We used the softwares TISEAN (Hegger *et al.*, 1999) and Chaos Data Analyzer Professional Version 2.1 of the Academic Software Library of the American Physical society for performing the tests on the time series.

Fig. 6.2 plots the frequency decomposition (cf. sec. 1.4.3) of the shear stress, which shows a broadband spectrum decaying exponentially with frequency. This is character-

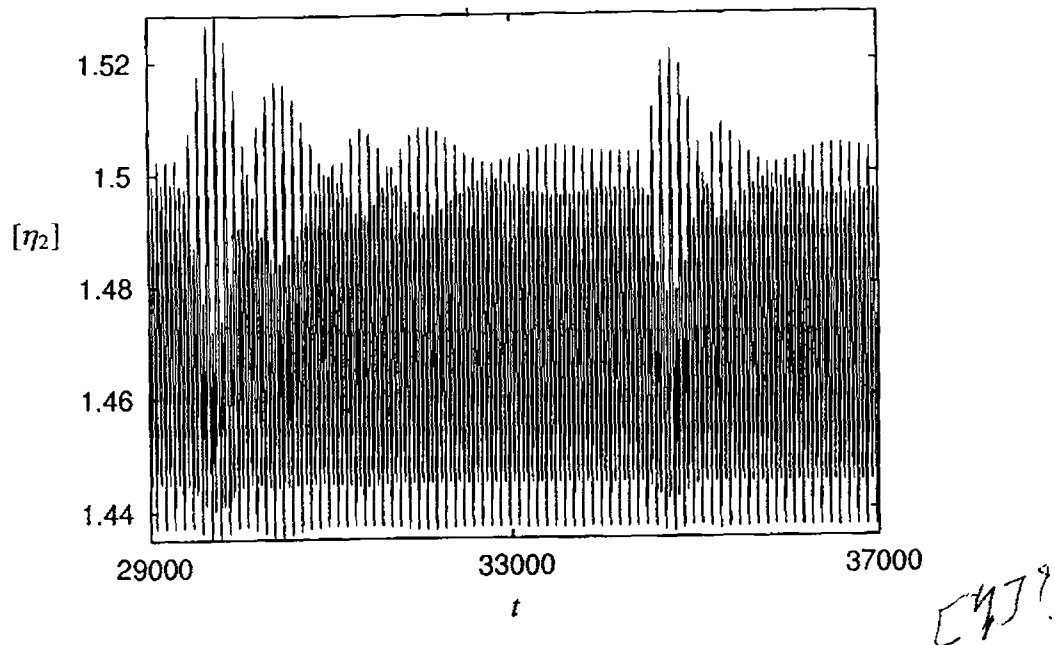


Figure 6.1: A part of the time series of $[\eta_2]$ for $\bar{P}e = 0.01$, $k_1 = k_3 = 0$, $k_2 = 0.1$ and $\omega = 1$.

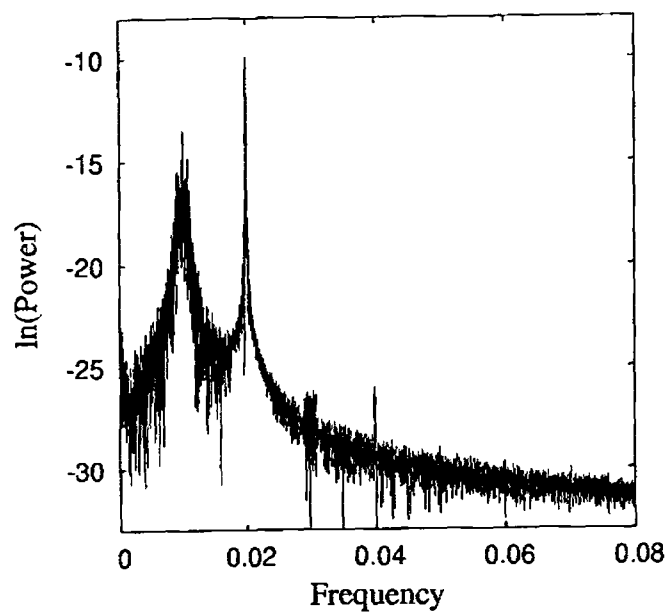


Figure 6.2: Plot of the power vs. frequency of $[\eta_2]$. The figure is typical of both chaotic and linear stochastic signals

istic of both deterministic chaos and linear autocorrelated noise (Schuster, 1988; Tsonis, 1992) and suggests further analysis of the system. The first step in any such investigation is the characterization of the attractor, a bounded subset of the phase space to which the system behavior eventually converges. This is usually done by reconstructing the attractor of the system from the available time series, say $y(t)$, using *delay reconstruction* (cf. sec. 1.4.5). Let $y(t)$ be the delay vector constructed from the time series $y(t)$ such that

$$y(t) = (y(t), y(t + \tau), \dots, y(t + (m - 1)\tau),$$

where m is a positive integer and $\tau > 0$ is called the delay. According to the embedding theorems of Takens (1981) and its extensions (Sauer *et al.*, 1991; Sauer and Yorke, 1993), the dynamics of the original system can be recaptured from the flow defined by the vector $y(t)$. (sec. 1.4.5). This means that most of the dynamical and geometrical characteristics of the original unknown system are reflected in the reconstructed flow in a one-to-one manner. In particular, the topological and geometrical invariants of the system are preserved under the embedding and hence characteristics such as fractal dimension, Lyapunov exponents and entropies can be computed from the flow in the reconstructed space (Kantz and Schreiber, 1997; Ott *et al.*, 1994).

Although the embedding theorems do not place any restriction on the choice of the time delay, in practice, the choice of both time delay and embedding dimension is important and may significantly affect the inferences derived from reconstruction, particularly when the data comes from experiment. Small delays lead to highly correlated vectors $y(t)$, while large delays yield vectors with more or less uncorrelated components resulting in data randomly distributed in the embedding space. A first guess of the proper choice of the delay may be obtained from the autocorrelation function of the sample data; the time at which the autocorrelation attains its first zero, or its first local minimum, can be taken as the optimal delay (Kantz and Schreiber, 1997). For our time series this value was around $\tau = 15$ and we obtained topologically identical attractors for

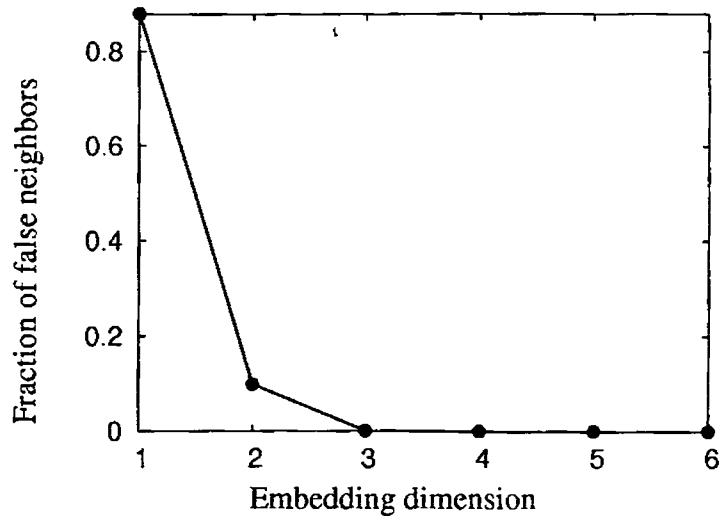


Figure 6.3: Fraction of false nearest neighbors as a function of the embedding dimension m for the $[\eta_2]$ series.

other choices of delay around this value. As for the embedding dimension m , it should be large enough for the attractor to fully unfold in the embedding space but choosing too large an m may cause the various algorithms to underperform (Kantz and Schreiber, 1997). A commonly used method to estimate the optimal value of m is the false nearest neighbor method (Kennel *et al.*, 1993; Abarbanel, 1994) which is based on the idea that a small value for m would not unfold the true geometry of the attractor and there may be self-intersections leading to false neighbors. Fig. 6.3 plots the fraction of false neighbors as a function of the embedding dimension m and yields $m = 3$ as an optimal choice, since for $m \geq 3$ the fraction of false neighbours become very small. This means that the behavior of the system can be eventually described by utmost 3 independent co-ordinates. Fig. 6.4 shows the attractor reconstructed from the time series of $[\eta_2]$ with $m = 3$ and $\tau = 15$. We experimented with higher dimensions and various delays but in all cases the attractor was found to be topologically identical to the one in the figure. We note that there is a definite structure in the phase phase plot of the stress component.

A quantitative measure of the structure and self-similarity of the attractor is provided

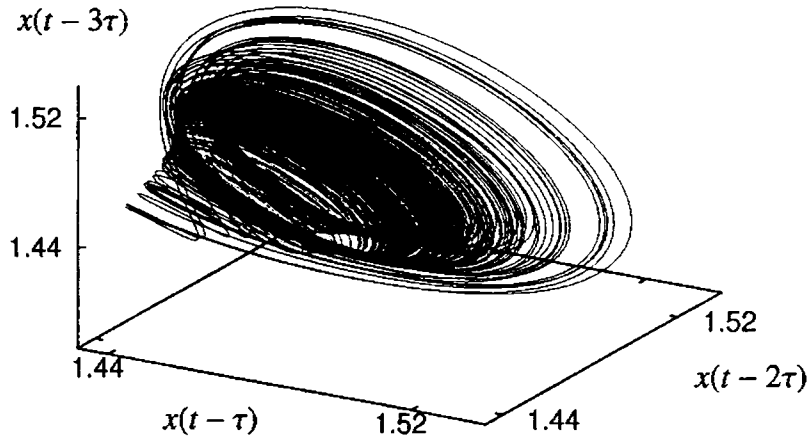


Figure 6.4: Three-dimensional embedding of the attractor of $[\eta_2]$ reconstructed from the time series with delay 15 and $m = 3$.

by various dimension estimates such as the box-counting dimension, the Hausdorff dimension etc. The correlation dimension, introduced by Grassberger (1983), Grassberger and Procaccia (1983) and others, is the easiest to compute from a time series (cf. sec. 1.4.3). The correlation dimension is estimated from the correlation sum $C(\epsilon, N)$, which is defined as the fraction of all possible pairs of points in the attractor which are closer than a given distance ϵ in a given norm; (Kantz and Schreiber, 1997)

$$C(\epsilon, m) = \frac{2}{N(N-1)} \sum_{i=1}^N \sum_{j=i+1}^N \Theta(\epsilon - \|\mathbf{x}_i - \mathbf{x}_j\|), \quad (6.5)$$

where $\Theta(x) = 1$ if $x > 0$, $\Theta(x) = 0$ if $x \leq 0$ and $\mathbf{x}(t)$ is the m -dimensional vector of time-delay co-ordinates. The correlation dimension is then given by

$$D = \lim_{\epsilon \rightarrow 0} \frac{\partial \ln C(\epsilon, m)}{\partial \ln \epsilon},$$

when m is sufficiently large. The scaling exponent $\ln C(\epsilon, m) / \ln \epsilon$ typically increases with m and saturates to a final value for sufficiently large m which is then taken as an

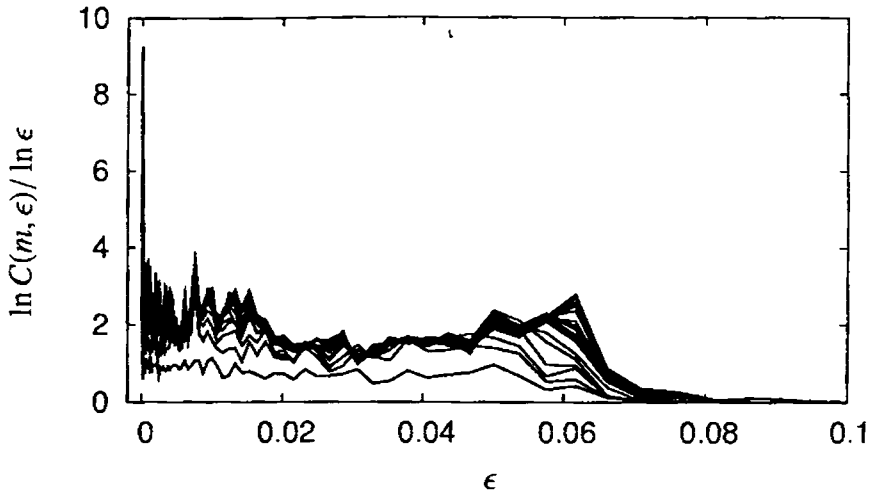


Figure 6.5: Plot of $\ln C(m, \epsilon) / \ln \epsilon$ vs. ϵ . The convergence of the curves for large m indicates low dimensionality.

estimate for D . In practice, the values $\ln C(\epsilon, m) / \ln \epsilon$ are plotted against ϵ for various m and the value corresponding to a plateau in the curves is identified as an approximation to D . In calculations, however, one has to be careful that the sum in Eq. (6.5) is not biased by temporal correlations, that is, the spatial closeness of the points appearing in Eq. (6.5) is not due to their being temporally close (Theiler, 1986). This is done by excluding from Eq. (6.5) the pairs of points which are closer in time by less than a *Theiler window*, which is approximately equal to the product of the time lag between the points and the embedding dimension (Theiler, 1986). In our calculations we used 50 as a Theiler window. Fig. 6.5 plots the correlation sums $C(\epsilon, m)$ obtained with these choice of parameters, which shows a convergence of the curves for larger m , an indication of low dimensionality of the attractor, and a plateau for the scaling exponent in the range $0.2 \leq \epsilon \leq 0.6$, suggesting a dimension approximately equal to 2. Together with the presence of definite structure in the attractor, this indicates that the apparent dimension of the system, governed by a set of 100 pairs of simultaneous equations, is far less than the number of degrees of freedom.

An interesting feature of some dynamical systems is their sensitive dependence on

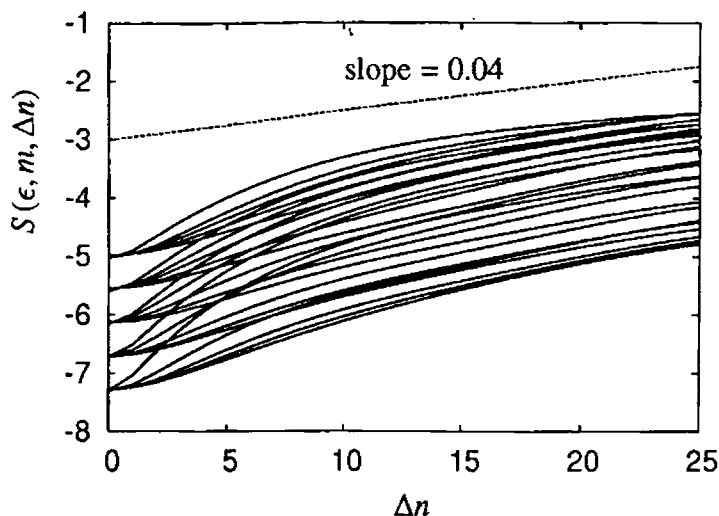


Figure 6.6: The functions $S(\epsilon, m, \Delta n)$ vs. Δn for various embedding dimensions. The curves are approximately linear with an overall slope of 0.04.

initial conditions, meaning that trajectories which start from neighboring initial conditions may diverge exponentially over time. An aperiodic bounded system having this property is termed a chaotic system (*cf.* sec. 1.4.2). The Lyapunov exponents (*cf.* sec. 1.4.3) quantify the average rate of divergence or convergence of nearby orbits, and the existence of a positive Lyapunov exponent is one of the most striking signatures of chaos (Schuster, 1988; Ott, 1993). Lyapunov exponents describe the long term behavior of nearby trajectories and are invariant under smooth transformations of the attractor, hence they are preserved under delay reconstruction. We used the Kantz algorithm (Kantz and Schreiber, 1997; Kantz, 1994) to estimate the maximum Lyapunov exponent. This proceeds by computing the sum

$$S(\epsilon, m, \Delta n) = \frac{1}{N} \sum_{n_0=1}^N \ln \left(\frac{1}{|U(\mathbf{x}_{n_0})|} \sum_{\mathbf{x}_n \in U(\mathbf{x}_{n_0})} |\mathbf{x}_{n_0+\Delta n} - \mathbf{x}_{n_0}| \right)$$

for a point \mathbf{x}_{n_0} of the time series in the embedded space and over a neighborhood $U(\mathbf{x}_{n_0})$ of \mathbf{x}_{n_0} with diameter ϵ . If the plot of $S(\epsilon, m, \Delta n)$ against Δn is linear over small Δn and for a reasonable range of ϵ , and all have identical slope for sufficiently large values of

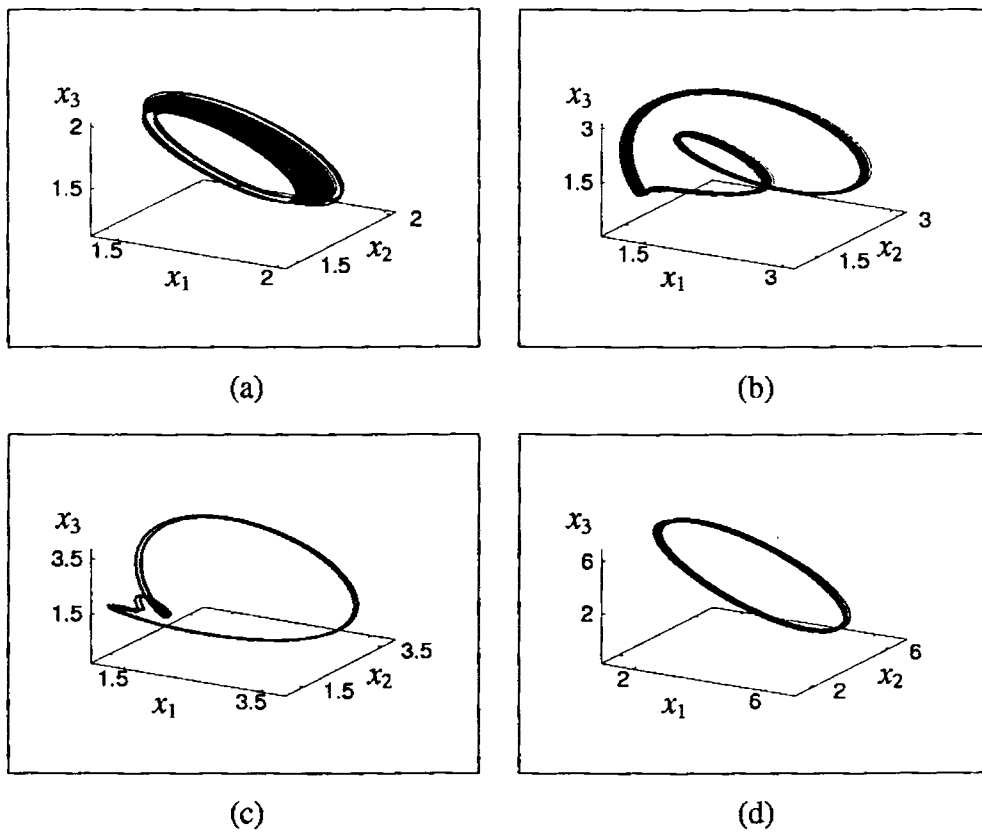
the embedding dimension m , then that slope can be taken as an estimate of the maximum Lyapunov exponent (Kantz and Schreiber, 1997). For our time series, Fig. 6.6 shows that $S(\epsilon, m, \Delta n)$ increases linearly with Δn and that the slope is roughly independent of the embedding dimension m for large m . An approximate estimate for the maximum Lyapunov exponent as obtained from the figure is 0.04. These observations indicate that the dynamics of the stress component is (weakly) chaotic in the range of parameters considered and that the system has a low dimensional chaotic attractor in this case.

The response of the system to variations in the strength of the force field, with the field orientation kept unchanged, are plotted in Figs. 6.7(a) through (d). Shown in the figures are the three-dimensional embedding of the attractors of the system for certain increasing values of k_2 , viz., $k_2 = 0.3, 0.42, 0.5$ and 1.0 respectively. For other values of k_2 in the range we got attractors which are topologically identical to the ones in the figures. This suggests that the system takes a quasi-periodic route to chaos as the parameter k_2 is decreased from 1.0 to 0.1 .

The flow parameter $\dot{\gamma}$ tends to drive the particle distribution to an anisotropic state, which is either complemented or opposed by the interaction of the imposed force field, and the interplay between these forces can lead to chaotic fluctuations, both in the dynamics and in the rheology, in the absence of diffusion (Kumar *et al.*, 1995; Kumar and Ramamohan, 1995). The Brownian parameter D , has a smoothing effect on the distribution and tends to drive the system to an isotropic equilibrium. It is, therefore, interesting to observe that the bulk system response can be chaotic in the weak diffusion regime also, as we have demonstrated above, and we expect the system to revert to regular behavior when diffusion gets stronger. This is illustrated by Figs. 6.8(a) through (c), plotting the three-dimensional embeddings of the attractors corresponding to $\tilde{P}e = 0.0, 0.1$ and 1.0 .

$$Pe = \infty, 10, 1$$

We note that the chaotic behavior of the rheological parameters could not have been picked up by many of the diffusion equation approaches that have been used to solve



$$\begin{aligned}
 x_1 &= x(t - \tau) \\
 x_2 &= x(t - 2\tau) \\
 x_3 &= x(t - 3\tau)
 \end{aligned}$$

Figure 6.7: Three-dimensional embedding of the attractors reconstructed from the time series of $[\eta_2]$ for $Pe = 0.01$, $k_1 = k_3 = 0$ and various values of k_2 ; (a) $k_2 = 0.3$, (b) $k_2 = 0.42$, (c) $k_2 = 0.5$ and (d) $k_2 = 1.0$

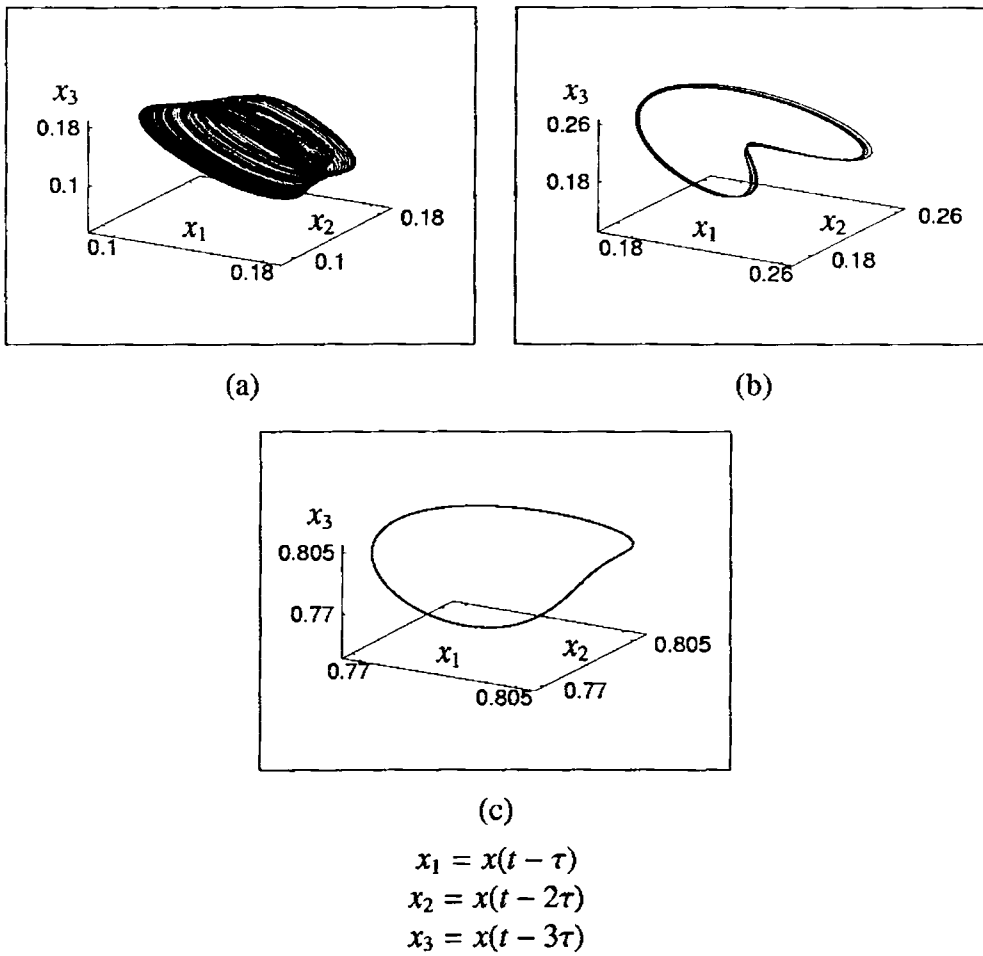


Figure 6.8: Three-dimensional embedding of the attractors reconstructed from the time series of $[\eta_2]$ for $k_2 = 0.1$, $k_1 = k_3 = 0$ and various values of $\tilde{P}e$; (a) $\tilde{P}e = 0.0$, (b) $\tilde{P}e = 0.1$ and (c) $\tilde{P}e = 1.0$

similar problems in the literature, either due to the deficiency of the approximation schemes employed to solve the diffusion equation or possibly due to more fundamental problems. Strand and Kim (1992), for example, used an expansion of the ODF into a series of orthogonal functions and applied the Galerkin method to an appropriately truncated series to express the rheological parameters in terms of the expansion coefficients. Strand (1989) has applied this method to treat periodically forced systems of dipolar particle suspensions. Their expansion for the ODF permits only the driving frequency and higher harmonics of the shear and external field and is generally not valid in regimes where the stress fluctuations may have subharmonic periodicity, such as the chaotic parameter regimes we have explored, where the range of the frequencies is a continuum. Thus if we take the Poincaré sections (*cf.* sec. 1.4.3) of the time series $[\eta_2]$ versus $[\tau_1]$, i.e. snapshots of the attractor $[\eta_2] \times [\tau_1]$ taken at regular time intervals corresponding to the driving frequency, the method of Strand should give only a single point, whereas our method results in a continuum of points for the set of parameters considered above (Fig. 6.9).

6.4 Other Orientations

Fig. 6.10(a) through (e) shows the results for $[\eta_1]$ and $[\tau_1]$ when the external force is oriented in the Z- direction. Note that $[\eta_1]$ and $[\eta_2]$ have identical values in this case. Simulations were carried out for a set of values of $\tilde{P}e$ in the range $0 \leq \tilde{P}e \leq 1$, typical plots of which are shown in the figure. It can be seen that the stress components remain in the regular regime for the values of $\tilde{P}e$ considered. The change in the magnitude of $\tilde{P}e$ affects only the range of the values assumed by the stress coefficients and does not cause any topological changes in the attractor of the system.

Chaotic behaviour, however, was observed for some other parametric regimes corresponding to a different orientation of the force field. The attractors for $[\eta_2]$ and $[\tau_1]$

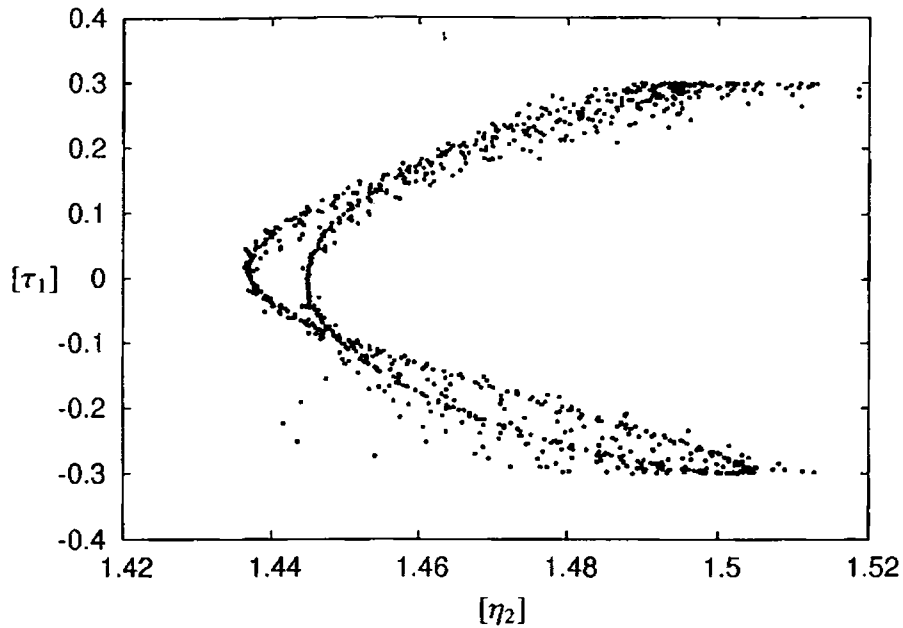


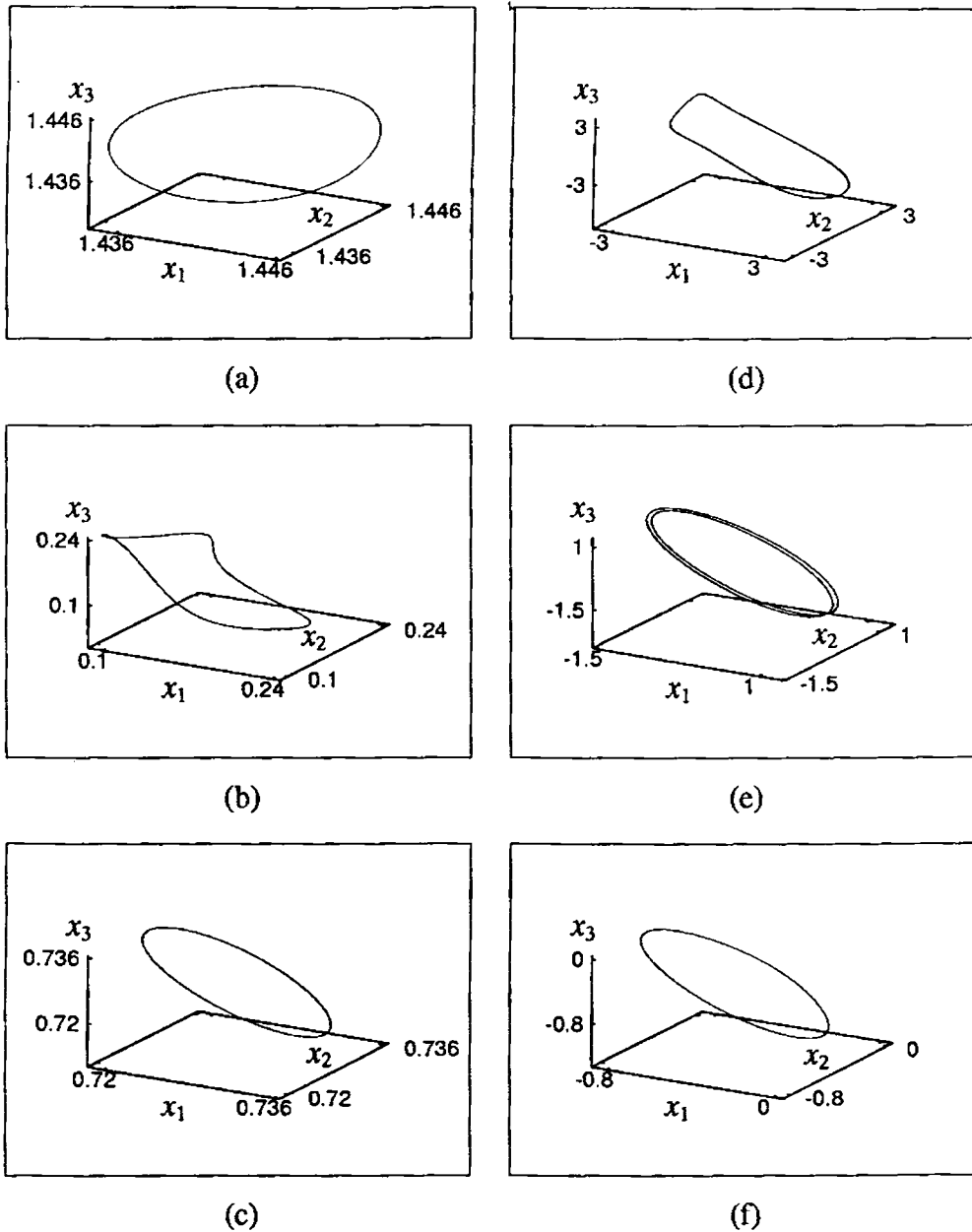
Figure 6.9: Poincaré section of the attractor of $[\eta_2] \times [\tau_1]$ for $\tilde{P}e = 0.01$, $k_2 = 0.1$, $k_1 = k_3 = 0$

when external force is parallel to $(1, 1, 0)$ are shown in figs. 6.11 (a) through (d) for several values of $\tilde{P}e$. The plots indicate that $[\eta_2]$ remains in the chaotic regime for a larger range $\tilde{P}e$ than in the previous case, for moderate values of k_3 . Here again the system comes back to regular behaviour when the effects of diffusion or of the external force become stronger. Table 6.1 lists the Lyapunov exponents and correlation dimensions for the attractors shown in the figure.

When the external force is parallel to $(1, 1, 0)$, both $[\eta_2]$ and $[\tau_1]$ exhibit chaos in the

$\tilde{P}e$	$[\eta_2]$	
	Lyap. exp.	Corr. dim.
0.00	0.030	1.7
0.01	0.025	1.5
0.10	0.015	1.3

Table 6.1: The estimated Lyapunov exponents and approximate correlation dimensions of the attractors in fig. 6.11



$$\begin{aligned}
 x_1 &= x(t - \tau) \\
 x_2 &= x(t - 2\tau) \\
 x_3 &= x(t - 3\tau)
 \end{aligned}$$

Figure 6.10: Three-dimensional embedding of the attractors reconstructed from the time series of $[\eta_1]$ and $[\tau_1]$ for $k_1 = k_2 = 0$, $k_3 = 1.0$ and various values of $\tilde{P}e$; (a) & (d) $\tilde{P}e = 0$; (b) & (e) $\tilde{P}e = 0.1$; (c) & (f) $\tilde{P}e = 1.0$

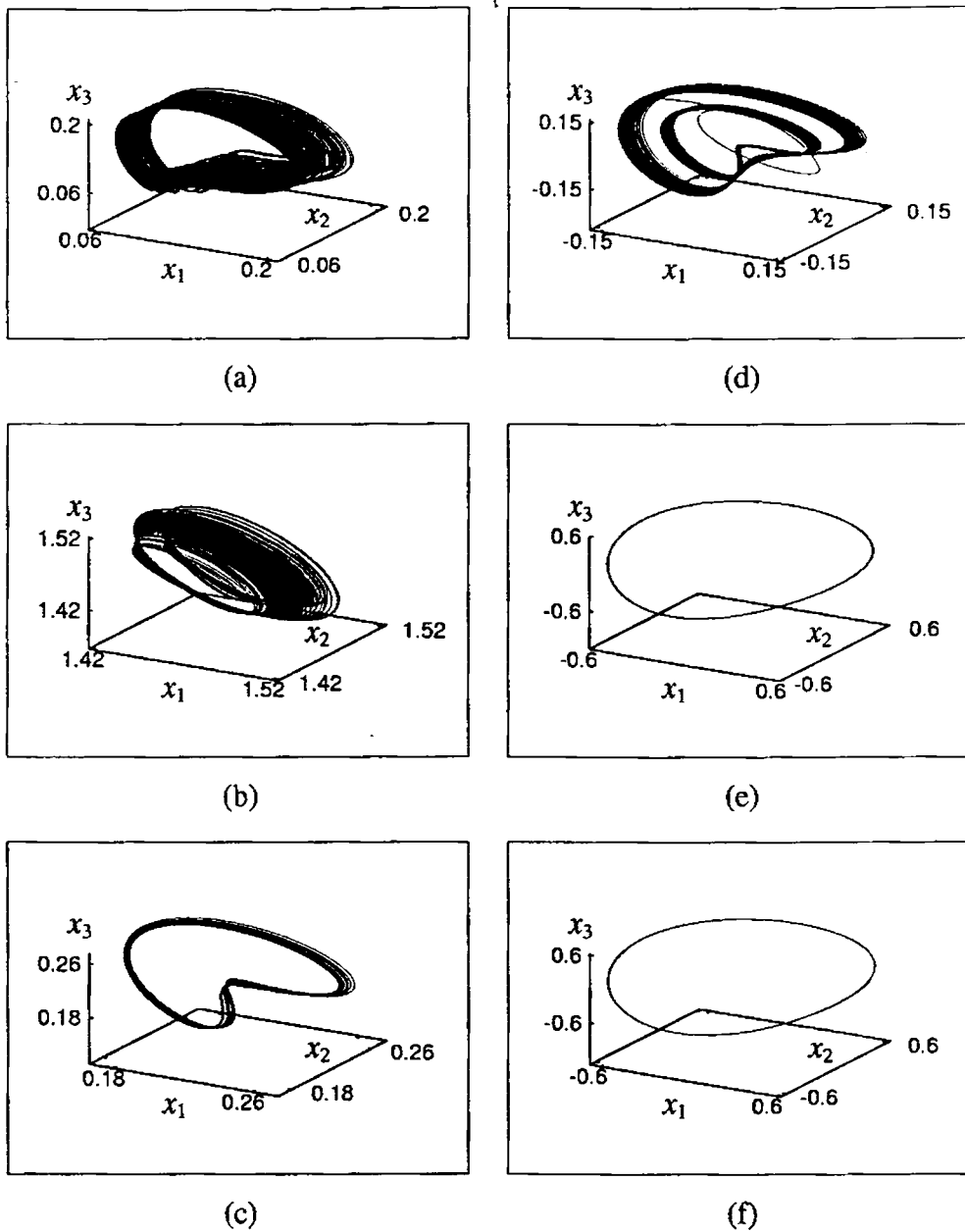
$\tilde{P}e$	[η_2]		[τ_1]	
	Lyap. exp.	Corr. dim.	Lyap. exp.	Corr. dim.
0.00	0.030	2.0	0.030	2.0
0.01	0.025	1.7	0.020	1.5
0.10	1.025	1.2	0.025	1.2

Table 6.2: The estimated Lyapunov exponents and approximate correlation dimensions of the attractors in fig. 6.12

range $0 \leq \tilde{P}e \leq 0.1$ for $k_1 = k_2 = 0.1$ (figs. 6.12 (a) through (e)). In both the cases chaos appears as a broadening of the attractor as $\tilde{P}e$ is reduced. The range of the diffusion strength for which chaos is observed is also larger as in the previous case. Table 6.2 lists the geometric invariants of the attractors for various values of $\tilde{P}e$.

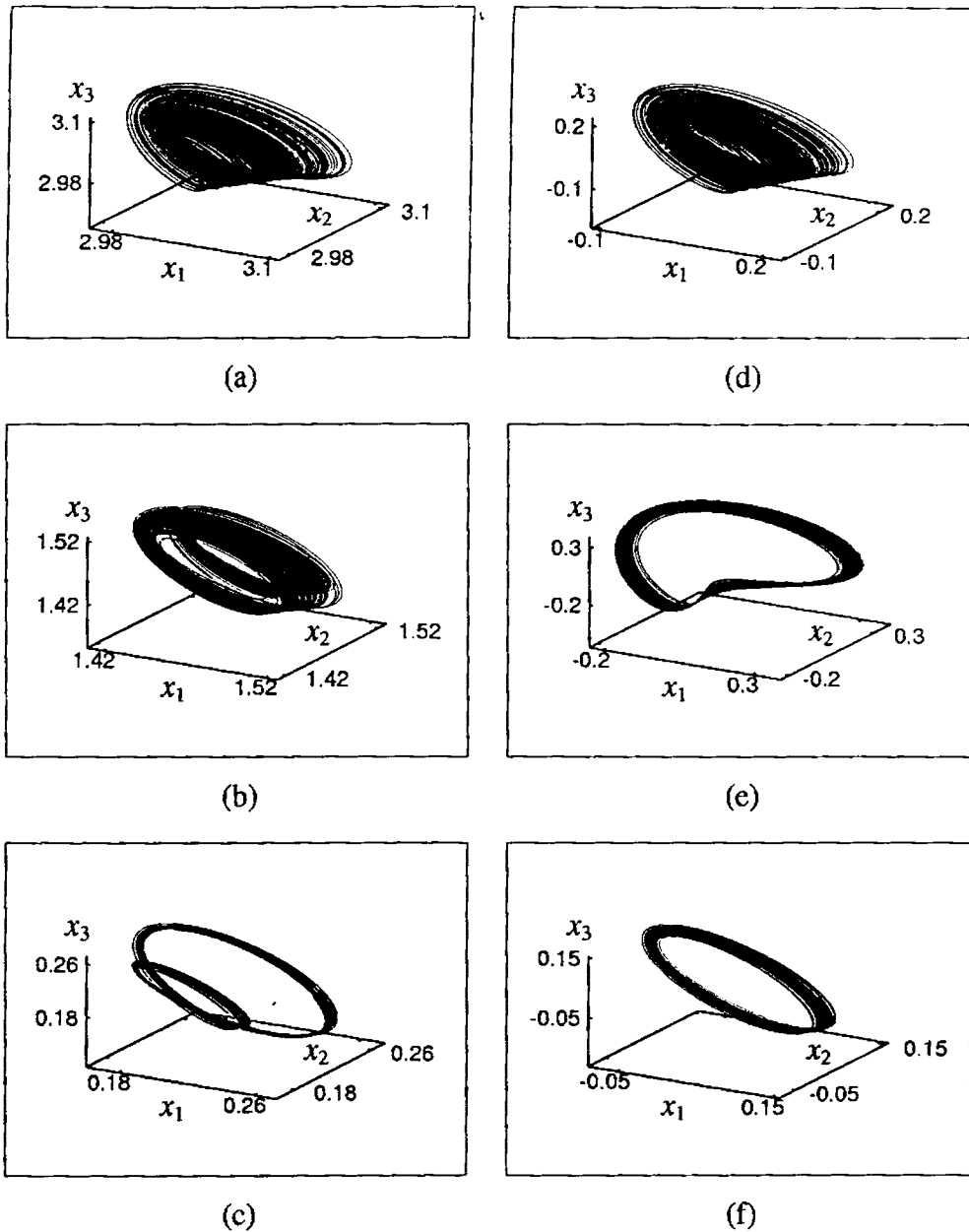
In all the cases where chaos was observed, the system returns to regular behaviour in favour of stronger orientational effects, either due to the external force or Brownian rotation.

Another important point to note is that all the above results pertain to the region of small Brownian motion where the solution of the Fokker-Planck equation becomes otherwise intractable. In the limit of weak diffusion, the Fokker-Planck equation changes from a second order partial differential equation to a first order partial differential equation, and the fundamental character of the equation changes from a diffusion equation type to a Liouville type. In perturbation methods, this often leads to a breakdown of the regular perturbation and requires a singular perturbation to be used. This usually means sharp gradients in the solution which are difficult to handle in the normal way. The Langevin equation method is more preferable in this case since, together with the paired-moment scheme for generating moments, it works fine even when diffusion is weak and is capable of capturing possible complex behaviours of the system which methods based on singular perturbations may not be able to pick up.



$$\begin{aligned}x_1 &= x(t - \tau) \\x_2 &= x(t - 2\tau) \\x_3 &= x(t - 3\tau)\end{aligned}$$

Figure 6.11: Three-dimensional embedding of the attractors reconstructed from the time series of $[\eta_2]$ and $[\tau_1]$ for $k_1 = 0, k_2 = k_3 = 0.1$ and various values of $\tilde{P}e$; (a) & (d) $\tilde{P}e = 0$; (b) & (e) $\tilde{P}e = 0.01$; (c) & (f) $\tilde{P}e = 0.1$



$$\begin{aligned}
 x_1 &= x(t - \tau) \\
 x_2 &= x(t - 2\tau) \\
 x_3 &= x(t - 3\tau)
 \end{aligned}$$

Figure 6.12: Three-dimensional embedding of the attractors reconstructed from the time series of $[\eta_1]$ and $[\tau_1]$ for $k_3 = 0, k_1 = k_2 = 0.1$ and various values of $\tilde{P}e$; (a) & (d) $\tilde{P}e = 0$; (b) & (e) $\tilde{P}e = 0.01$; (c) & (f) $\tilde{P}e = 0.1$

Conclusions

7.1 Summary

We have developed a novel theoretical framework, based on and extending the traditional Langevin equation approach, for modelling the dynamics and calculating the bulk properties of orientable particles dispersed in a simple shear flow subject to various orientational effects. For computing the various moments, this method relies on the direct equations of motion for the particles, in contrast to the familiar Fokker-Planck equation route which involves finding the solution of an appropriate partial differential equation for the statistical distribution of the orientations. It turns out that the Langevin approach has many advantages over the Fokker-Planck equation method, both in efficiency and scope.

In the presence of rotational Brownian motion, the microscopic equations for the evolution of the particle orientation vectors are stochastic differential equations, each containing a noise term. The nature and properties of the noise term were determined by applying a novel theory for non-linear noisy systems, introduced recently by Coffey *et al.* (1996). It was shown that an ensemble of these equations is collectively equivalent to the governing Fokker-Planck (Diffusion) equation of the system. To show this, we demonstrated that the averaging procedures of both the methods led to the same equation

for the dynamics of the spherical harmonics.

We have outlined a general procedure for deriving the exact equation for the evolution of any orientation moment, as the particles change orientations due to various orientational torques. These are ordinary differential equations even in the presence of noise, with the additional advantage that they do not require the explicit computation of the orientation distribution function. However, due to the closure problem, the moment equations are hard to solve directly. Hence we developed a way for simulating the moments in suitable pairs using a brute force technique. For the simulations, we used a large number of pairs of ordinary differential equations describing the motions of a set of tracer orientation vectors in the orientation space, and computed the moments by suitably averaging the iterated solutions of the equations dynamically. Each of these equation pairs was deduced from a suitably chosen moment pair by rewriting the moment equations appropriately. To test the validity of the method as well as the software, we generated the steady state values of a few moments for the case of force-free fibres in simple shear and compared the results with those of Chen and Koch (1996) and Chen and Jiang (1999) and found that the results were in perfect agreement. Several advantages of the new method were discussed and demonstrated; in particular, it is significantly faster than the above methods, about four times faster in computing simple orientation moments.

The method can be extended to more general systems subject to additional particle orientation effects without any significant change in the basic strategy. We studied the special case in which the particles had dipole moments interacting with an external force field. Two different possibilities were considered for the force field; (i) the force field does not vary with time and (ii) the force field varies sinusoidally with time. In each case the Langevin equation was obtained by adding suitable terms corresponding to the force field to the equation derived for force-free particles. For a constant force field, the intrinsic viscosity of the system was calculated for several parameter values representing

different field strengths and orientations, many particle aspect ratios and varying degrees of diffusion. In all cases, the results were in good agreement with those of Brenner and Weissman (1972) and Strand and Kim (1992). These simulations served to demonstrate the validity of the general procedure to be followed while using the Langevin method in standard flow problems.

When the external field is periodic the Langevin equations are non-autonomous and the tracer orientation vectors are described by pairs of simultaneous non-autonomous non-linear differential equations. This leads to the possibility of chaotic dynamics for certain stress components in some parametric regimes, as revealed by a detailed and careful analysis of the time series. Chaos was observed in situations where none of the orientational effects were strong; in particular, the strength of diffusion and the force field needed to be moderate for the onset of chaos.

7.2 Future work and applications

The results of this analysis have both fundamental and theoretical importance. Accurate and efficient computation of rheological properties of suspensions is important both in theoretical studies as well as practical applications. The diffusion equation approach has been, by and large, the most widely used method for this purpose. Solving the diffusion equation has been a major hurdle in this case and a common strategy that can be used to approximate the solution in all parametric ranges is still elusive. The Langevin equation approach presented in this work can serve as a viable alternative in this case for solving flow problems. The method can, in principle, be used to model any suspension system with noise, in which the microscopic equations governing the evolution of the system are stochastic differential equations with multiplicative white noise and for which the form of the noise term is explicitly known.

Our method has also pointed out the deficiency of the diffusion equation methods currently in use, in that they cannot pick up possible subharmonics in the system or

chaotic behaviour of the averages as demonstrated in this work. The important implication of this observation is that systems which are in some sense governed by the Fokker-Planck equation can show chaos in averages and hence this system could become an important physically realisable system to determine the conditions under which chaos in microscopic dynamics can result in chaos in macroscopic averages.

On the technological front, the new observations may lead to the development of new methods to characterize magneto rheological suspensions by parameters like Lyapunov exponents. The observed chaos in the system can be put to use by controlling chaos using appropriate control of chaos algorithms and making the system behave as desired. This opens up the possibility of computer controlled intelligent rheology. Reviews of various chaos control algorithms and their applications to different fields can be found in Shinbrot (1993), Ditto *et al.* (1995), Ott and Spano (1995), Laksmanan and Murali (1996) and a special algorithm that is particularly suited for controlling fluctuations in rheological parameters is described in Kumar (1997).

It is well known in the chaos literature that chaotic signals from two different sources may be combined to produce a resultant non-chaotic signal. This points to the possibility of synchronizing chaos in the rheology of suspensions with chaotic signals from other sources and killing the undesirable oscillations in the latter. For example, the observed chaos in the dynamics of a rolling railway wheel set at higher velocity (Knudsen *et al.*, 1991; Knudsen *et al.*, 1994) may be controlled in this manner by converting it into mechanical signals and then synchronizing with chaotic response from a suspension system.

There are many directions in which the present study can be extended, apart from envisaging it as a model for analysing other flow problems using the tools of the Langevin method. Additional orientational effects can be considered, if such effects can be included in the Langevin equation through superposition. An example is to extend this study to suspensions of charged fibres (Chen and Koch, 1996) by modifying the Langevin

equation and the expression for the stress tensor to take care of the additional factors. The method may also be used to simplify the study of other similar systems, such as systems of polymeric liquids in the presence of Brownian rotation. Kumar (1997) has used a novel algorithm to control chaotic rheological parameters to make them oscillate in desired periodic orbits. To explore the possibility of implementing this algorithm in conjunction with the Langevin equation formalism, in the presence of diffusion, will be an interesting problem.

Program listing

The source code(GNU FORTRAN 77) of the programme we developed to simulate the stress components for the case of suspensions of fibres under periodic forcing is given below. This can be easily modified to compute the stress components for the case of spheres under constant external force. Subroutine odeint is adapted from Press *et al.* (1986).

```
Program stress
c  implicit double precision(a-h,o-z)
parameter(int=11,nop=100,nav=10)
character*2 i01
dimension y(2),ave(nav,2),aa(int),bb(int),y2(nav,2,nop)
common /area1/ak1,ak2,ak3,pe,cc,re
common /path/kmax,kount,dxsav,xp(200),yp(2,200)
common /coeff/ah,bh,ch,fh,cf,cm,cp
common /avepass/iave
common /pforce/pk1,pk2,pk3
open(unit=11,file="pc.dat")
ak=1.0
re=1000.0      !particle aspect ratio
pe=0.1

c  components of force field
```

```

ak1 =ak
ak2 =ak
ak3 =0.0

re21=(re*re-1.0)
cc=1.0          !shape factor=1 for fibres
akc=1
pi=3.141592653589793
cm = (1.0-cc)/2.0
cp = (1.0+cc)/2.0

c   stress coefficients for fibres(scaled)
ah=3.0
bh=0.0
ch=0.0
fh=18.0
cf=6.0

nvar=2
eps =0.000001  !tolerance for step-size control
kmax=2
dx2=100.0*h1*akc
dxsav=dx2/20.0
hhh=2.0*pi/100.0      !input step-size
h1=hhh
hmin=h1/200.0
xx1=0.0
xx2=xx1+hhh

c   assigning initial conditions -- 100 in number
c   the three dimensional array y2 contains
C   the polar and azimuthal angles
thy=2.0/(float(int-1))
ph=2.0*pi/(float(int-1))
do i=1,int-1

```

```

xpp=-1.0+float(i-1)*thy
aa(i)=acos(xpp)
enddo
aa(int)=acos(1.0)
do j=1,int
bb(j)=float(j-1)*ph
enddo
iint=int-1
do iave=1,nav
do i=1,iint
do j=1,iint
y2(iave,1,j+(i-1)*iint)=(aa(i)+aa(i+1))* .5
y2(iave,2,j+(i-1)*iint)=(bb(j)+bb(j+1))* .5
enddo
enddo
enddo

do 51 j=1,50000

c   periodic forcing
wt=w*xx2
wt=mod(wt,2.0*pi)
pk1=ak1*cos(wt)
pk2=ak2*cos(wt)
pk3=ak3*cos(wt)
do 61 iave=1,nav
c   if((iave.eq.8))goto 61
do 71 i3=1,nop
y(1)=y2(iave,1,i3)
y(2)=y2(iave,2,i3)
i01="OK"
call odeint(i01,y,nvar,xx1,xx2,eps,h1,hmin,nok,nbad)
call ynorm(y,nvar)
y2(iave,1,i3)=y(1)
y2(iave,2,i3)=y(2)

```

```

71      continue
61      continue
          call avefun(y2,ave)
          call stress(ave,eta1,eta2,tau1,tau2)
xx1=xx2
xx2=xx1+hhh
          write(11,'(i7,4(1x,f12.5))')j,eta1,eta2,tau1,tau2
51      continue
1000    close(11)
          stop
          end

c      computing the orientation moments
subroutine avefun(y2,ave)
c      implicit double precision(a-h,o-z)
common /area1/ak1,ak2,ak3,pe,cc,re
parameter(nop=4,nav=10)
dimension y2(nav,2,nop),ave(nav,2)
dimension sums(10,2)
do 10 iav=1,nav !*iav corresponds to iave in main()*
do i=1,2
ave(iav,i)=0.0
sums(iav,i)=0.0
enddo
10     continue
do 23 iav=1,nav
do 20 i3=1,nop
          qx=sin(y2(iav,1,i3))*cos(y2(iav,2,i3))
          qy=sin(y2(iav,1,i3))*sin(y2(iav,2,i3))
          qz=cos(y2(iav,1,i3))
          sums(1,1)=qz*qz
          sums(1,2)=qx*qx*qy*qy
          sums(3,1)=qx
          sums(3,2)=qy
          sums(4,1)=qx*qx

```

```

        sums(4,2)=qy*qy
        sums(5,1)=qx*qx*qy
        sums(5,2)=qx*qy*qy
        sums(7,1)=qz*qz*qz
        sums(7,2)=qx*qy*qz
        sums(8,1)=qx*qy
        sums(8,2)=qx*qy*qz
        sums(9,1)=qx*qx*qz
        sums(9,2)=qz*qy*qy
        sums(10,1)=qx**3
        sums(10,2)=qy**3
    ave(iav,1)=ave(iav,1)+sums(iav,1)
    ave(iav,2)=ave(iav,2)+sums(iav,2)
20    continue
23    continue
c    here
    do 30 iav=1,nav
    do i=1,2
        ave(iav,i)=ave(iav,i)/float(nop)
    enddo
30    continue
    return
    end

c    computing the stress components
    subroutine stress(ave,eta1,eta2,tau1,tau2)
    parameter(nav=10)
c    implicit double precision(a-h,o-z)
    dimension ave(nav,2)
    common /area1/ak1,ak2,ak3,pe,cc,re
    common /coeff/ah,bh,ch,fh,cf,cm,cp
    common /pforce/pk1,pk2,pk3
    s1=pk1*ave(5,1)+pk2*ave(5,2)+pk3*ave(7,2)
    s2=pk1*ave(10,1)+pk2*ave(5,1)+pk3*ave(9,1)
c
        s2=<(sig_kiui)u1^2>

```

```

      s3=pk1*ave(5,2)+pk2*ave(10,2)+pk3*ave(9,2)
c          s3=<(sig_kiui)u2^2>
      s4=ave(9,1)+ave(9,2)+ave(7,1)
c          s4=<u3>
      s5=pk1*ave(3,1)+pk2*ave(3,2)+pk3*s4
c          s5=<sig_kiui>
      s6=s5-s2-s3
c          s6=<(sig_kiui)u3^2>
      s7=ave(2,1)-ave(6,2)-ave(6,1)
c          s7=<u1u2 u3^2>
      eta1 = 4.0*ah*ave(1,2)+2.0*bh*(ave(4,1)+ave(4,2))+ch
*          +(cf/cc)*(cc*s1+pk2*cm*ave(3,1)-pk1*cp*ave(3,2))
*          +fh*ave(2,1)
      eta2 = 4.0*ah*ave(1,2)+2.0*bh*(ave(4,1)+ave(4,2))+ch
*          +(cf/cc)*(cc*s1+pk1*cm*ave(3,2)-pk2*cp*ave(3,1))
*          +fh*ave(2,1)
      tau1 = 4.0*ah*(ave(6,2)-s7)+4.0*bh*ave(2,1)
*          +cf*(s2-s6+pk3*s4-pk1*ave(3,1))
*          +fh*(ave(4,1)-ave(2,2))
      tau2 = 4.0*ah*(ave(6,1)-s7)+4.0*bh*ave(2,1)
*          +cf*(s3-s6+pk3*s4-pk2*ave(3,2))
*          +fh*(ave(4,2)-ave(2,2))
      return
      end

      subroutine derivs(x,y,yprime)
c      implicit double precision(a-h,o-z)
c      user defined routine called by ode integrator

      dimension y(2),yprime(2)
      common /area1/ak1,ak2,ak3,pe,cc,re
      common /avepass/iave
      common /pforce/pk1,pk2,pk3
      pi=3.141592653589793
      q1=y(1)

```

```

q2=y(2)
q12=2.0*q1
q24=4.0*q2
pe2=pe/2.0
st=sin(q1)
ct=cos(q1)
sp=sin(q2)
cp=cos(q2)
c2t=cos(q12)
c4p=cos(q24)
sf=1.0
ah1=(pk1*ct*cp+pk2*ct*sp-pk3*st)  !*** force terms**
ah2=(1.0/st)*(-pk1*sp+pk2*cp)
rh1=sf*cc*st*ct*sp*cp+ah1
rh2=-sf*cc*sp*sp-(1.0-cc)/2.0+ah2

c  noise part specific to each pair of moments chosen
if(iave.eq.1)then      !generates <u1^2 u2^2> and <u3^2>
  f1=4.0*(st**3)*ct*sp*sp*cp*cp
  f2=(st**4)*cos(2.0*q2)*sin(2.0*q2)
  u=2.0*st*st-20.0*(st**4)*sp*sp*cp*cp
  g1=-2.0*st*ct
  g2=0.0
  v=-2.0*(3.0*ct*ct-1.0)
endif
if(iave.eq.2)then      !generates <u1 u2> and <u3^2>
  f1=2.0*st*ct*sp*cp
  f2=st*st*cos(2.0*q2)
  u=-3.0*st*st*sin(2.0*q2)
  g1=-2.0*st*ct
  g2=0.0
  v=-2.0*(3.0*ct*ct-1.0)
endif
if(iave.eq.3)then      !***generates <u1> and <u2>*
  f1=ct*cp

```

```

    f2=-st*sp
    u=-2.0*st*cp
    g1=ct*sp
    g2=st*cp
    v=-2.0*st*sp
endif
if(iave.eq.4)then      !generates <u1^2> and <u2^2>
    f1=2.0*st*ct*cp*cp    !**cross checked with <u3^2>**
    f2=-2.0*sp*cp*st*st
    u=2.0-6.0*st*st*cp*cp
    g1=2.0*st*ct*sp*sp
    g2=2.0*sp*cp*st*st
    v=2.0-6.0*st*st*sp*sp
endif
if(iave.eq.5)then      !generates <u1^2 u2> and <u1 u2^2>
    f1=3.0*st*st*ct*cp*cp*sp
    f2=(st**3)*(cp*cp*cp-2.0*sp*sp*cp)
    u=2.0*st*sp-12.0*(st**3)*sp*cp*cp
    g1=3.0*st*st*ct*cp*sp*sp
    g2=(st**3)*(2.0*sp*cp*cp-sp*sp*sp)
    v=2.0*st*cp-12.0*(st**3)*cp*sp*sp
endif
if(iave.eq.6)then      !generates <u1 u2^3> and <u1^3 u2>
    f1=4.0*(st**3)*ct*(sp**3)*cp
    f2=(st**4)*sp*sp*(3.0*(cp**2)-(sp**2))
    u=3.0*st*st*sin(2.0*q2)-10.0*(st**4)*(sp**2)*sin(2.0*q2)
    g1=4.0*(st**3)*ct*(cp**3)*sp
    g2=(st**4)*cp*cp*(cp**2-3.0*(sp**2))
    v=3.0*st*st*sin(2.0*q2)-10.0*(st**4)*(cp**2)*sin(2.0*q2)
endif
if(iave.eq.7)then      !generates <u3^3> and <u1u2u3>
    f1=-3.0*st*ct*ct
    f2=0.0
    u=-3.0*(ct+cos(3.0*q1))
    g1=st*(2.0*ct*ct-st*st)*sp*cp

```

```

    g2=st*st*ct*(cos(2.0*q2))
    v=-6.0*ct*st*st*sin(2.0*q2)
endif
if(iave.eq.8)then          !generates <u1u2> and <u1u2u3>
    f1=1.0*st*ct*sin(2.0*q2)
    f2=1.0*st*st*cos(2.0*q2)
    u=-3.0*st*st*sin(2.0*q2)
    g1=st*(2.0*ct*ct-st*st)*sp*cp
    g2=st*st*ct*(cos(2.0*q2))
    v=-6.0*ct*st*st*sin(2.0*q2)
endif
if(iave.eq.9)then          !generates <u1^2 u3> and <u3 u2^2>
    f1=cp*cp*(2.0*st*ct*ct-st*st*st)
    f2=-2.0*sp*cp*st*st*ct
    u=2.0*ct-12.0*st*st*cp*cp*ct
    g1=st*sp*sp*(2.0*ct*ct-st*st)
    g2=2.0*st*st*ct*sp*cp
    v=2.0*ct-12.0*st*st*ct*sp*sp
endif
if(iave.eq.10)then        !generates <u1^3> and <u2^3>
    f1=3.0*(st**2)*ct*(cp**3)
    f2=-3.0*sp*(cp**2)*(st**3)
    u=6.0*st*cp-12.0*(st**3)*(cp**3)
    g1=3.0*(st**2)*ct*(sp**3)
    g2=3.0*(sp**2)*cp*(st**3)
    v=6.0*st*sp-12.0*(st**3)*(sp**3)
endif

    rat1=sf*pe*(g2*u-f2*v)/dr
    rat2=sf*pe*(g1*u-f1*v)/dr
    yprime(1)=rh1+rat1
    yprime(2)=rh2-rat2
37  return
    end
c

```

```

        subroutine odeint(i01,ystart,nvar,x1,x2,eps,h1,hmin,
!   nok,nbad)
c   implicit double precision(a-h,o-z)
c   runge kutta driver with adaptive stepsize control.
c   Integrate the nvar starting values ystart from x1 to x2
c   with accuracy eps, storing intermediate results in the
c   common block /path/. h1 should be set as a guessed first
c   stepsize. hmin as the minimum allowed stepsize
c   (can be zero). On output nok and nbad are the num.
c   of good and bad (but retried and fixed)steps taken,
c   and ystart is dpreplaced by values at the end of the
c   integration interval.
c   derivs is the user supplied subroutine while rkqc is the
c   name of the stepper routine to be used. path contains its
c   own information about how often an intermediate value is
c   to be stored.
        external derivs
        external rkqc
        character*2 i01
        parameter(maxstp=1000000,nmax=2,two=2.0,zero=0.0,
!   tiny=1.e-30)
        common /path/kmax,kount,dxsav,yp(200),yp(2,200)

c   user storage-intermediate results. Preset dxsav and kmax
        dimension ystart(nvar),yscal(nmax),y(nmax),dydx(nmax)
        x=x1
        h=sign(h1,x2-x1)
        nok=0
        nbad=0
        kount=0
        do 11 i=1,nvar
        y(i)=ystart(i)
11      continue
        if(kmax.gt.0) xsav=x-dxsav*two
c   assures storage of first step

```

```

do 16 nstp=1,maxstp '
c   take at most maxstp steps
   call derivs(x,y,dydx)
   do 12 i=1,nvar

c   scaling used to monitor accuracy. This general purpose
c   choice can be modified if need be

   yscal(i)=abs(y(i))+abs(h*dydx(i))+tiny
12  continue
   if(kmax.gt.0) then
   if(abs(x-xsav).gt.abs(dxsav)) then
   if(kount.lt.kmax-1) then
   kount=kount+1
   xp(kount)=x
   do 13 i=1,nvar
   yp(i,kount)=y(i)
13  continue
   xsav=x
   endif
   endif
   endif
   if((x+h-x2)*(x+h-x1).gt.zero) h=x2-x
c   if step can overshoot end, cut down stepsize

   call rkqc(i01,y,dydx,nvar,x,h,eps,yscal,hdid,hnext)
   if(hdid.eq.h) then
   nok=nok+1
   else
   nbad=nbad+1
   endif
   if((x-x2)*(x2-x1).ge.zero) then
c   Are we done?

```

```

        do 14 i=1,nvar
        ystart(i)=y(i)
14      continue
        if(kmax.ne.0) then
        kount=kount+1

c      Save final step
        xp(kount)=x
        do 15 i=1,nvar
        yp(i,kount)=y(i)
15      continue
        endif
        return
c      normal exit

        endif
        if(abs(hnext).lt.hmin) i01="N1"
        h=hnext
16      continue
        i01="N2"
        return
        end

        subroutine rkqc(i01,y,dydx,n,x,htry,eps,yscal,hdid,hnext)
c      implicit double precision(a-h,o-z)
c
c      Fifth order runge-kutta step with monitoring of local
c      truncation error to ensure accuracy and adjust stepsize.
c      Input are the dependent variable vector y of length n and
c      its derivative dydx at the starting value of the
c      independent variable x. Also input are the stepsize to be
c      attempted htry, the required accuracy eps, and the vector
c      yscal against which the error is scaled. On output, y and
c      x are replaced by their new values, hdid is the stepsize

```

```

c      which was actually accomplished, and hnext is the
c      estimated next stepsize. derivs is the user supplied
c      subroutine that computes the right hand side derivatives.

      character*2 i01
      parameter (nmax=2,pgrow=-0.2,pshrink=-0.25,fcor=1.0/15.0,
! one=1.0,safety=0.9,errcon=6.e-04)
c      the value errcon equals (4/safety)**(1/pgrow)

      external derivs
c      common /area1/ak1,ak2,ak3,pe,cc,re
      dimension y(n),dydx(n),yscal(n),ytemp(nmax),ysav(nmax),
! dysav(nmax)
      xsav=x
c      save initial values

      do 11 i=1,n
      ysav(i)=y(i)
      dysav(i)=dydx(i)
11      continue
      h=htry

c
c      set stepsize to the initial trial value
c
1      hh=0.5*h
      call rk4(ysav,dysav,n,xsav,hh,ytemp)
      x=xsav+hh
      call derivs(x,ytemp,dydx)
      call rk4(ytemp,dydx,n,x,hh,y)
      x=xsav+h
      if(x:eq.xsav) i01="N0"
      call rk4(ysav,dysav,n,xsav,h,ytemp)

c      take the large step
      errmax=0.0

```

```

c      evaluate accuracy
      do 12 i=1,n
      ytemp(i)=y(i)-ytemp(i)
      errmax=max(errmax,abs(ytemp(i)/yscal(i)))
12     continue
c      ytemp now contains the error estimate

      errmax=errmax/eps
      if(errmax.gt.one) then
      h=safety*h*(errmax**pshrink)
c      truncation error too large, reduce stepsize

      go to 1
      else
c      step succeeded. compute size of next step
      hdid=h
      if(errmax.gt.errcon) then
      hnext=safety*h*(errmax**pgrow)
      else
      hnext=4.0*h
      endif
      endif
      do 13 i=1,n
c      mop up fifth order truncation error
      y(i)=y(i)+ytemp(i)*fcor
13     continue
      return
      end

      subroutine rk4(y,dydx,n,x,h,yout)
c      implicit double precision(a-h,o-z)
c
c      given values for n variables y and their derivatives
c      dydx known at x, use the fourth order runge kutta method

```

```

c      to advance the solution over an interval h and return
c      the incremented variables as yout, which need not be a
c      distinct array from y. The user supplies the subroutine
c      derivs(x,y,dydx) which returns derivatives dydx at x.
c
      external derivs
      parameter(nmax=2)
c      Set to the maximum number of functions

c      common /area1/ak1,ak2,ak3,pe,cc,re
      dimension y(n),dydx(n),yout(n),yt(nmax),dym(nmax),
!      dym(nmax)
      hh=0.5*h
      h6=h/6.0
      xh=x+hh
      do 11 i=1,n
      yt(i)=y(i)+hh*dydx(i)
11      continue
      call derivs(xh,yt,dyt)
      do 12 i=1,n
      yt(i)=y(i)+ hh*dyt(i)
12      continue
      call derivs(xh,yt,dym)
      do 13 i=1,n
      yt(i)=y(i)+h*dym(i)
      dym(i)=dym(i)+dyt(i)
13      continue
      call derivs(x+h,yt,dyt)
      do 14 i=1,n
      yout(i)=y(i)+h6*(dydx(i)+dyt(i)+2.0*dym(i))
14      continue
      return
      end

c
c      subroutine that normalizes the orientation vector

```

```
      subroutine ynorm(u,m)
c      implicit double precisibn(a-h,o-z)
      dimension u(m)
      pi=3.141592653589793
      u(1)=mod(u(1),pi)
      u(2)=mod(u(2),2.0*pi)
      return
      end
```

Notes on notation

The various notations used in the thesis are collected here for immediate reference. In general the font attributes of a letter or symbol represent the nature of the physical quantity it denotes according to the following conventions;

- lightface italic: scalar (eg. s)
- boldface italic: vector (eg. \mathbf{u})
- boldface Greek: second order tensor (eg. $\boldsymbol{\sigma}$)
- boldface sans serif: tensor of arbitrary order (eg. \mathbf{E})

a	polar radius of a spheroid in the suspension
$a_{n,k}^{m,j}$	Bird-Warner coefficients
$a_{n,m}$	coefficients in the expansion of ψ in terms of spherical harmonics (eq. (3.8))
A_H	coefficient in the expression for the stress tensor (see eqns. (5.4) and (5.5))
b	equatorial radius of a spheroid in the suspension
B_H	coefficient in the expression for the stress tensor (see eqns. (5.4) and (5.5))
C	$= (r^2 - 1)/(r^2 + 1)$, a shape factor for the particle
C_H	coefficient in the expression for the stress tensor (see eqns. (5.4) and (5.5))

$C(\epsilon, m)$	time series analysis: correlation sum
D	time series analysis: correlation dimension
D_0	rotary diffusivity of a sphere of volume equal to that of the particle
D_r	diffusion coefficient
\mathbf{E}	rate of deformation tensor
F_H	coefficient in the expression for the stress tensor (see eqns. (5.4) and (5.5))
h_1, h_2	deterministic parts of the Langevins equation of the system (see eqs. (5.11) and (6.2))
\mathbf{H}	external force field vector
H_\perp	projection of \mathbf{H} in the direction perpendicular to \mathbf{u}
i	unit vector along the X -direction
j	unit vector along the Y -direction
\mathbf{k}	the scaled dimensionless form of the external force
k_1, k_2, k_3	Cartesian components of \mathbf{k}
k_B	Boltzmann constant
\mathbf{m}	particle dipole moment
m	time series analysis: embedding dimension of the attractor
p	pressure
Pe	Péclet number ($= \dot{\gamma}/D_r$)
$P_n(x)$	Legendre polynomial of degree n
$P_n^m(x)$	associated Legendre function
r	aspect ratio of the particle
T	absolute temperature
T^{hyd}	hydrodynamic torque on the particle
T^{Ext}	torque on the particle due to the external field
\mathbf{u}	unit vector indicating the orientation of the particle
u_1, u_2, u_3	Cartesian components of \mathbf{u}

v	undisturbed velocity profile of the flow
$Y_{n,m}, Y_{n,m}^*$	spherical harmonics and complex conjugate (see sec. 3.1)
$\dot{\gamma}$	shear rate
Γ	Gaussian white noise vector
$\Gamma_1, \Gamma_2, \Gamma_3$	Cartesian components of Γ
δ	unit tensor
δ_{ij}	Kronecker delta (=1 if $i = j$ and 0 if $i \neq j$)
ζ	hydrodynamic resistance tensor
ζ_{\parallel}	component of ζ parallel to the particle axis
ζ_{\perp}	component of ζ perpendicular to the particle axis
$[\eta_1], [\eta_2]$	the apparent viscosities
η_s	viscosity of the solvent
θ	polar angle in spherical co-ordinates
$\bar{\Lambda}(\psi)$	linear operator in the definition of diffusion equation (see eq. (3.7))
σ	the averaged bulk fluid stress tensor
σ^a	anti-symmetric part of the stress
σ^p	stress contributed by the suspension particles alone
σ^s	symmetric part of the stress
τ	time series analysis: delay in attractor reconstruction
$[\tau_1]$	the first normal stress difference
$[\tau_2]$	the second normal stress difference
τ^s	stress of the solvent in the absence of particles
ϕ	azimuthal angle in spherical co-ordinates
Φ	the volume fraction of the particles in the fluid
$\psi(\mathbf{u}, t)$	particle orientation distribution function
ω	frequency of the external force driver
ω	angular velocity of the particle
Ω	vorticity vector

$\bar{\Omega}(\psi)$ linear operator in the definition of diffusion equation (see eq. (3.7))

Bibliography

- Abarbanel, H. D. I., *Analysis of Observed Chaotic Data*, Springer, Berlin, 1996.
- Advani, S. G. and C. L. Tucker, "The use of tensors to describe and predict fiber orientation in short fiber composites", *J. Rheol.* **31**, 751–784 (1987).
- Advani, S. G. and C. L. Tucker, "Closure approximations for three dimensional structure tensors", *J. Rheol.* **34**, 367–386 (1990).
- Alligood, K. T., T. D. Sauer and J. A. Yorke, *Chaos: An introduction to dynamical systems*, Springer Verlag, New York, 1997.
- Almog, Y. and I. Frankel, "Rheology of dilute suspensions of Brownian dipolar axisymmetric particles", *J. Fluid Mech.* **366**, 289–310 (1998).
- Anczurowski, E. and S. G. Mason, "The kinetics of flowing dispersions, III. Equilibrium orientations of rods and disks (experimental)", *J. Colloid Int. Sci.* **23**, 533–546 (1967).
- Arfken, G. B. and H. J. Weber, *Mathematical methods for Physicists*, Academic, Newyork, 1995.
- Banks, J., J. Brooks, G. Cairns, G. Davis and P. Stacey, "On Devaney's definition of chaos", *Amer. Math. monthly* **99**, 332 (1992).
- Barthés-Biesel, D. and A. Acrivos, "The rheology of suspensions and its relation to phenomenological theories for non-Newtonian fluids", *Int. J. Multiphase Flow* **1**, 1–24 (1973).

- Batchelor, G. K., "The stress system in a suspension of force-free particles", *J. Fluid Mech.* **41**, 545–570 (1970).
- Batchelor, G. K. and J. T. Green, "The determination of the bulk stress in a suspension of spherical particles to order c^2 ", *J. Fluid Mech.* **56**, 401–427 (1972).
- Beasley, M. R. and B. A. Huberman, "Chaos in Josephson's junctions", *Comments on Sol. Stat. Phys.* **10**, 155 (1982).
- Bird, R. B., O. Hassager, R. C. Armstrong and C. Curtiss, *Dynamics of Polymeric Liquids*, Vol. 2, Wiley, New York, 1987.
- Bird, R. B., H. R. Warner and D. C. Evans, "Kinetic theory and Rheology of Dumbbell suspensions with Brownian motion", *Adv. Polymer Sci.* **8**, 1 (1971).
- Brenner, H., "Rheology of a dilute suspension of dipolar spherical particles in an external field", *J. Colloid Interface Sci.* **42**, 141–158 (1970).
- Brenner, H., "Rheology of a dilute suspension of axisymmetric Brownian particles", *Int. J. Multiphase Flow* **1**, 195–341 (1974).
- Brenner, H. and D. W. Condiff, "Transport mechanics in systems of orientable particles. IV. Convective transport", *J. Colloid Interface Sci.* **47**, 199–264 (1974).
- Brenner, H. and M. H. Weissman, "Rheology of a dilute suspension of dipolar spherical particles in an external field. II. Effect of rotary Brownian motion", *J. Colloid Interface Sci.* **41**, 499–531 (1972).
- Bretherton, F. P., "The motion of rigid particles in a shear flow at low Reynolds number", *J. Fluid Mech.* **14**, 284–304 (1962).
- Bryant, P., R. Brown and H. Abarbanel, "Lyapunov exponents from observed time series", *Phys. Rev. Lett.* **65**, 1523 (1990).

- Buevich, Yu. A., S. V. Syutkin and V. V. Tetyukhin, "Theory of a developed magnetofluidized bed", *Magnetohydrodynamics* (N. Y.) **20**, 333–339 (1984).
- Cebers, A., "Chaos: New trend of magnetic fluid research", *J. Magn. Magn. Mater.* **122**, 281–285 (1993).
- Chandrasekhar, S., "Stochastic problems in Physics and Astronomy", *Rev. Mod. Phys.* **15**, 1 (1943).
- Chen, S. B. and L. Jiang, "Orientation distribution in a dilute suspension of fibres subject to simple shear flow", *Phys. Fluids* **11**, 2878–2890 (1999).
- Chen, S. B. and D. L. Koch, "Rheology of dilute suspensions of charged fibres", *Phys. Fluids* **8**, 2792–2807 (1996).
- Chua, L. O., M. Komuru and T. Matsumoto, "The double scroll family", *IEEE Trans. on Cir & Sys.* **CAS 33**, 1073 (1986).
- Cintra, J. S. and C. L. Tucker, "Orthotropic closure approximations for flow-induced fibre-orientations", *J. Rheol.* **39**, 1095 (1995).
- Coffey, W. T., Kalmykov, Yu. P. and J. T. Waldron, *The Langevin Equation*, World Scientific, Singapore, 1996.
- Devaney, R. L., *An introduction to chaotic dynamical systems*, Addison-Wesley, New York, 1989.
- Ditto, W. L., M. L. Spano and J. F. Lindner, "Technique for the control of chaos", *Physica D* **86**, 198 (1995).
- Doob, J. L., *Stochastic Processes*, Wiley, New York, 1953.
- Doob, J. L. in Wax N., *Selected papers on noise and stochastic processes*, Dower, New York, 1954.

- Eckmann, J.-P., S. O. Kamphorst, D. Ruelle and S. Ciliberto, "Liapunov exponents from time series", *Phys. Rev. A* **34**, 4971 (1986).
- Einstein, A., "Eine neue bestimmung der molekuldimension", *Ann. Phys.* **19**, 286–306 (1906).
- Einstein, A., "Berichtigung zu meiner Arbeit: Eine neue Bestimmung der Molekuldimension", *ibid.* **34**, 591– (1911).
- Einstein, A in R. H. Furth, *Investigations on the theory of the Brownian movement*, Methuen, London, 1926.
- Feigenbaum, M. J., "Quantitative universality for a class of nonlinear transformations", *J. Stat. Phys.* **19**, 25 (1978).
- Feigenbaum, M. J., "The Universal metric properties of nonlinear transformations ", *J. Stat. Phys.* **21**, 69 (1979).
- Feigenbaum, M. J., "Universal behavior in nonlinear systems", *Los Alamos Sci.* **1**, 4 (1980).
- Field, R. and M. Burger, *Oscillations and Travelling Waves in Chemical Systems*, John Wiley, New York, 1985.
- Folgar, F. and C. L. Tucker, "Orientation behaviour of fibres in concentrated suspensions", *J. Reinf. Plast. Composites* **3**, 98 (1984).
- Gardiner, C. W., *Handbook of stochastic methods for physics, chemistry and natural sciences*, Springer-Verlag, Newyork, 1985.
- Gillespie, D. T., "The mathematics of Brownian motion", *Am. J. Phys.* **64**, 225–240 (1996).

- Gillespie, D. T., "The multivariate Langevin and Fokker-Planck equations", *Am. J. Phys.* **64**, 1246–1257 (1996).
- Glendinning, P., *Stability, Instability and Chaos: An introduction to the theory of nonlinear differential equations*, Cambridge University Press, Cambridge, 1994.
- Grassberger, P., "Generalized dimension of strange attractors", *Phys. Letters A.* **97**, 227 (1983).
- Grassberger, P. and I. Procaccia, "Measuring the strangeness of strange attractors", *Physica D.* **9**, 189 (1983).
- Guckenheimer, J. and P. Holmes, *Nonlinear oscillations, dynamical systems and bifurcations of vector fields*, Springer Verlag, New York, 1983.
- Hall, W. F. and S. N. Busenberg, "Viscosity of magnetic suspensions", *J. Chem. Phys.* **51**, 137–144 (1969).
- Han, K. H. and Y. T. Im, "Modified hybrid closure approximation for prediction of flow-induced fibre-orientation", *J. Rheol.* **43**, 569 (1999).
- Hao, Bai-Lin, *Chaos II*, World Scientific, Singapore, 1990.
- Harrison, R. G. and D. J. Biswas, "Chaos in light", *Nature* **321**, 394 (1986).
- Hegger, R., H. Kantz, T. Schreiber, "Practical implementation of nonlinear time series methods: The TISEAN package", *Chaos* **9**, 413 (1999).
- Hénon, M., "A two-dimensional mapping with a strange attractor", *Commun. Math. Phys.* **50**, 69 (1976).
- Hinch, E. J. and L. G. Leal, "The effect of Brownian motion on the rheological properties of non-spherical particles", *J. Fluid. Mech.* **52**, 683–712 (1972).

- Hinch, E. J. and L. G. Leal, "Constitutive equations in suspension mechanics. Part 2. Approximate forms for a suspension of rigid particles affected by Brownian rotations", *J. Fluid Mech.* **76**, 187 (1976).
- Hua, C. C., and J. D. Schieber, "Application of kinetic theory models in spatiotemporal flows for polymer solutions, liquid crystals and polymer melts using the CONNFES-SIT approach", *Chem. Eng. Sci.* **51**, 1473–1485 (1995).
- Hur, D. U., "Flow of semi-dilute glass fibre suspensions in tubular entry flows", Ph. D. thesis, University of Melbourne, 1987.
- Ignatenko, N. M., Yu. Melik-Gaikazyan, V. M. Polunin and A. O. Tsebers, "Excitation of ultrasonic vibrations in a suspension of uniaxial ferromagnetic particles by volume magnetostriction", *Magnetohydrodynamics (N. Y.)* **20**, 237–240 (1984).
- Jansons, K. M., "Determination of the constitutive equations for a magnetic field", *J. Fluid Mech.* **137**, 187–216 (1983).
- Jeffery, G. B., "Motion of ellipsoidal particles immersed in a viscous fluid", *Proc. R. Soc. London (Ser. A)* **102**, 161–179 (1922).
- Kantz, H., "A robust method to estimate the maximal Lyapunov exponent of a time series", *Phys. Lett. A* **185**, 77 (1994).
- Kantz, H. and T. Schreiber, *Nonlinear Time Series Analysis*, Cambridge University Press, Cambridge, 1997.
- Kennel, M. B., R. Brown and H. D. I. Abarbanel, "Determining embedding dimension for phase-space reconstruction using a geometrical construction", *Phys. Rev. A* **45**, 3403 (1992).

- Kim, S. and C. J. Lawrence, "Similarity solutions for the orientation distribution function and rheological properties of suspensions of axisymmetric particles with external couples", *J. Non-Newtonian Fluid Mech.* **24**, 297–310 (1987).
- Knudsen, C., R. Feldberg and A. Jaschinski, "Nonlinear dynamic phenomena in the behaviour of a railway wheelset model", *Nonlinear Dynamics* **2**, 389 (1991).
- Knudsen, C., E. Silvsgaard, M. Rose, H. True and R. Feldberg, "Dynamics of a model of a railway wheelset", *Nonlinear Dynamics* **6**, 215 (1994).
- Kumar, C. V. and T. R. Ramamohan, "Controlling chaotic dynamics of periodically forced spheroids in simple shear flow: Results for an example of a potential application", *Sadhana* **23**, 131–149 (1998).
- Kumar, C. V. and T. R. Ramamohan, "New Class I intermittency in the dynamics of periodically forced spheroids in simple shear flow", *Phys. Lett. A* **227**, 72–78 (1997).
- Kumar, C. V., K. S. Kumar and T. R. Ramamohan, "Chaotic dynamics of periodically forced spheroids in simple shear flow with potential application to particle separation", *Rheol. Acta.* **34**, 504–511 (1995).
- Kumar, K. S., "Studies on the chaotic rheological parameters of periodically forced suspensions of weak Brownian slender bodies in simple shear flow", Ph. D. thesis, Cochin University of science and Technology, India, 1997.
- Kumar, K. S. and T. R. Ramamohan, "Chaotic rheological parameters of periodically forced slender rods in simple shear flow", *J. Rheol.* **39**, 1229–1241 (1995).
- Kumar, K. S., S. Savithri and T. R. Ramamohan, "Chaotic dynamics and rheology of suspensions of periodically forced slender rods in simple shear flow", *Jpn. J. Appl. Phys.* **35**, 5901–5908 (1996).

- Lakshmanan, M. and K. Murali, *Chaos in nonlinear operators*, World Scientific, Singapore, 1996.
- Lakshmanan, M. and S. Rajasekhar, *Nonlinear Dynamics: Integrability, Chaos and Patterns*, Springer, 2003.
- Landau, L. D., "On the problem of turbulence", *C. R. Acad. Sci. URSS* **44**, 311 (1944).
- Lauterborn, W. and U. Parlitz, "Methods of chaos physics and their application to acoustics", *J. Acoust. soc. Am.* **84**, 1975 (1988).
- Leal, L. G. and E. J. Hinch, "The effect of weak Brownian rotations on particles in shear flow", *J. Fluid mech.* **46**, 685–703 (1971).
- Leal, L. G. and E. J. Hinch, "The rheology of a dilute suspension of nearly spherical particles subject to Brownian rotations", *J. Fluid Mech.* **55**, 745 (1972).
- Lemons, D. S. and Gythiel, A., "Paul Langevin's 1908 paper on the theory of Brownian motion", *Am. J. Phys.* **65**, 1079–1081 (1997).
- Libchaber, A., C. Laroche and S. Fauve, "Period doubling cascade in mercury, a quantitative measurement", *J. Physique Lett.* **43**, L211 (1982).
- Lipscomb, G. G., "Analysis of suspension rheology in complex flows", Ph. D. thesis, University of California, Berkeley, 1986.
- Lipscomb II, G. G., M. M. Denn, D. U. Hur and D. V. Boger, "The flow of fibre suspensions in complex geometries", *J. Non-Newtonian Fluid mech.* **26**, 297–325 (1988).
- Lorenz, E. N., "Deterministic nonperiodic flow", *J. Atmos. Sci.* **20**, 130 (1963).
- Madan, R., *Chua's circuit: paradigm for chaos*, World Scientific, Singapore, 1993.
- May, R. M., "Simple mathematical models with very complicated dynamics", *Nature* **261**, 459 (1976).

- McTague, J. P., "Magnetoviscosity of magnetic colloids", *J. Chem. Phys.* **51**, 133 (1969).
- Moon, F. C. and P. J. Holmes, "A magnetoelastic strange attractor", *J. Sound. Vib.* **65**, 275 (1979).
- Nayfeh, A. H. and B. Balachandran, *Applied nonlinear dynamics—Analytical, computational and experimental methods*, John Wiley, New York, 1995.
- Nelson, E., *Dynamical theories of Brownian motion*, Princeton University Press, Princeton, 1967.
- Newhouse, S., D. Ruelle and F. Takens, "Occurance of strange axiom attractors near quasiperiodic flows on T^m , $m > 3$ ", *Commun. Math. Phys.* **64**, 35 (1978).
- Okagawa, A. and S. G. Mason, "Particle behavior in shear and electric fields: VII. Orientation distribution of cylinders", *J. Colloid Interface Sci.* **47**, 568 (1974).
- Olsen, L. F. and H. Degn, "Chaos in biological systems", *Quart. Rev. Biophys.* **18**, 165 (1985).
- Ott, E., *Chaos in Dynamical Systems*, Cambridge University Press, Cambridge, 1993.
- Ott, E., and M. L. Spano, "Controlling chaos", *Physics Today* **5**, 34 (1995).
- Ott, E., T. Sauer and J. A. Yorke, *Coping with Chaos*, Wiley, New York, 1994.
- Packard, N. H., J. P. Crutchfield, J. D. Farmer and R. S. Shaw, "Geometry from a time series", *Phys. Rev. Lett.* **45**, 712 (1980).
- Parlitz, U., "Identification of true and spurious Lyapunov exponents from time series", *Int. J. Bif. Chaos* **2**, 155 (1992).
- Pedersen, N. F., "Chaos in Josephson junctions and SQUIDS", *Europhys. News* **19**, 53 (1988).

- Pedley, T. J. and J. O. Kessler, "A new continuum model for suspension of gyrotactic micro-organisms", *J. Fluid Mech.* **122**, 155–182 (1990).
- Pedley, T. J. and J. O. Kessler, "Hydrodynamic phenomena in suspensions of swimming micro-organisms", *Ann. Rev. Fluid Mech.* **24**, 313–358 (1992).
- Pomeau, Y. and P. Manneville, "Intermittent transition to turbulence in dissipative dynamical systems", *Commun. Math. Phys.* **74**, 189 (1980).
- Press, W. H., B. P. Flannery, S. A. Teukolsky and W. T. Vetterling, *Numerical Recipes, The Art of Scientific Computing*, Cambridge University Press, Cambridge, 1986.
- Radhakrishnan, K., K. Asokan, J. Dasan, C. C. S. Bhat and T. R. Ramamohan, "Numerical evidence for the existence of a low-dimensional attractor and its implications in the rheology of dilute suspensions of periodically forced slender bodies", *Phys. Rev. E* **60**, 6602–6609 (1999).
- Ramamohan, T. R., S. Savithri, R. Sreenivasan and C. C. S. Bhat, "Chaotic dynamics of a periodically forced slender body in a simple shear flow", *Phys. Lett. A* **190**, 273–278 (1994).
- Risken, H., *The Fokker–Planck equation*, Springer Verlag, Berlin, 1984.
- Rössler, O. E., "An equation for continuous chaos", *Phys. Lett. A* **57**, 397 (1976).
- Roux, J. C., R. H. Simoyi and H. L. Swinney, "Observation of a strange attractor", *Physica D* **8**, 257 (1983).
- Ruelle, D. and F. Takens, "On the nature of turbulence", *Commun. Math. Phys.* **20**, 167 (1971).
- Salueña, C., A. Pérez-Madrid and J. M. Rubí, "The viscosity of a suspension of rod-like particles", *J. Colloid Interface Sci.* **164**, 269–279 (1994).

- Sauer, T. and J. A. Yorke, "How many delay coordinates do you need?", *Int. J. Bifurcation and Chaos* **3**, 737 (1993).
- Sauer, T., J. A. Yorke, and M. Casdagli, "Embedology", *J. Stat. Phys.* **65**, 579 (1991).
- Schaffer, W. M., "Can nonlinear dynamixs elucidate mechanisms in ecology and epidemiology ?", *IMA J. Math Applied in Medicine and Biology* **2**, 221 (1985).
- Schuster, H., *Deterministic Chaos*, Physik-Verlag, Weinheim, Germany, 1988.
- Shinbrot, T., "Chaos: unpredictable yet controllable", *Nonlinear Science Today* **3**, 1 (1993).
- Simoyi, R. H., A. Wolf and H. L Swinney, "One-dimensional dynamics in a multicomponent chemical reaction", *Phys. Rev. Lett.* **49**, 245 (1982).
- Smith, T. L. and C. A. Bruce, "Intrinsic viscosities and other rheological properties of flocculated suspensions of nonmagnetic and magnetic ferric oxides", *J. Colloid Interface Sci.* **72**, 13–26 (1979).
- Sparrow, C., *The Lorenz Equations: Bifurcations, Chaos and strange Attractors*, Springer Verlag, New York, 1982.
- Stover, C. A., D. L Koch and C. Cohen, "Observations of fibre orientation in simple shear flow of semi-dilute suspensions", *J. Fluid Mech.* **238**, 277–296 (1992).
- Strand, S. R., "Dynamic rheological and rheo-optical properties of dilute suspensions of dipolar Brownian particles", Ph. D. thesis, University of Wiscosin, Madison, 1989.
- Strand, S. R. and S. Kim, "Dynamics and rheology of a dilute suspension of dipolar non-spherical particles in an external field: Part I. Steady shear flows", *Rheol. Acta* **31**, 94–117 (1991).
- Strogatz, S. H., *Nonlinear dynamics and chaos*, Addison-Wesley, New York, 1994.

- Sudou, K., Y. Tomita, R Yamane, Y Ishibashi and H Otowa, "Ferromagnetic fluid flow through a circular channel", *Bul. Jpn. Soc. Mech. Eng.* **26**, 2120 (1983).
- Szeri, A. J. and L. G. Leal, "A new computational method for the solution of flow problems microstructured fluids. Part I. Theory", *J. Fluid Mech.* **242**, 549–576 (1992).
- Szeri, A. J. and D. J. Lin, "A deformation tensor model of Brownian suspensions of orientable particles—The non-linear dynamics of closure models", *J. Non-Newtonian Fluid mech.* **64**, 43–69 (1996).
- Szeri, A. L. and L. G. Leal, "A new computational method for the solution of flow problems of microstructured fluids. Part 2. Inhomogeneous shear flow of a suspension", *J. Fluid Mech.* **262**, 171 (1994).
- Takens, F., *Detecting Strange Attractors in Turbulence*, Lecture Notes in Math. Vol. 898, Springer, New York, 1981.
- Theiler, J., "Spurious dimension from correlation algorithms applied to limited time series data", *Phys. Rev. A* **34**, 2427 (1986).
- Touhey, P., "Yet another definition of chaos", *Amer. Math. Monthly* **1045**, 411 (1997).
- Tsonis, A., *Chaos: From Theory to Application*, Plenum, New York, 1992.
- Tucker, C. L., "Flow regimes for fibre suspensions in narrow gaps", *J. Non-Newtonian Fluid Mech.* **39**, 239–268 (1991).
- van Kampen, N. G., *Stochastic processes in Physics and Chemistry*, North-Holland Physics Publishing, Amsterdam, 1981.
- Weiss, C. O. and J. Brock, "Evidence for Lorenz-type chaos in a laser", *Phy. Rev. Lett.* **57**, 2804 (1986).

- Weiss, C. O. and W. Kische, "On observability of Lorenz instability in lasers", *Opt. Commun.* **51**, 47 (1984).
- Weser, T. and K Stierstadt, "Magnetoviscosity of concentrated ferrofluids", *Z. Phys. B.* **59**, 257 (1985).
- Wolf, A., J. B. Swift, H. Swinney and J. A. Vastano, "Determining Lyapunov exponents from a time series", *Physica D* **16**, 285 (1985).
- Zirnsak, M. A., D. U. Hur and D. V. Boger, "Normal stresses in fibre suspensions", *J. Non-Newtonian Fluid Mech.* **54**, 153–193 (1994).

List of publications

1. K. Radhakrishnan, **K. Asokan**, J. Dasan, C. C. Bhat and T. R. Ramamohan, “Numerical evidence for the existence of a low dimensional attractor and its implications in the rheology of dilute suspensions of periodically forced slender bodies”, *Physical Review E*, **60**, 6602–6618(1999), American Physical Society.
2. K. Radhakrishnan, **K. Asokan**, C. C. Bhat and T. R. Ramamohan, “Suspension rheology as a paradigm for study of aspects of spatio-temporal chaos”, *Non-linear dynamics: Integrability and chaos*, 305–312, Narosa Publishing House (2000)
3. **K. Asokan**, T. R. Ramamohan and V. Kumaran, “A novel approach to computing the orientation moments of spheroids in simple shear flow at arbitrary Péclet number”, *Physics of Fluids*, **14**(1), 75–84(2002), American Institute of Physics.
4. **K. Asokan** and T. R. Ramamohan, “The rheology of a dilute suspension of Brownian dipolar spheroids in a simple shear flow under the action of an external force”, Communicated.

G18631

